FUNCTIONAL STUDY OF KCV POTASSIUM CHANNEL THROUGH MANIPULTION OF INDIVIDUAL SUBUNITS

A Dissertation

Presented to

The Faculty of the Graduate School

University of Missouri - Columbia

In Partial Fulfillment

Of the Requirements for the Degree

Doctor of Philosophy

---

by

QIULIN TAN

Dr. Li-Qun (Andrew) Gu, Dissertation Supervisor

MAY 2010

The undersigned, appointed by the Dean of the Graduate School, have examined the dissertation titled

Functional study of Kcv potassium channel through manipulation of individual subunits

Presented by Qiulin Tan

A candidate for the degree of Doctor of Philosophy

And herby certified that in their opinion it is worthy of acceptance.

_____

Li-Qun (Andrew) Gu, Ph. D.

_____

Mark A. Milanick, Ph. D.

_____

Kevin D. Gillis, D. Sc.

_____

Fuhung Hsieh, Ph. D.

_____

Tzyh-Chang Hwang, Ph. D.

ACKNOWLEDGEMENTS

I would like to gratefully and sincerely thank Dr. Li-Qun (Andrew) Gu for his insightful guidance, understanding and patience during my Ph. D. study. He encouraged me to not only grow as an experimentalist but also as an independent thinker. His great mentorship has provided a well rounded experience for my long-term career goals.

I would also like to thank my doctoral committee members: Dr. Mark Milanick, Dr. Kevin Gillis, Dr. Fuhung Hsieh and Dr. Tzyh-Chang Hwang. I am so grateful for their input, valuable discussions and comments, which greatly elaborate my research.

Additional, I would like to thank all of the members of the Dr. Gu research group: Yong Wang, Kai Tian, Insoon Kang and Zhongchao Huang for their kind assistance during my graduate studies. These friends and co-workers provided not only their expertise and collaboration but also some humor and entertainment in the laboratory.

Importantly, I would like to thank my parents for their faith in me and allowing me to be as ambitious as I wanted. I also would like to thank my wife Pan Tian for her encouragement, quiet patience and unwavering love, which helped me overcome setbacks and fulfill my graduate study.

TABLE OF CONTENTS

LIST OF FIGURES

LIST OF TABLES

FUNCTIONAL STUDY OF KCV POTASSIUM CHANNEL THROUGH MANIPULTION OF INDIVIDUAL SUBUNITS

Qiulin Tan

Dr. Li-Qun Gu, Dissertation Supervisor

ABSTRACT

Potassium channels make up a ubiquitous, physiologically essential class of integral membrane proteins. Many K+ channels contain four identical symmetrically associated subunits. To explore the role of an individual subunit in the channel functions, i.e. functional stoichiometry, one can genetically manipulate individual subunits and characterize the variation of channel functions with subunit composition. The functional stoichiometry of ion channels can be studied through the co-expression and concatemer methods. In this report, we utilized Kcv as a potassium model for functional stoichiometric study. The chlorella virus-encoded Kcv can form a homo-tetrameric potassium (K+) channel in the lipid membrane. This miniature peptide can be synthesized *in vitro*, and the tetramer purified from the SDS polyacrylamide gel retains the K+ channel functionality. Based on this capability, here we propose a simple, straightforward method for detecting the contribution from individual subunits to the channel functions. By using this approach, several mechanisms for ion permeation and potassium channel blocker binding regulated by subunit composition were identified. For example, the structural change from only one subunit in the selectivity filter G65C is sufficient to cause permanent channel dysfunction (“all-or-none” mechanism), whereas the mutation near the extracellular entrance L70Y additively modifies the ion permeation with the

number of mutant subunits in the tetramer (“additive” mechanism). This study also demonstrates that four subunits of Kcv channel interact simultaneously with the potassium channel blocker tetraethylamonium (TEA) and each subunit contributes equally to the TEA binding free energy.

CHAPTER 1

INTRODUCTION

1.1. Structure and function of potassium channels

Potassium ions diffuse rapidly across cell membranes through proteins called potassium channels. K^+ channels make up a ubiquitous, physiologically essential class of integral membrane proteins (Jan and Jan, 1994). These channels play an important role in fundamental biological processes such as electrical signaling in the nervous system, heart beat, skeletonal muscle contraction, etc.

Potassium channels use diverse mechanisms of gating (the processes by which the pore opens and closes) (Tombola et al., 2006). For example, many potassium channels are voltage-gated (Long et al., 2005a, b). These channels contain a voltage-sensing domain (VSD) in helix S_4 voltage sensor which contains several positively charged amino acids (Arginine or Lysine). Several different models have been proposed for interpretation of the structure and molecular motion of the voltage sensor by using different techniques including crystallography, fluorescence analysis, and electrophysiology (Baker et al., 1998; Chanda et al., 2005; Ruta et al., 2005). Under depolarization condition, a conformation change occurs in this domain to turn the ion channel on, thereby triggering the efflux of potassium from the cell. This causes the membrane potential to be repolarized and the action potential is consequently terminated. Another important potassium channel family is inward-rectifying channel (Kir)

(Schachtman et al., 1992; Ho et al., 1993). Under hyperpolarization condition, Kir channels exhibit higher inward potassium current. The inward rectifying property is caused by the high affinity block of endogenous polyamine and Mg^{2+} which bind to the acidic residues in the cytoplasmic region of the channel (Nichols et al., 1993; Nishida et al., 2007). When depolarized, the binding of the blockers to the inner pore is enhanced, therefore plugging the channel pore and decreasing the outward current. In addition to voltage-gating mechanism, some channels are also gated by ions. For example**, c**alcium-activated potassium channels (BK, IK, SK channels) are activated by membrane potential and/or increasing concentration of Ca^{2+} in the cells (Vergara et al., 1998). Activation of BK (Big conductance Calcium-activated potassium channel) can cause hyperpolarization of cell membrane and play an important role in regulating neuronal cell excitability.

Potassium channels show a high selectivity for K^+, e.g., relative to Na^+, which is largely determined by a conserved sequence of TXXTXG(Y/F)G (MacKinnon et al., 1998; Shealy et al., 2003). One of the extensively studied potassium channels is KcsA, which has well-defined crystal structure (Fig. 1A) (Doyle et al., 1998). Encoded by Gram-positive bacterium *Streptomyces lividans*, KcsA encode a protein of 17.6 kDa with two predicted transmembrane (TM) helices connected by a linker region (Schrempf et al., 1995; Heginbotham et al., 1997). Despite the absence of a voltage sensor in KcsA, its open probability (P_0) is regulated by transmembrane potentials. It has been shown that the intracellular TM2 inner helices from four subunits constitute a bundle crossing domain, which function as an intracellular gate (Perozo et al., 1999; Del Camino and Yellen, 2001; Liu et al., 2001; Blunck et al., 2006). KcsA gating is also pH- dependent. KcsA opens at pH<5.5 at the intracellular side (Cuello et al., 1998). The proton binding site is

believed to be in the bundle crossing region as revealed by truncation constructs and NMR study (Cortes et al., 2001; Takeuchi et al., 2007). At neutral pH, they form a complex network of inter- and intrasubunit salt bridges and hydrogen bonds near the bundle crossing, thereby stabilize the closed state. At acidic pH, the proton binding can disturb this network and lead to channel opening (Thompson et al., 2008).

Although KcsA is a two transmembrane-spanning channel, its amino acid sequence shows high homolog to those eukaryotic six membrane-spanning channel proteins. It includes a signature motif (T_{72}ATTVGYG_{79}). In the K^+ selectivity filter the amino acid sequence TVGYG forms an extended strand that directs the threonine hydroxyl oxygen and four carbonyl oxygen atoms toward the ion conduction pore. Four strands (one from each subunit) come together to create five layers of four in-plane oxygen atoms; half way between each layer a K^+ interacts favorably with eight oxygen atoms, four from each adjacent layer. These favorable positions, or K^+ binding sites, are labeled 1–4 from the extracellular to the intracellular side of the selectivity filter (Fig. 1B) (Noskov et al., 2004; Zhou and MacKinnon, 2004). In addition to the selective K+ permeation, the selectivity filter is also suggested to participate in regulation of channel multimerization (Splitt et al., 2000) and gating behavior (Bernèche and Roux, 2005).

Another good example of potassium channel is Kcv. Encoded by Cholorella virus PBCV-1, Kcv channel protein plays an important physiological role in early infection cycle of the virus. Briefly, incorporation of Kcv channel to host plasma membrane during infection leads to an increased K+ conductance followed by a hyperpolarization of host cell membrane. This hyperpolarization consequently facilitates the DNA release from the virus into the host cells (Frohns et al., 2006). As one of the shortest potassium channel

ever found (Gazzarrini et al., 2009), Kcv encodes a peptide of 94 amino acids with an isoelectric point of 8.7 and a molecular weight of 10.6k Dalton (Plugge et al., 2000). Expression of the Kcv mRNA or cDNA can form functional K+ channels in *Xenopus laevis* oocytes or mammalian cells such as HEK293 cell sand Chinese hamster ovary (CHO) cells (Gazzarrini et al., 2002; Kang et al., 2004). And Kcv protein via in vitro synthesis or overexpression in eukaryotic system can be purified and functionally reconstituted into artificial lipid bilayer at a single channel level (Pagliuca et al., 2007; Shim et al., 2007).

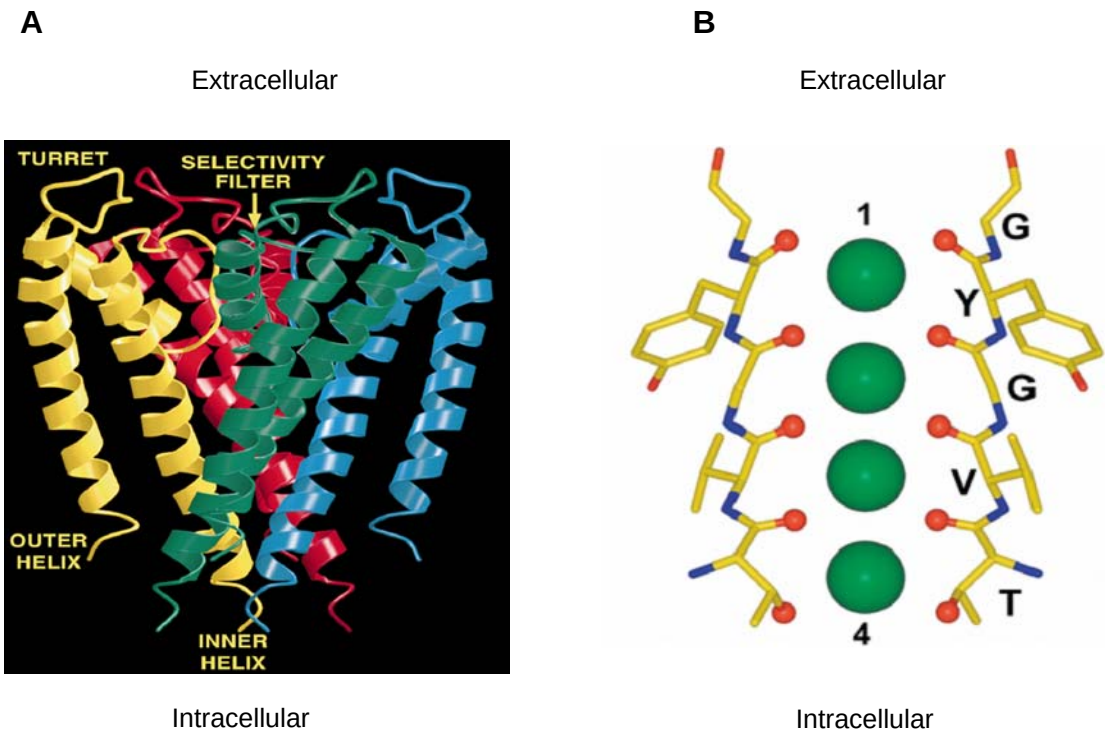

Figure 1. Structure of KcsA potassium channel. A. Homo-tetrameric KcsA (Doyle et al, 1998). B. Ion binding sites (represented as green spheres) in the selectivity filter of KcsA (Zhou et al, 2004).

Hydropathy analysis of Kcv reveals two putative transmembrane domains (Fig. 2) separated by 44 amino acids that contain the K^+ channel signature sequence T_{60}THSTVGFG_{67}. An unusual feature of Kcv is its short (12 amino acids) cytoplasmic NH2-terminus, which is required for the functional expression of Kcv channel (Moroni et al., 2002). The COOH-terminus of the Kcv protein is part of the second transmembrane region. Kcv thus appears to lack a COOH-terminal cytoplasmic tail. These structural data suggest that Kcv represents a very primitive K^+ channel. Due to its small size, it is a good archetypal potassium channel for the structure-function studies.

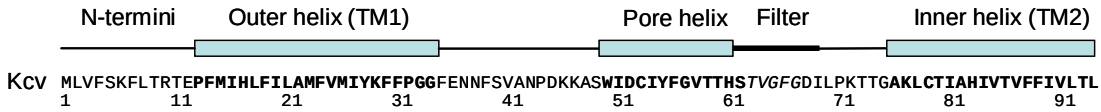

Figure 2. Amino acid sequence of chlorella virus PBCV-1 Kcv protein. Two transmembrane domains (TM1,TM2) and pore region (P) are boldface. The selectivity filter sequence $T_{63}V_{64}G_{65}F_{66}G_{67}$ is shown in italic.

1.2. Mutagenesis study of potassium channels

Many details of potassium channel structure-function relations have been well studied, mainly because of high-resolution electrophysiological analysis of genetically manipulated ion channels.

Heginbotham et al. investigated the effect of mutations in the signature sequence of the Shaker channel on K^+ selectivity determined under bi-ionic conditions (Heginbotham et al., 1994). Nonconservative substitutions of two threonine residues and the tyrosine residue leave selectivity intact. In contrast, mutations at some positions render the

channel nonselective among monovalent cations. These findings are consistent with a proposal that the signature sequence contributes to a selectivity filter. Furthermore, the results illustrate that the hydroxyl groups at the third and fourth positions, and the aromatic group at position seven, are not essential in determining K^+ selectivity.

Another study showed that designed mutations within kcsA gene resulted in a set of mutant proteins, which were characterized in respect to their assembly and channel activities (Splitt et al., 2000). Substitution of the first glycine (G77) residue within the GYG motif by an alanine (A) or substitution of the tyrosine (Y) residue 78 by a phenylalanine (F) led to mutant proteins which form tetramers of reduced stability. In contrast to the AYG mutant protein, GFG functions as an active K^+ channel whose characteristics correspond to those of the wild-type KcsA channel. The mutant proteins, which carry different mutations (T72A, T72C, V76A, V76E, G77E, Y78A, G79A, G79D, G79E) within the signature sequence of the pore region, do not at all or only to a very small degree assemble as tetramers and lack channel activities.

1.3. Techniques in electrophysiological study

1.3.1. Patch clamp techniques

The patch clamp technique has been widely used in the study of single or multiple ion channels in a variety of cells, especially in excitable cell such as neurons, cardiomyocytes and muscle fibers. The patch clamp technique can be applied in variable configurations including cell-attached, whole-cell, inside-out and outside-out. Conventional patch clamp recording uses a micropipette as an electrode. A well polished micropipette is patched on

the cell surface with high seal resistance (Giga-ohm GΩ) between the glass and cell membrane. This gigaseal can not only reduce the electronic noise but also provide more mechanic stability, thus allowing for high-fidelity recording of current of ion channels in the cell membrane. To use this technique, mRNA or CDNA template of potassium channels were injected into *xenopus laevis* oocytes or mammalian cells such as HEK293 or COS-1 cells. Upon expression of ion channels in the heterologous expression system, the current recordings were carried out with different type of patch clamp techniques.

1.3.2. Planar lipid bilayer recording

Another method for channel study is plannar lipid bilayer recording. Instead of overexpression of potassium channels in cells, the purified potassium channels are reconstituted into an artificial lipid bilayer for channel study under voltage clamp condition. In this study, the lipid bilayer composition is very important for the channel functions. For example, the function of membrane protein varies with the hydrophobic thickness of the lipid bilayer, which is determined by the acyl chain length of the phospholipid (Yuan et al., 2004). The property of lipid headgroup is also very important for the proper function of channel proteins. It has been suggested an anionic phospholipid (phosphatidylglycerol or phosphatidylserine) is required for KcsA to form functional channel in artificial lipid bilayer, probably due to the regulation of gating process via interaction between the anionic lipid and the transmembrane *a* helices (Williamson et al., 2002; Alvis et al., 2003; Williamson et al., 2003).

The artificial lipid bilayer can be formed by a monolayer-folding method. An aperture with a diameter of ~100um was formed in the center of the 25um thick teflon film by

electric discharge. This Teflon film is clamped between two chambers, thus serving as a septum. The aperture was pretreated with 10ul of 10% (v/v) hexadecane in pentane. Half volume of the desired solution is added to each chamber (*cis* or *trans*). About 10ul of designed phospholipid in pentane is added into each chamber to disperse on the surface of the water solution. After the organic solvent evaporated, the monolayer of the phospholipid is formed at the water-air interface. Upon addition of another half volume of solution, the lipid bilayer is formed when the lipid monolayer is raised to cover the aperture. The quality of lipid bilayer can be monitored by measuring the capacitance (~100-150pF).

This planar lipid bilayer recording techniques allows the investigator to manipulate easily the solution composition such as ion concentration, pH and ion channel blocker from either side of potassium channels. Also this technique is suitable for single channel recording which provides more detailed information about gating kinetics. By using this method, functions of potassium channel Kcv were investigated in this study. Kcv proteins were synthesized by in vitro transcription and translation. The tetrameric channel proteins were resolved and purified from SDS-PAGE gel. The purified potassium channels were then reconstituted into an artificial lipid bilayer for single channel recording. In combination with a mass-tagging method, a set of heteromeric Kcv channels carrying different number of mutated subunits were separated and purified from SDS-PAGE gel. By detecting each type of hetero-channel activity, different mechanisms for contribution of each subunit to the overall channel functions (eg., Ion permeation and gating, K^+ channel blocker sensitivity) have been identified.

CHAPTER 2

SEPARATION OF HETEROMERIC KCV TOWARDS PROBING SUBUNIT COMPOSITION-REGULATED ION PERMEATION AND GATING

2.1. Introduction

2.1. 1. Functional stoichimetry of potassium channels

Many K+ channels are composed of four identical subunits, which are symmetrically associated and work concertedly in conferring unique properties on channels, including ion selectivity and voltage-dependent gating. To explore the role of an individual subunit in the channel functions, i.e. functional stoichiometry, one can genetically manipulate individual subunits and characterize the variation of channel functions with subunit compositions (Isacoff et al., 1990; Liman et al., 1992; Tytgat and Hess, 1992; Ogielska et al., 1995; Pathak et al., 2005). The understanding of functional stoichiometry is not only beneficial for dissecting structure-determined channel mechanisms and programming channel activities with subunit composition, but also has significant medical implications. In many channelpathies such as Andersen's syndrome, the heterogeneous phenotypes are contributed by hetero-multimerization of the pathogenic channel protein (mutants) with other members in a channel family (Jongsma and Wilders, 2001; Plaster et al., 2001; Preisig-Müller et al., 2002).

The functional stoichiometry of ion channels can be studied through the detection of heteromeric channels that are hybridized by different types of subunits such as the wild-type and mutant subunits (MacKinnon et al., 1993). These subunit proteins are co-expressed in *Xenopus* oocyte and mammalian cells, and co-assemble in the cell membrane to form various hybrid channels. In the condition that the participating subunits are expressed at the same level and assemble randomly, the levels of hybrid channels will follow a binominal distribution. The levels of hybrid channels are determined by the amounts of mRNAs or cDNAs introduced, and their functions can be deduced from the sum of overall functions (Fig. 3A). As an example, this method has been used to study the inhibition of the Shaker K+ channel by scorpion toxin charybdotoxin, in which both the wild-type channel and wild-type/mutant hybrid channels were found to be inhibited by the toxin, leading to the conclusion that one wild-type subunit is enough to grant the tetrameric channel high toxin sensitivity (MacKinnon, 1991). Hybrid channels can also be formed between different members of channel family. For instance, co-expression of the voltage-gated K^+ channel Kv1.4 with Kv1.1 or Kv1.2 exhibited distinct cell surface expression pattern determined by subunit composition (Manganas and Trimmer, 2000). This method, however, is less effective in distinguishing between two types of hetero-channels that exhibit similar functionality. An alternative method of learning subunit contribution relies on concatemeric hetero-channels (Hurst et al., 1992; Kirsch et al., 1995; Mannuzzu and Isacoff, 2000). The concatemer protein is composed of two or more different types of subunits that are sequentially linked with a polypeptide linker. The concatemer proteins can be expressed in *Xenopus* oocytes or mammalian cells, and form tandem-linked hybrid channels in the membrane (Fig. 3B).

Compared with the co-expression approach, the concatemer approach can give more uniform (homogeneous) population of hybrid channels, and has significant implications for channelopathies and pharmacological distinction (Akhtar et al., 2002; Sokolov et al., 2007). However, some constructs showed lower expression efficiency, improper assembling and disturbance of function from the inter-subunit linker (Groot-Kormelink et al., 2004; Minier and Sigel, 2004; White, 2006). The constitution and length of intersubunit polypeptide linker has been shown to be important and need to be empirically decided.

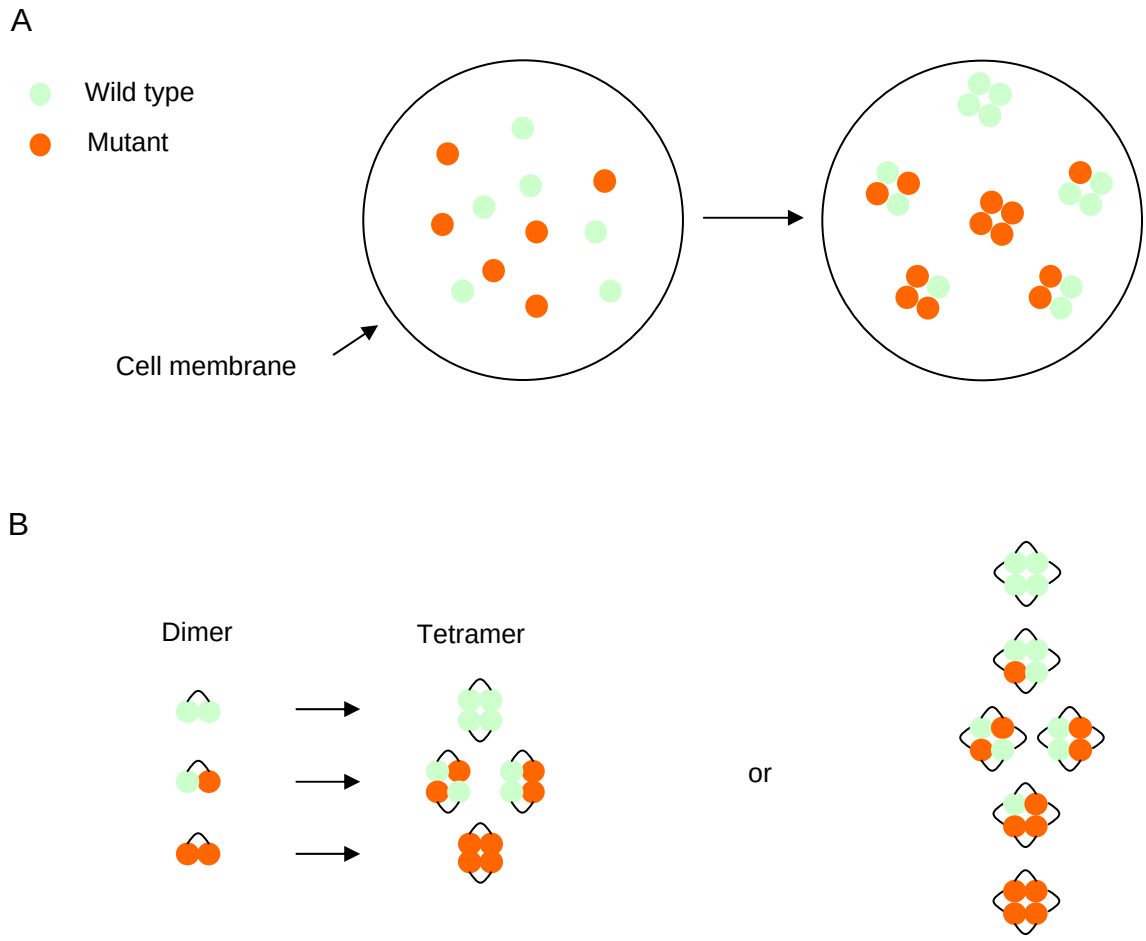

Figure 3. Conventional methods for study of functional stoichiometry. A. Coexpression in cell membrane. B. Construction of concatemers.

2.1.2. Generation of hetero-channels by mass-tagging method

In this report, we utilized the K+ channel Kcv as a model to propose a simple, straightforward method of studying functional stoichiometry. Recently, we uncovered a useful property of this protein: The *in vitro*-synthetic Kcv can form stable tetramers in the detergent SDS, and the Kcv tetramer collected from the SDS electrophoresis gel retains functions as a K+ channel (Shim et al., 2007). Based on this capability, we designed a tagged-Kcv (attached with a polypeptide tag) that can hybridize with an untagged-Kcv (e.g. mutant Kcv) to form hetero-tetramers. As these hetero-tetramers migrate in different mobility during electrophoresis, they can be well separated on the gel. The stability of Kcv tetramers in SDS allows us to purify each type of electrophoretically separated tetramers from the gel, and examine its single channel functionality (Fig. 4). The designed tagged-Kcv should also function as a wild-type Kcv, therefore providing a "wild-type background" when forming hetero-tetramers with untagged mutant subunits. By detecting the channel activity of each heterotetramer, the correlation between the channel function and subunit combination can be established.

Using this hetero-channel method, we are able to identify different mechanisms for subunit contributions to the channel activities. We found the mutation in the selectivity filter of Kcv regulate the ion permeation in an "all-or-none" manor. Substitution in one subunit is sufficient to result in permanent channel inactivation. In contrast, the mutation in the position near the extracellular entrance of the channel regulates the ion permeability in an "additive" mechanism. The channel's rectifying current can be additively modified with increasing number of mutant subunits in the tetramer.

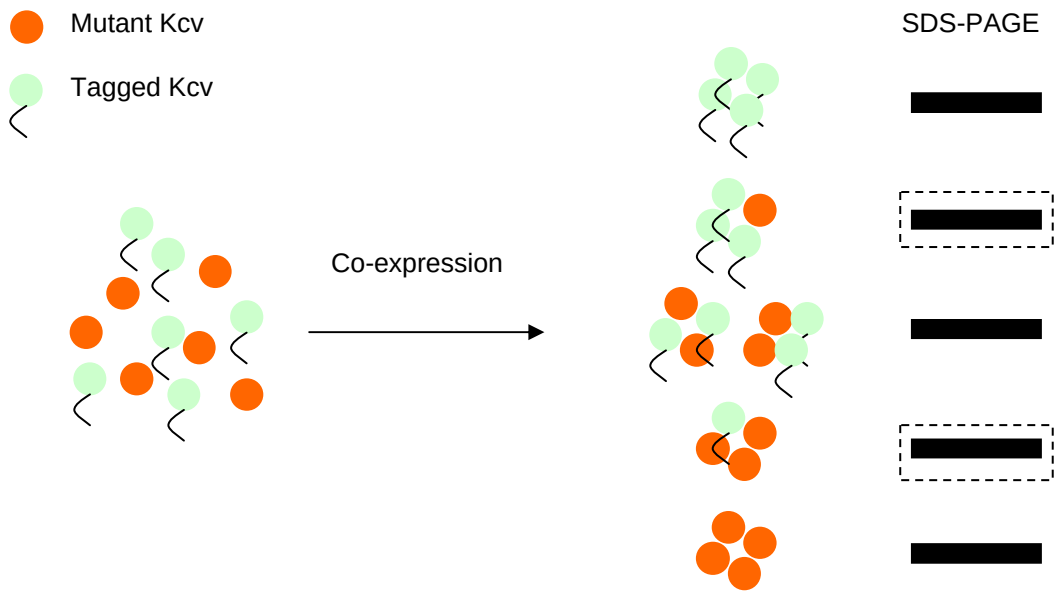

Figure 4. Generation of Kcv hetero-channels by mass-tagging method. Co-expression of tagged and untagged Kcv forms a set of SDS-stable tetrameric ion channels with different subunit composition. Homo- and heteromeric channels are separated by SDS-polyacrylmide gel electrophoresis due to their different electrophoretic mobility. Each type of tetramer can be purified from SDS gel for further single channel study individually.

2.2. Methods

2.2.1. Synthesis of Kcv gene

The sequence of the Kcv gene has been reported earlier (Shim et al., 2007). The Kcv gene in pUC57 with restriction sites for NdeI at the 5'-terminal and HindIII at the 3'-terminal was synthesized by GeneScript Corporation, NJ. The synthesized Kcv gene in pUC57 was cleaved with NdeI (New England biolabs R0111S) and HindIII (New England biolabs R0104S). The digestion products were resolved in 1.5% agarose gel. The

DNA band was then cut from the gel and the DNA was extracted by using Qiaquick gel extraction kit (Qiagen 28074). The Kcv gene was then ligated into the predigested vector pGS-21a (GeneScript Corporation) that contains a T7 promoter for protein expression. The plasmid pGS-21a-Kcv was transformed into competent XL-10 gold cells (Stratagene) by heat shock method. Briefly, 10ng of plasmid was added to 50ul of XL-10 gold cells. After incubation on ice for 40 minutes, the mixture was put in 42^0C water bath for 45-60 seconds. The cells were plated onto LB agar containing 50 ug/ml of Ampicillin and grew at 37^0C for > 16 hours. One colony was picked and grew in 100ml of LB medium containing 50 ug/ml of Ampicillin at 37^0C in the shaker for > 16 hours. The whole culture was spin at 4000g for 10 minutes, and the cell pellet was used for large preparation of plasmid by using Qiafilter plasmid midi Kit (Qiagen 12243)

2.2.2. Construction of tagged-Kcv genes

Using PCR, the tagged-Kcv genes containing the NdeI site (5'-terminal) and HindIII site (3'-terminal) were amplified. The PCR was performed as the following condition: 95^0C 5min – (95^0C 30sec, 56^0C 30sec, 72^0C 30sec) x 30 cycles – 6^0C 2min. The PCR product (~ 300bp) was resolved in 1.5% argarose gel. Purified DNA from the gel was digested with both NdeI and HindIII, and subcloned into pGS-21a, which has been predigested with the same enzymes. To construct tagged-Kcv genes, the forward primers containing NdeI site were,

D4 TAGTAGCATATG**GACGATGACGAC**TTAGTGTTTTCTAAATTCCTGACC

E4 TAGTAGCATATG**GAGGAAGAGGAG**TTAGTGTTTTCTAAATTCCTGACC

K4 TAGTAGCATATG**AAGAAGAAGAAG**TTAGTGTTTTCTAAATTCCTGACC

R4 TAGTAGCATATG**CGACGACGACGA**TTAGTGTTTTCTAAATTCCTGACC

N2 TAGTAGCATATG**AACAAT**TTAGTGTTTTCTAAATTCCTGACC

N4 TAGTAGCATATG**AACAATAACAAC**TTAGTGTTTTCTAAATTCCTGACC

N8 TAGTAGCATATG**AACAACAACAACAACAATAACAAC**TTAGTGTTTTC

TAAATTCCTGACC

The common reverse primer containing HindIII site was,

TAGTAGAAGCTTATCACAGGGTTAAAACAATAAAGAAC

2.2.3. Kcv mutagenesis

The Kcv mutants with single amino acid substitution were constructed using QuikChange® Site-Directed Mutagenesis Kit (Stratagene 200519). According to the protocol, the PCR was performed as the following condition: 95^0C 30sec – (95^0C 30sec, 55^0C 1min, 68^0C 5min) x 16 cycles. 50 μL PCR product was digested with 1 μL DpnI (10 U/μL) at 37 °C for 1 hour. 1ul solution was then transformed into XL-1 blue supercompetent cells by heat shock. The cells were plated onto LB agar containing 80 μg/mL X-GAL, 20 mM IPTG and 50ug/ml of Ampicillin, and grew at 37 °C for over 16 hours. One colony was picked and grew on 10 ml of LB medium containing 50ug/ml of Ampicillin at 37 °C for over 16 hours. Finally, the plasmids were extracted using QIAprep Spin Miniprep Kit (Qiagen 27104). The sequence was verified by DNA sequencing. The Primers for gene construction of Kcv mutants were:

G65C:

Forward: GTGACCACCCACTCTACCGTT**TGC**TTCGGTGATATCTTAC

Reverse: GTAAGATATCACCGAA**GCA**AACGGTAGAGTGGGTGGTCAC

G67Q:

Forward: ACCCACTCTACCGTTGGTTTC**CAA**GATATCTTACCAAAAACGA CG

Reverse: CGTCGTTTTTGGTAAGATATC**TTG**GAAACCAACGGTAGAGTGGGT

L70Y:

Forward: CCGTTGGTTTCGGTGATATC**TAT**CCAAAAACGACGGGC

Reverse: GCCCGTCGTTTTTGG**ATA**GATATCACCGAAACCAACGG

2.2.4. *In vitro* synthesis of Kcv proteins

S^{35}-labeled Kcv proteins were synthesized from coupled *in vitro* transcription and translation (IVTT) in *E. coli* T7 S30 Extract System for circular DNA (L1130, Promega). The IVTT mix contained premix solution, amino acids minus methionine, S30 extract pretreated with rifampicin, [35S]-methionine (10 uCi/25ul reaction, MP biomedicals 0151001.5), and plasmid template (4ul/reaction, 400ng/ul). To get the hetero-tetramer, the 4ul of template with various ration of tagged DNA to untagged DNA (4:0, 3:1, 2:2, 1:3, 0:4) was added. The IVTT mix was incubated at 37 C for 1hour.

2.2.5. Purification of Kcv proteins from the SDS gel

The IVTT mix (6ul) was added to 40ul 1x Laemmli sample buffer. The radio-labeled protein was resolved in a 12.5% SDS polyacrylamide gel, followed by autoradiography of the dried gel. Using the developed autoradiogram as a template, the slices containing Kcv tetramers were cut from the gel and rehydrated in 250ul sterile ddH_2O. The slice was then crushed with a disposable pestle (Kimble-Knotes Products 749521–1590). After 6

hours at room temperature, the gel fragment was removed with a spin filter Qiashredder (Qiagen 79654). The filtrate was then aliquoted and stored at -20^{0}C.

2.2.6. Single channel recording on lipid bilayer

Planar lipid bilayer recording was performed at 25^{0}C as described (Shim et al., 2007). Briefly, a 25um-thick Teflon film (Goodfellow, MA) with 100-150 uM diameter orifice separated the two 2-ml Teflon chambers. The aperture was pretreated with 10% (v/v) hexadecane in n-pentane. Planar lipid bilayer was formed with 1,2-diphytanoylsn-glycerophosphatidylcholine (Avanti Polar Lipids) over the orifice by a mono-layer folding method. Bilayer formation was monitored by the increase in the membrane capacitance to 100-150 pF. Gel –purified Kcv protein was added to the *cis* chamber, which was grounded. A potential was applied across this bilayer by Ag/AgCl electrodes with 1.5% agarose (Ultra Pure DNA Grade, Bio-Rad) containing 3M KCl. The voltage was applied from the *trans* chamber so that at positive potential a positive current was recorded. Currents were recorded with an Axopatch 200B patch clamp amplifier (Molecular Device Inc.). The signal was filtered at 1 kHz with a 4-pole low-pass Bessel filter, and acquired with Clampex 9.0 software (Molecular Device Inc.) through a Digidata 1332 A/D converter (Molecular Device Inc.) at a sampling rate of 20 kHz. The data were analyzed using Clampex 9.0. The magnitudes of the recorded currents were determined by fitting the peaks in amplitude histograms to Gaussian functions. Conductance values were given as means ± S.D. based on n separate experiments (n>=3).

2.3. Results and discussion

2.3.1. Construction and properties of the tagged-Kcv

We designed a series of tagged-Kcv that are distinct from each other in the tag's charge and/or molecular weight (Table 1). All the proteins of tagged-Kcv and untagged-Kcv were synthesized using coupled *in vitro* transcription and translation (see Methods).

Table 1. Tagged-Kcv and their tag sequences

Tagged-Kcv	K4	R4	D4	E4	N2	N4	N8
Tag sequences	KKKK	RRRR	DDDD	EEEE	NN	NNNN	NNNNNNNN

2.3.1.1. Tetramerization capability of tagged Kcv

We first examined the tetramerization capability of tagged-Kcv proteins. Fig. 5 shows the result of electrophoresis running on a 12.5% SDS polyacrylamide gel for 8 hours. For the wild-type Kcv (WT), we observed a light band and a heavy band. Consistent with our earlier study, the light band is the WT monomer and the heavy band the tetramer (Shim et al., 2007). All Kcvs carrying a charged tag, D4, E4, K4 and R4, also show a light band that is attributed to the monomer form. However, no heavy band can be identified for D4 and E4, and a very thin heavy band was seen in K4 and R4 lanes, suggesting D4 and E4 can not assemble homo-tetramers, and the tetramerization of K4 and R4 is not as efficient as WT. According to the electrophoresis result, D4, R4, E4 and K4 were ruled out for further test because of their low oligomerization efficiency. Probably their monomers are prevented from assembling by the repulsive electrostatic interaction among charged tags.

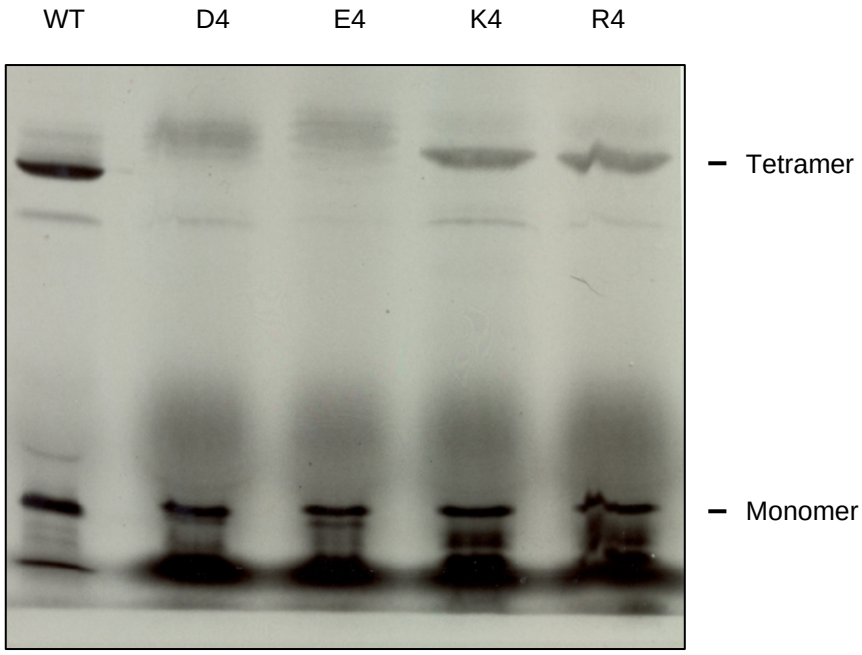

Figure 5. Tetramerization capacity of Kcv (D4, E4, K4 or R4). The S35-labeled Kcv proteins were run on a 12.5% SDS-polyacrylamide gel for 8 hours, and visualized by autoradiograph. The light band was the monomer and the heavy band the tetramer. Compared with wild type Kcv, D4 and E4 can not assemble into tetramers, and K4 and R4 assembly in a lower efficiency.

We further examined the tetramerization capability of tagged Kcvs (N2. N4, and N8) carrying different length of neutral Asparagine tags (Fig. 6). All three tagged Kcvs demonstrate both light and heavy hands in the same electrophoresis condition. The protein ratio of two bands for each tagged-Kcv is similar to that of WT, suggesting their similar tetramerization efficiency. N2 and N4 tetramers migrate at almost the same rate as the WT tetramer, but the N8 tetramer much slower with a distinguishable gap from the WT tetramer. The lowest electrophoretic mobility of N8 tetramer is attributed to the largest mass of its tag.

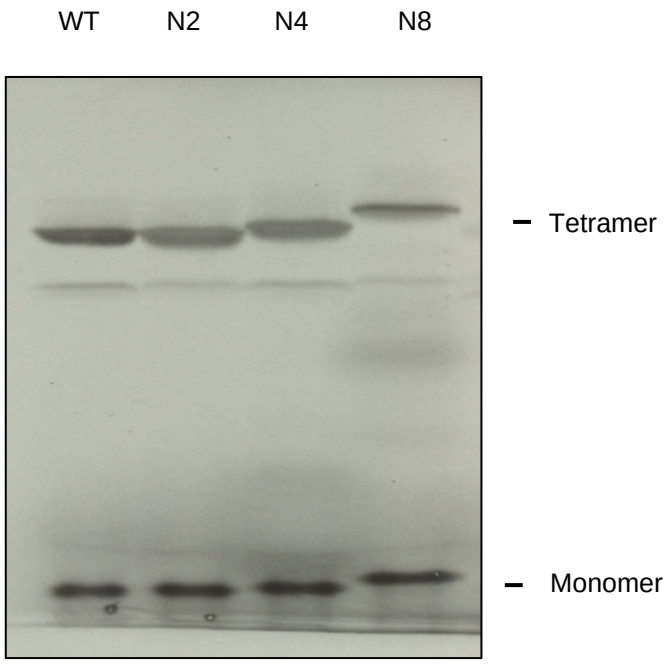

Figure 6. Tetramerization capacity of Kcv (N2, N4 or N8). The S35-labeled Kcv proteins were run on a 12.5% SDS-polyacrylamide gel for 8 hours, and visualized by autoradiograph. N2, N4 and N8 show similar tetramerization efficiency with wild type Kcv. N2 and N4 tetramers migrate at almost the same rate as the WT tetramer, but the N8 tetramer much slower with a distinguishable gap from the WT tetramer.

2.3.1.2. Electrophoretic separation of tagged Kcv N8 and untagged wild type Kcv

After identification of tetramerization capability of different tagged Kcv proteins, we tested whether the tagged-Kcv can co-assemble with WT, and whether their hetero-tetramers can be well separated by SDS-polyacrymide gel electrophoresis. We focused on N8 for this test because Fig. 5 has revealed that its tetramer is well separated from the WT tetramer compared to N2 and N4. To visualize all types of hetero-tetramers, WT and N8 were co-expressed at five WT/N8 plasmid ratios, 4:0, 3:1, 2:2, 1:3 and 0:4. Fig. 7 shows their product separation on a 12.5% SDS gel running for 16 hours. Lane-A and

Lane-E only show the WT and N8 homo-tetramer bands. In Lane-B, -C and -D, the co-expressed products split into five distinguishable bands. The relative protein amounts in the five bands are highly dependent on the DNA ratio. When the DNA quantity of WT is two-fold more than that of N8, the faster-migrating bands dominate (Lane-B); as their DNA quantities are equal, the intermediate bands thicken (Lane-C); and when the WT DNA falls to one third of the N8 DNA, the slower-migrating bands dominate (Lane-D), an inverse trend to Lane-B. Given the tetrameric stoichiometry, the fastest- and slowest-migrating bands should be the WT and N8 homo-tetramers (WT_4 and $N8_4$), and three intermediate bands are associated with WT/N8 hetero-tetramers in three subunit combination: from the fast- to slow-migrating, WT_3N8_1, WT_2N8_2 and WT_1N8_3. The subscripts denote the number of each subunit in the tetramer.

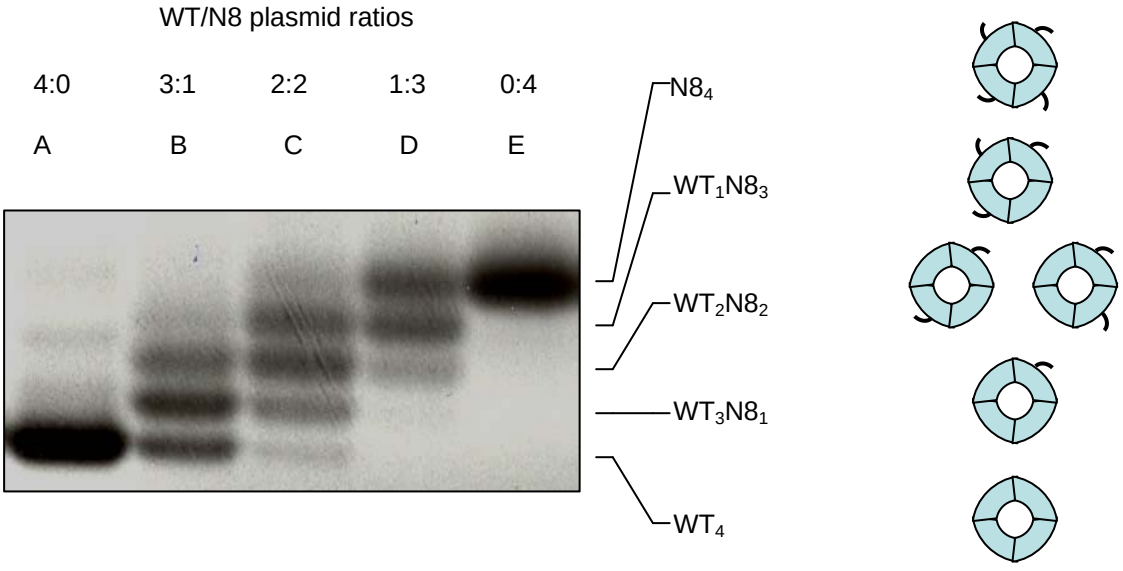

Figure 7. Electrophoretic separation of WT/N8 tetramers. The synthesized S^{35}-labeled proteins were run on a 12.5% SDS-polyacrylamide gel for 16 hours. Lane A through E were tetramers formed at WT:N8 plasmid ratios of 4:0, 3:1, 2:2, 1:3 and 0:4. The five bands identified represent all possible subunit combinations, $WT_{4-n}N8_n$ (n = 0, 1, 2, 3 and 4 is the number N8 in the tetramer).

2.3.1.3. Electrophysiological properties of tetrameric Kcv channels containing tagged subunit N8

Following the electrophoresis detection, our greatest interest was to know whether each WT/N8 tetramer purified from the gel can form a channel that functions as the wild-type Kcv. We recorded their single channel currents in symmetric solutions containing 150 mM KCl (Fig. 8). Their current-voltage relations (Fig. 10A) show that all the four tetramers containing N8 subunits form ion channels in the lipid bilayer with similar conductance to the WT tetramer at various voltages between ±120 mV. For instance, the conductance of the five tetramers at +40 mV are, WT_4, 213±5 pS; WT_3N8_1, 203±36 pS; WT_2N8_2, 216±5pS; WT_1N8_3, 216±16 pS; and $N8_4$, 194±19 pS (Table 2). We also measured the conductance under the bi-ionic condition (150 mM NaCl *cis* vs. 150 mM KCl *trans*) to determine the selectivity. Single channel recordings (Fig. 9) show that all the five tetramers only produce a positive current but never a negative current at high negative voltage. Their reverse potential (V_r, Table 2) obtained from the I-V curves (Fig. 10B) are also similar, WT_4, -60.2±5.9 mV, WT_3N8_1, -62.9±7.7 mV; WT_2N8_2, -62.0±5.2 mV; WT_1N8_3, -56.1±2.7 mV; and $N8_4$, -61.5±6.5 mV. This result suggests that the channels formed by all the WT/N8 tetramers are highly K+ selective.

Table 2. Conductance and reverse potentials of the five WT/N8 tetramers

	g (+40 mV, pS)	g (-40 mV, pS)	V_r (mV)
WT_4	213 ± 5	168 ± 15	-60.2 ± 5.9
WT_3N8_1	203 ± 36	145 ± 8	-62.9± 7.7
WT_2N8_2	216 ± 5	165 ± 5	-62.0 ± 5.2
WT_1N8_3	216 ± 16	159 ± 8	-56.1 ± 2.7
$N8_4$	194 ± 19	169 ± 9	-61.5 ± 6.5

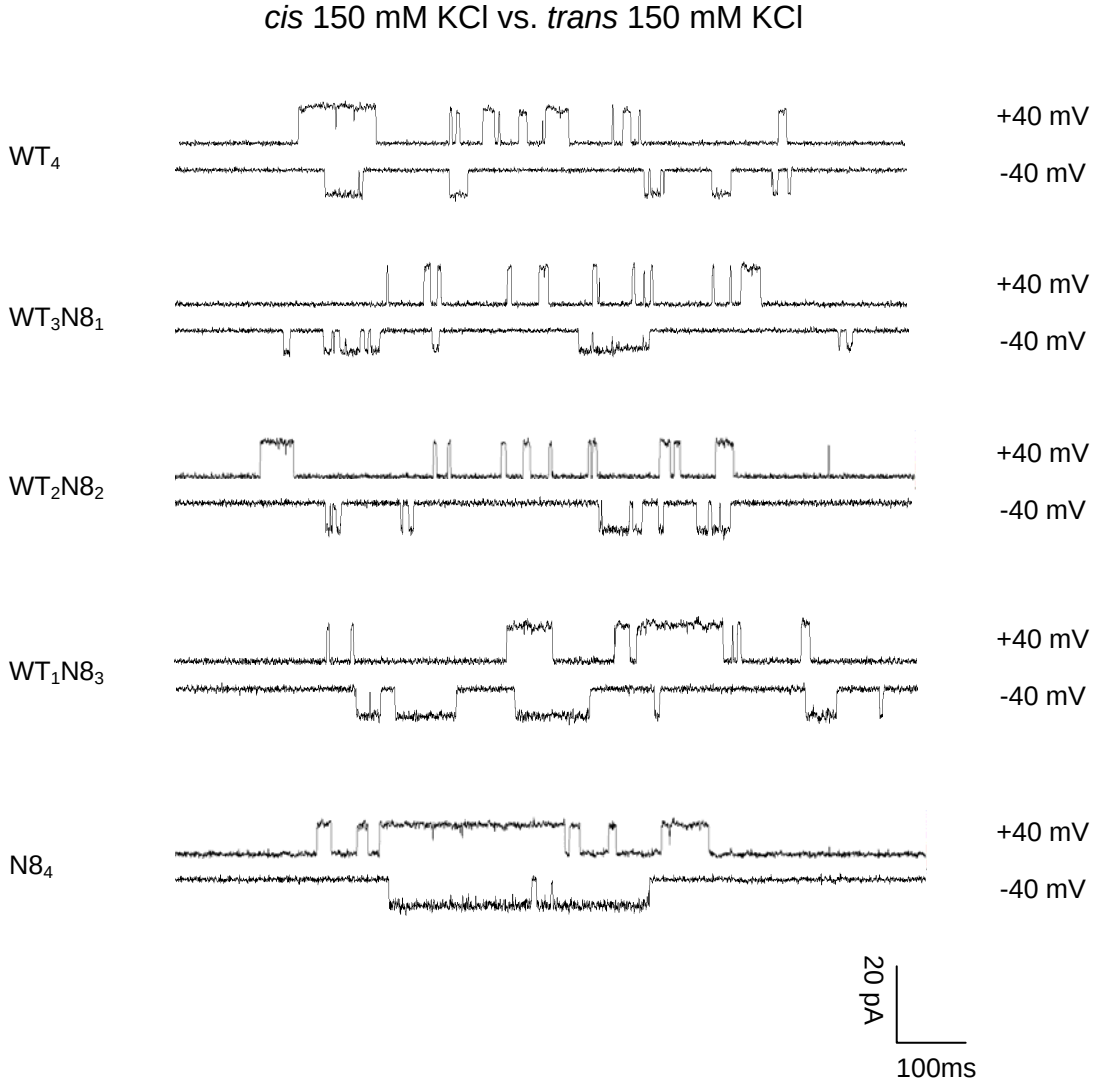

Figure 8. Single channel recordings of WT/ N8 tetramers under symmetric condition. The homo- and heterotetramers co-assembled by wild type (WT) and tagged Kcv (N8) were collected from SDS-polyacrylmide gel and dissolved in water. Each type of tetrameric Kcv channel was reconstituted into a 1,2-diphytanoylsn-glycerophosphatidylcholine (DMPC) lipid bilayer. Currents were recorded in symmetric solutions with 150mM KCl, 10mM Tris.Cl, pH = 7.2 in both trans and cis side. Representative current trace at +40 mV and -40 mV are shown.

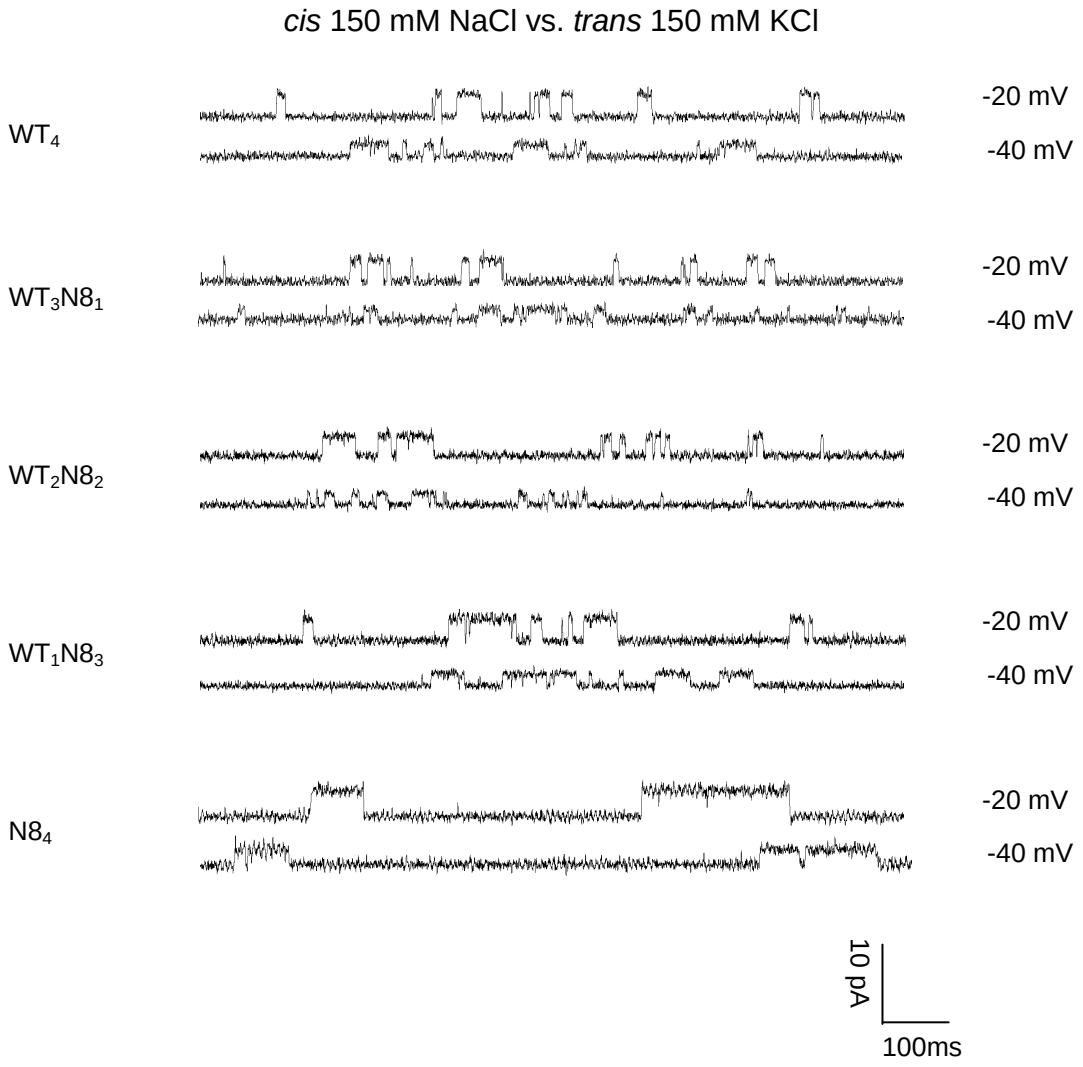

Figure 9. Single channel recordings of WT/ N8 tetramers under bi-ionic condition. Gel purified homo- and heterotetramers from wild type (WT) and tagged Kcv (N8) were reconstituted into (DMPC) lipid bilayer. Currents were recorded in symmetric solutions with 150mM KCl in *trans* and 150mM NaCl in *cis* (10mM Tris.Cl, pH = 7.2). Representative current trace recorded at -20 mV and -40 mV are shown.

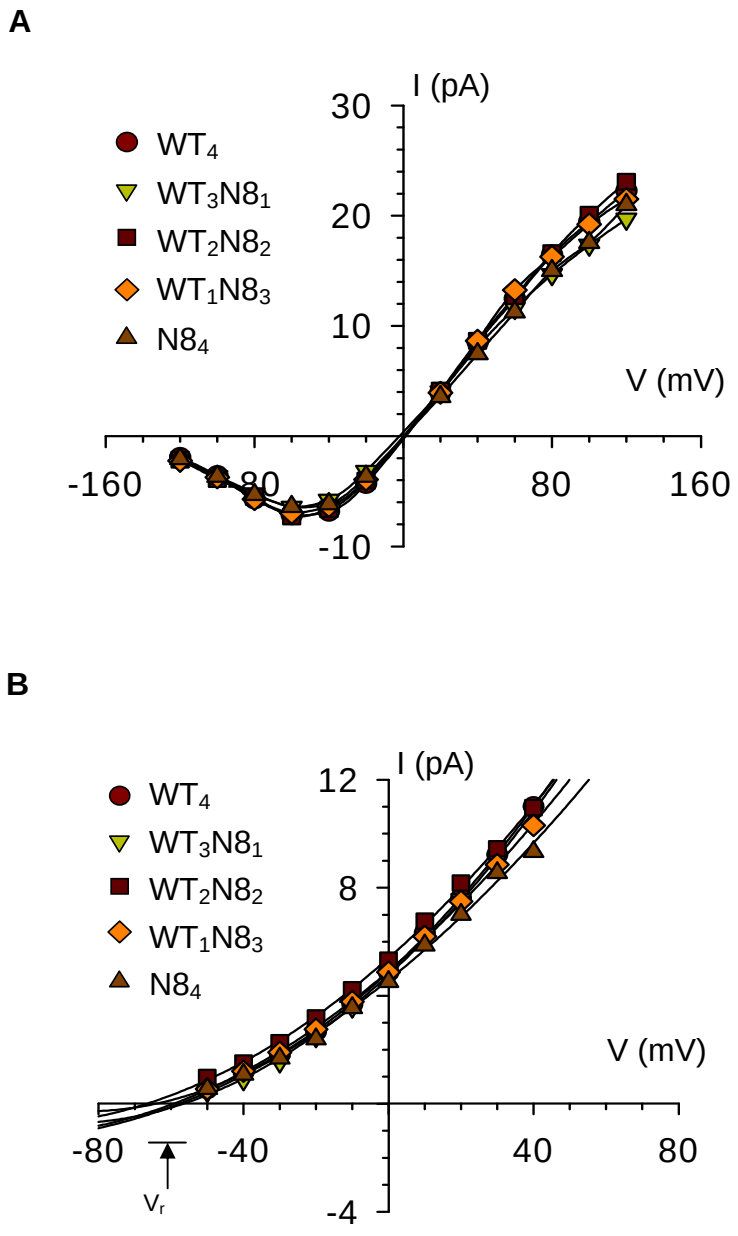

Figure 10. Current-voltage relations of WT/N8 tetramers. A. I-v curves corresponding to current recordings from Fig. 8. All five tetramers showed similar ion conductance in 150mM KCl symmetric solution. **B. I-v curves corresponding to current recordings from Fig. 9.** The data were obtained from single channel current recorded in bi-ionic solution with 150mM NaCl in *cis* and 150mM KCl in *trans*. The reversal potentials (V_r) were calculated by fitting the data to polynomial functions.

In summary, N8 is a tagged-Kcv that can form both homo- and hetero-tetramers with WT. The tetramers can be separated using electrophoresis, and each type of tetramers purified from the gel functions as a K+ channel with similar conductance and selectivity to the wild-type Kcv. Based on both findings from electrophoresis and electrophysiology detections, N8 is qualified for exploring the channel's functional stoichiometry, which are exemplified in the next two sections.

2.3.2. "All-or-none" channel inactivation by Gly^{65} in the selectivity filter

2.3.2.1. Mutagenesis study of Kcv mutants in selectivity filter

The crystallographic structures have revealed that the selectivity filter of a K+ channel comprises a symmetric ion pathway that is assembled by the backbone carbonyls contributed from four identical signature sequences. Many studies have confirmed the important role of the selectivity filter in maintaining the rapid and selective conduction of K+ ions. For instance, the Shaker K^+ channel with an altered selectivity filter has been turned into a non-selective pore for monovalent cations (Heginbotham et al., 1994). The KcsA channel with a substitution on the first glycine in the selectivity filter TVGYG (G77A) completely loses the permeability, and the mutant on the second glycine (G79A) can not even assemble into a tetramer (Splitt et al., 2000). Therefore, the filter of potassium channels at least plays key roles in both selective ion permeation and channel multimerization. Similar to KcsA, the mutant G67Q on the second glycine in the selectivity filter TVGFG can not tetramerize (Fig. 11). The Kcv mutant G65C (the first glycine in the filter) can form a tetramer. However, this tetrameric channel exhibited no

ion conductance (a non-conducting state) under either symmetrical (150mM KCl in both trans and cis side) or bi-ionic condition (150mM KCl trans VS. 150mM NaCl cis).

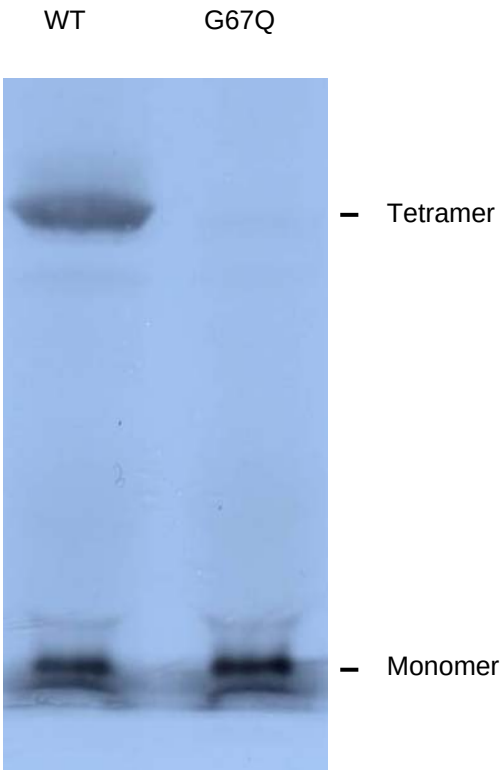

Figure 11. Tetramerization of Kcv mutant G67Q. G^{65} is the first glycine in the selectivity filter $T^{65}V^{66}G^{67}F^{68}G^{69}$. The in vitro synthesized S^{35}-labeled proteins were run on a 12.5% SDS-polyacryamide gel for 8 hours. Compared with the wild-type Kcv, G67Q did not show the tetramer band, indicating that this mutant can not tetramerize in the presence of SDS.

2.3.2.2. Electrophoretic separation of tetramers co-assembled from tagged Kcv N8 and Kcv mutant G65C

Because the selectivity filter is contributed by four identical signature sequences, we wanted to know how the structural change in one or several subunits among four alters

the channel permeability. To detect the channel regulation by individual subunits, we co-synthesized G65C with N8 at various plasmid ratios (4:0, 3:1, 2:2 1:3 and 0:4). Their products form five bands on the electrophoresis gel (Fig. 12). Similar to the WT/N8 co-expression products, the fastest-migrating (Lane A) and slowest-migrating band (Lane E) are the homotetramers $G65C_4$ and $N8_4$ respectively. The three intermediate bands appeared in Lane B, C and D are hetero-tetramers, from fast- to slow-migrating, $G65C_3N8_1$, $G65C_2N8_2$ and $G65C_1N8_3$.

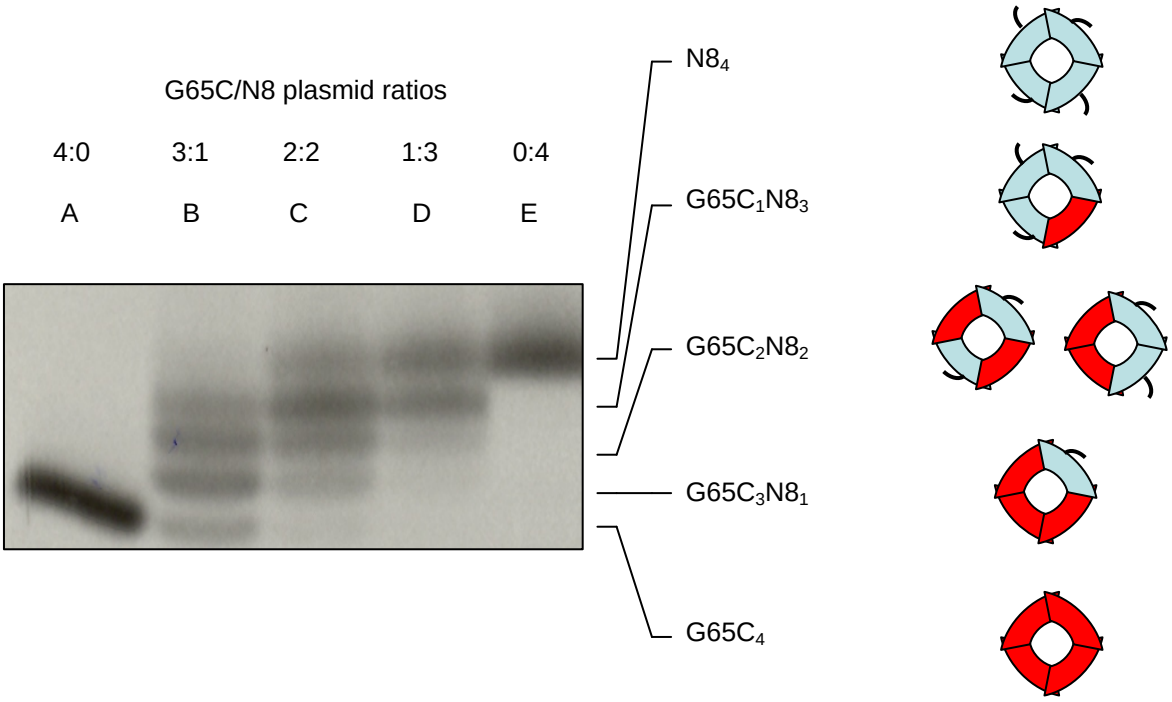

Figure 12. Electrophoretic separation of G65C/N8 tetramers. G^{65} is the first Glysine in the selectivity filter $T^{65}V^{66}G^{67}F^{68}G^{69}$. The synthesized S^{35}-labeled proteins were run on a 12.5% SDS-polyacryamide gel for 16 hours. Lane A through E were tetramer from co-synthesized G65C and N8 at a G65C/N8 plasmid ratios of 4:0, 3:1, 2:2, 1:3 and 0:4. The five bands identified represent all possible subunit combinations, $G65C_{4-n}N8_n$ (n = 0, 1, 2, 3 and 4 is the number N8 in the tetramer).

2.3.2.3. Channel activities of N8/G65C tetramers

After the G65C/N8 tetramers were purified from SDS-PAGE gel, their single channel properties were studied under either symmetric or bi-ionic condition. We found that, except $N8_4$ that functions as the wild-type Kcv, all other four tetramers containing different number of G65C subunits stay in a permanent inactivation state without opening events. Fig.13 shows the single channel recordings of five categories of N8/G65C tetramers under bi-ionic condition. The concentration factor for this result was ruled out because the stock concentrations of all purified proteins were similar (Fig. 14). Actually, the $N8_4$ channels were easily formed a few minutes after addition of 1 μl stock protein, but no channel was identified for all other tetramers while waiting for 1 hour with 5-10 fold increase of sample amount, and the channel activity of each tetramer was confirmed by at least ten tests. Overall, the finding from single channel currents confirms that all the four Gly^{65} in the selectivity filter are required to retain the K^+ ion conduction. Substitution of one Gly^{65} among four is sufficient to disable the channel permanently.

This "all-or-none" functional stoichiometry could be correlated with the selectivity filter's function in gating regulation. There has been increasing evidence supporting that the selectivity filter can regulate the gating of of K+ channels (Lu et al., 2001; VanDongen, 2004; Cordero-Morales et al., 2006a; Cordero-Morales et al., 2006b). The molecular dynamics (MD) simulation on the KcsA channel suggested that two peptide linkages in the selectivity filter (T-V and V-G amides in TVGYG) can transition to another orientation that leads to a stable "non-conducting" conformational state (Bernèche and Roux, 2005). The initiation of this conformational transition is sensitive to the configurations of the ion occupancy in the selectivity filter and inter-subunit

interactions. Thus the selectivity filter with such a conformational transition might function as a gate to regulate channel's opening and closing. The functional stoichiometry of Kcv revealed by the WT/G65C hetero- channels provides an experimental support on this theoretical analysis. The substitution of Gly^{65} in this mutation may give rise to a "reorientation" of the selectivity filter that "locks" the Kcv channel in the non-conducting state. Strikingly, the MD simulation (Bernèche and Roux, 2005) further predicted that this reorientation of the selectivity filter only takes place in a single subunit, which is sufficient to lead to the non-conducting state. This prediction is in good agreement with our experimental finding that the substitution in the selectivity filter from one Kcv subunit is sufficient to inactivate the channel, transitioning it to the non-conducting state.

It is interesting that the similar functional stoichiometry also applies to other structures such as G-quadruplex that utilize similar tetra-carbonyls for binding K+ ions. The G-quadruplex is a special structure of nucleic acids folded by a series of G-tetrad planes stacking one on another. Each G-tetrad is assembled by four guanine bases through hydrogen bonding. Very similar to the precise K^+/carbonyl coordination in the K^+ channel's filter structure, a K^+ ion is intervened between adjacent G-tetrads, coordinating with eight carbonyls, each from a guanine base (Wong and Wu, 2003). We have found the substitution of any single guanine in a G-tetrad will completely disable the G-quadruplex formation (unpublished data). Interestingly, engineered G-quadruplexes have been found to form ion channels in the lipid bilayer in the presence of K^+ ions (Ma et al., 2008).

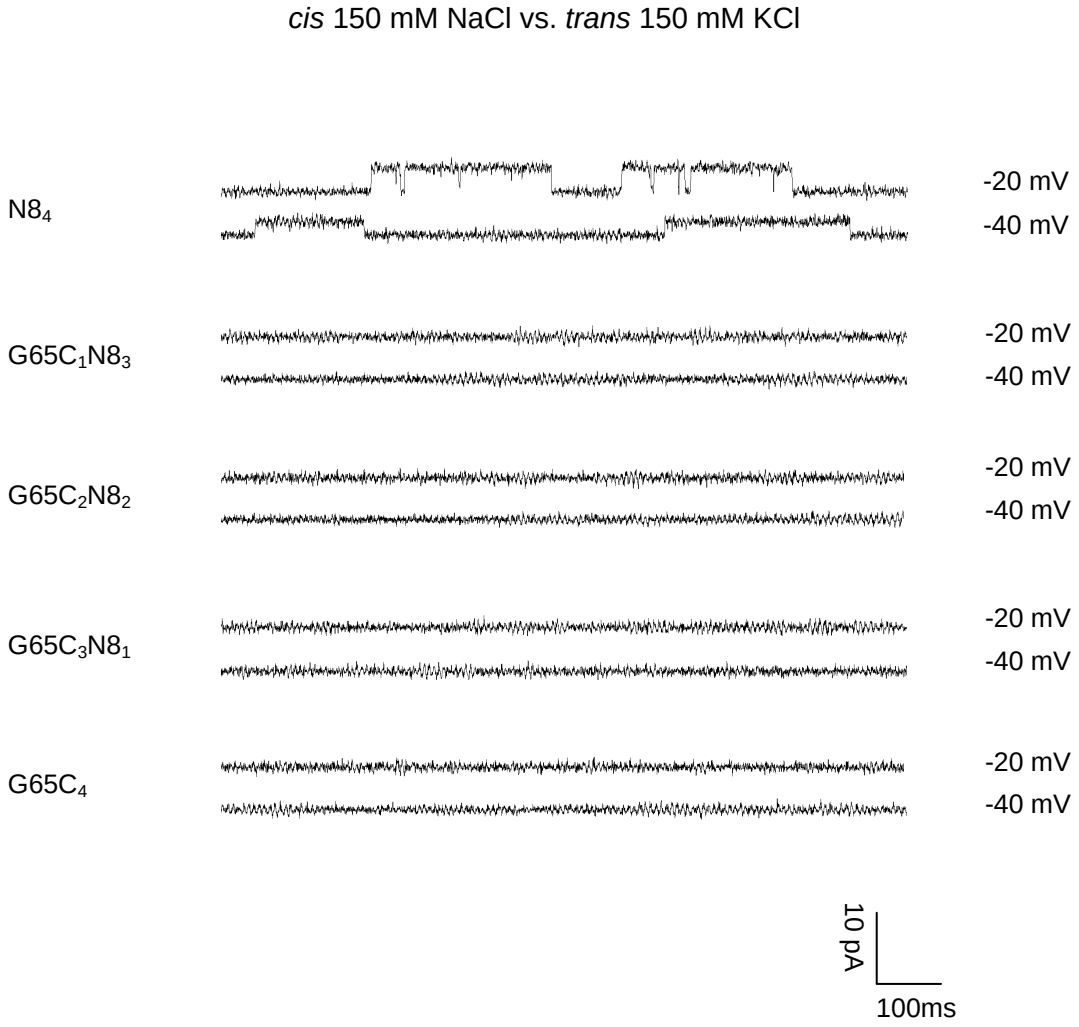

Figure 13. Single channel recordings of G65C/ N8 tetramers under bi-ionic condition. Gel purified homo- and heterotetramers from wild type (WT) and tagged Kcv (N8) were reconstituted into (DMPC) lipid bilayer. Currents were recorded under bi-ionic condition, *cis* 150 mM NaCl vs. *trans* 150 mM KCl, pH7.2. Only the N8 tetramer ($N8_4$) can form a K+ channel, but all other tetramers that contain at least one G65C subunit, i.e. $G65C_1N8_3$, $G65C_2N8_2$, $G65C_3N8_1$ and $G65C_4$, do not form opening channels.

Protocol #:14 Name:QUICK SWIPES 13-Mar-2008 14:46
Region A: LL-UL= 0.0-18.6 Lcr= 0 Bkg= 0.00 %2 Sigma=0.00
Region B: LL-UL=18.6-256. Lcr= 0 Bkg= 0.00 %2 Sigma=0.00
Region C: LL-UL=256.-2000 Lcr= 0 Bkg= 0.00 %2 Sigma=0.00
Time = 1.00 QIP = SIS
Luminescence Correction On

S#	TIME	CPMA	CPMB	CPMC	H3DPM	C14DPM	P32DPM	?ISOTO	tSIE	FLA
1	10.00	8.40	5.16	5.60	22	21	19	156	0.00	
2	1.00	48074.2	49772.8	0.40	123267	199091	1	826564	0.00	
3	1.00	6209.22	6234.64	0.00	15921	24939	0	104768	0.00	
4	1.00	6030.59	6357.44	0.00	15463	25430	0	104853	0.00	
5	1.00	3288.82	3539.04	0.40	8433	14156	1	57924	0.00	
6	1.00	3880.39	3790.64	0.40	9950	15163	1	64394	0.00	
7	1.00	2489.64	2487.64	0.00	6384	9951	0	41883	0.00	

Figure 14. Scintillation analysis of G65C/N8 tetramers. S# 1, background control; 2, wild-type Kcv from an 125 µl large reaction for comparison; 3 through 7, G65C4-nN8n (n=0, 1, 2, 3 and 4) from a 12.5 µl reaction. The proteins of G65C/N8 co-tetramers in the same gel were collected and purified as the stocks. 10 µl of each stock solution was used for scintillation analysis.

2.3.3. "Additive" regulation of ion permeation by Leu^{70} near the extracellular entrance of the channel

The wild-type Kcv forms a moderate voltage-dependent channel with a rectified current-voltage relationship (Fig. 10A): the single channel current increases almost linearly with positive voltages, whereas decays sharply at negative voltages. The asymmetric I-V curve is not caused by the binding of cations such as Mg^{2+} as in the inward-rectifier K+ (Kir) channels (Lopatin et al., 1994), in that Kcv was studied in the absence of multivalent ions. Through the mutagenesis screening, we have identified L^{70} near the extracellular entrance (the 3rd amino acid after the selectivity filter) as a key position for modulating the rectified I-V relationship. For example, the substitution of Leu^{70} with aromatic residues Tyr (L70Y) significantly increased the negative conductance, thus change the rectifying property.

2.3.3.1. Electrophoretic separation of N8/L70Y tetramers

To understand how the structural change in individual subunits alters the rectification property, L70Y and N8 were co-expressed at indicated plasmid ratios. Tetrameric Kcv proteins were then resolved in 12.5% SDS- polyacrylamide gel electrophoresis. Fig. 15 shows that the L70Y/N8 products split into five bands on the SDS gel. The fastest-migrating (Lane A) and slowest-migrating band (Lane E) are the homotetramers $L70Y_4$ and $N8_4$. The three intermediate bands in Lane B, C and D are hetero-tetramers, from fast- to slow-migrating, $L70Y_3N8_1$, $L70Y_2N8_2$ and $L70Y_1N8_3$ respectively.

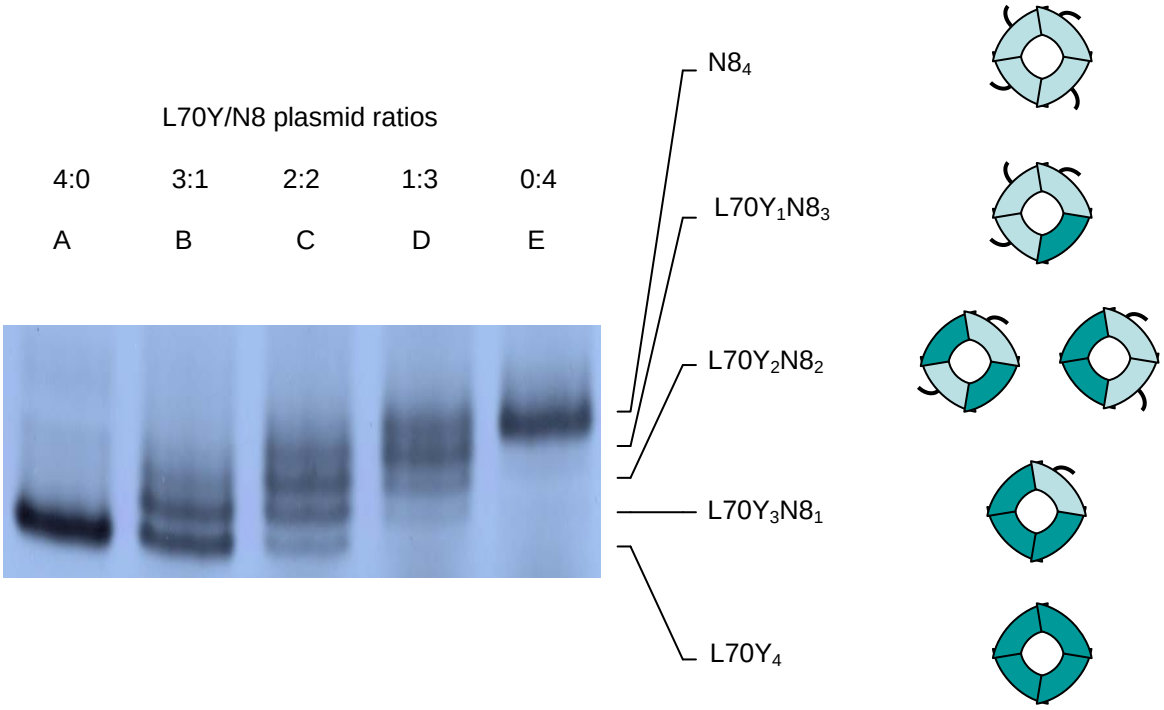

Figure 15. Electrophoretic separation of L70Y/N8 tetramers. The synthesized S^{35}-labeled proteins were run on a 12.5% SDS-polyacrylamide gel for 16 hours. The five bands identified represent all possible subunit combinations, $L70Y_{4-n}N8_n$ (n = 0, 1, 2, 3 and 4 is the number N8 in the tetramer).

2.3.3.2. Regulation of ion permeation by individual L70Y subunit in a Kcv tetramer

We collected the five tetramers from the gel and individually examined their channel activities. Fig. 16 shows their single channel currents recorded at -60 mV in 150 mM KCl. The I-V curves at various voltages between ±100 mV were determined in Fig. 17A, and their conductance at ±60 mV was compared in Table 3. We found all the L70Y/N8 tetramers show similar positive conductance with their currents increasing linearly with the voltage. In contrast to the positive conductance, the negative conductance for the five tetramers varies with the subunit composition. $N8_4$ does not contain any L70Y subunit, so behaves as the wild-type Kcv with a conductance of 112±2 pS at -60 mV. This conductance monotonically increases with the number of L70Y subunits in the tetramer, $L70Y_1N8_3$, 172±12 pS, $L70Y_2N8_2$, 218±10 pS, and $L70Y_3N8_1$, 268±5 pS (Table 3). As $L70Y_4$ has all the four subunits replaced, the conductance reaches the highest 292±12 pS, which represents a 2.5 folds increase from $N8_4$. Therefore the decayed negative current of Kcv is stepwise increased with the number of L70Y subunits. Fig. 17B shows that the change in the negative conductance (g) with the number of L70Y subunits (n) can be fitted to a straight line, and can be described using Eq.1

$$\begin{aligned} g_{M_nN8_{4-n}} &= (4-n)g_{N8} + ng_M \\ &= (4-n)g_{N8} + n(g_{N8} + \Delta g) \\ &= 4g_{N8} + n\Delta g \end{aligned} \qquad (1)$$

In this expression, g_{N8} is the conductance contributed by a single N8 subunit, $g_M = g_{N8} + \Delta g$ is the conductance by a L70Y mutant subunit, Δg is the increase. $g_{M_nN8_{4-n}}$ is the conductance of the tetramer containing n subunits of the mutant L70Y and 4-n subunits of N8. This model suggests a different mechanism for regulation of ion

permeation. Unlike Gly^{65} in the selectivity filter where four subunits work concertedly, each subunit at Leu^{70} contributes equally and independently to the conductance, and additively modulates the permeability without significant inter-subunit cooperation.

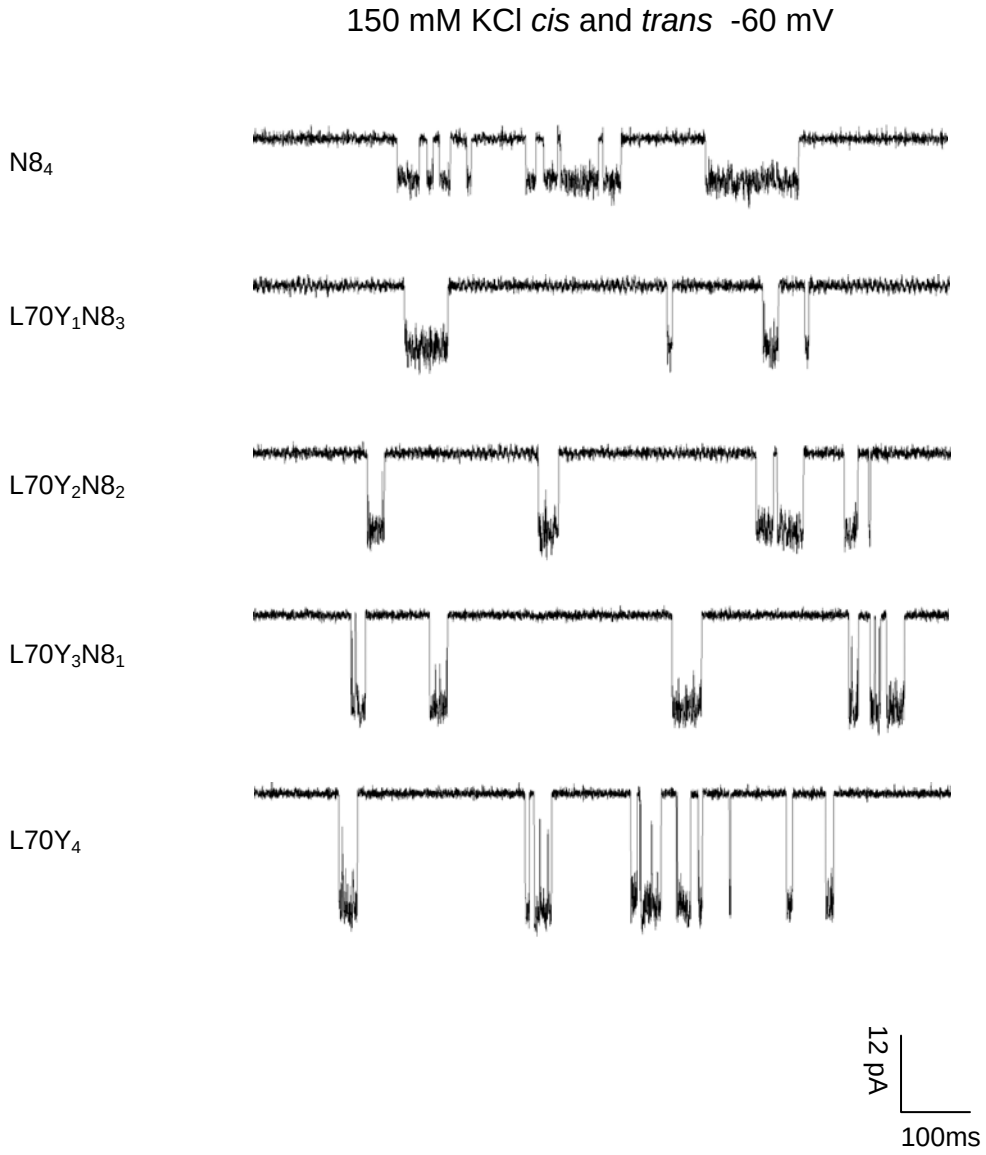

Figure 16. Single channel recordings of L70Y/ N8 tetramers under symmetric condition. Current of each tetramer was recorded in 150mM KC symmetric solution. Representative current traces at -60 mV are shown.

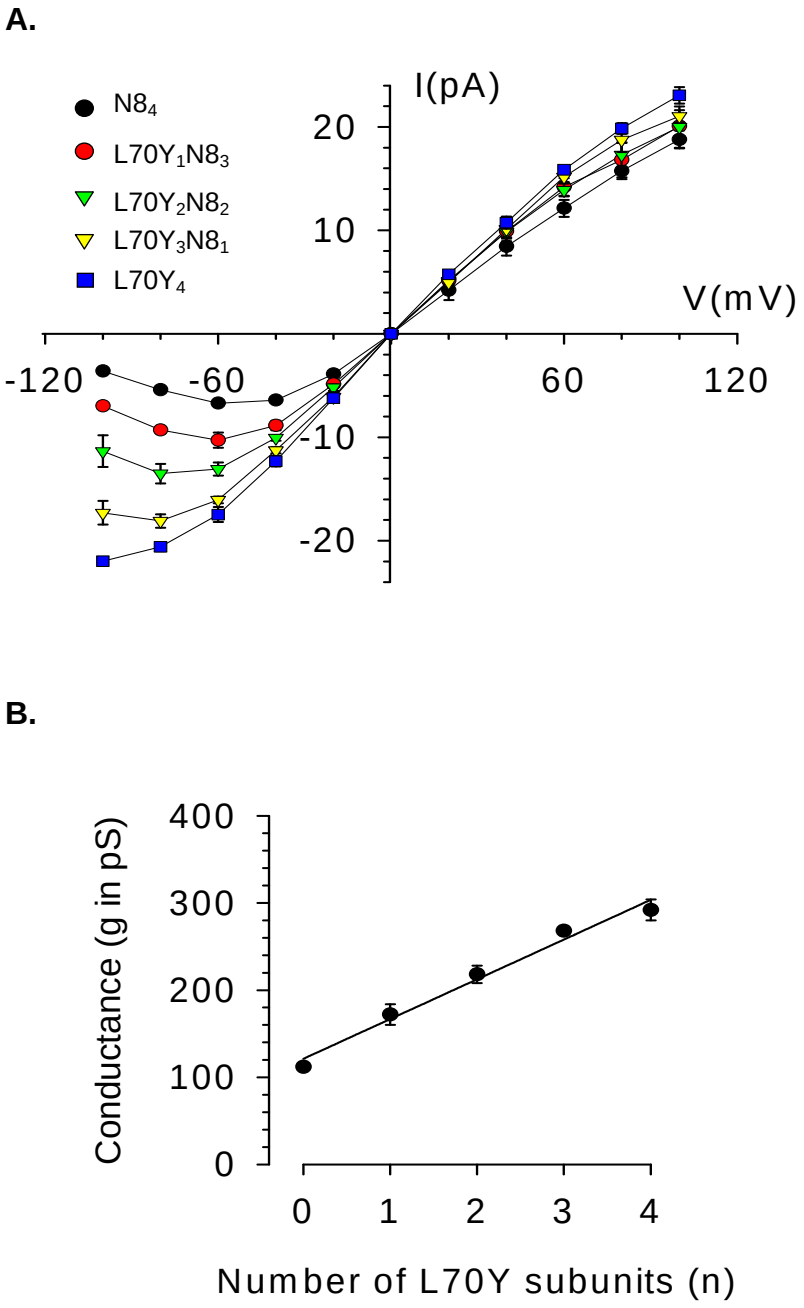

Figure 17. Regulation of ion conductance by individual L70Y subunit. A. Current-voltage relations of L70Y/N8 tetramers. The data were obtained from single channel current recorded in 150 mM KCl symmetric solution. **B. Correlation between the conductance for the five L70Y/N8 tetramers at -60 mV and the number of L70Y subunits in the tetramer.**

Table 3. Conductance of channels formed by the five L70Y/N8 tetramers

	g (+60 mV, pS) [a]	g (-60 mV, pS) [a]
$N8_4$	212 ± 14	112 ± 2
$L70Y_1N8_3$	236 ± 14	172 ± 12
$L70Y_2N8_2$	232 ± 10	218 ± 10
$L70Y_3N8_1$	253 ± 9	268 ± 5
$L70Y_4$	264 ± 13	292 ± 12

[a] : *cis* 150 mM KCl vs. *trans* 150 mV.

The "additive" regulation of ion permeation could originate from the "fast" gating, a mechanism proposed by Abenavoli et al (Abenavoli et al., 2009) to interpret the Kcv's decayed conductance in the single-channel I-V curve at extreme voltages. According to that study, the decayed conductance of Kcv formed in Xenopus oocytes is associated with a high level of current noise. This phenomenon is attributed to an open-close flicking that is too fast (microseconds) to be fully resolved at the filtering frequency and data acquisition rate provided by the electrophysiology instrument. Guided by a β-distribution analysis, the decayed conductance can be recovered to the original full conductance. By comparison, our Kcv channel in the artificial membrane shows similar single channel characters to that in the cell membrane. At negative voltage, the decayed conductance is always accompanied with flicking-like current noise (Fig.18). Based on the fast gating model and the functional stoichiometry studied above, we infer that that Leu^{70} is a key position to modulate the fast gating activity, and each subunit independently contributes a fast gating pattern to the overall conductance. Therefore, the observed apparent

conductance is an accumulation of four fast gating patterns, rather than a simple open-close two-state flicking. An advanced mathematic model is needed to describe this process.

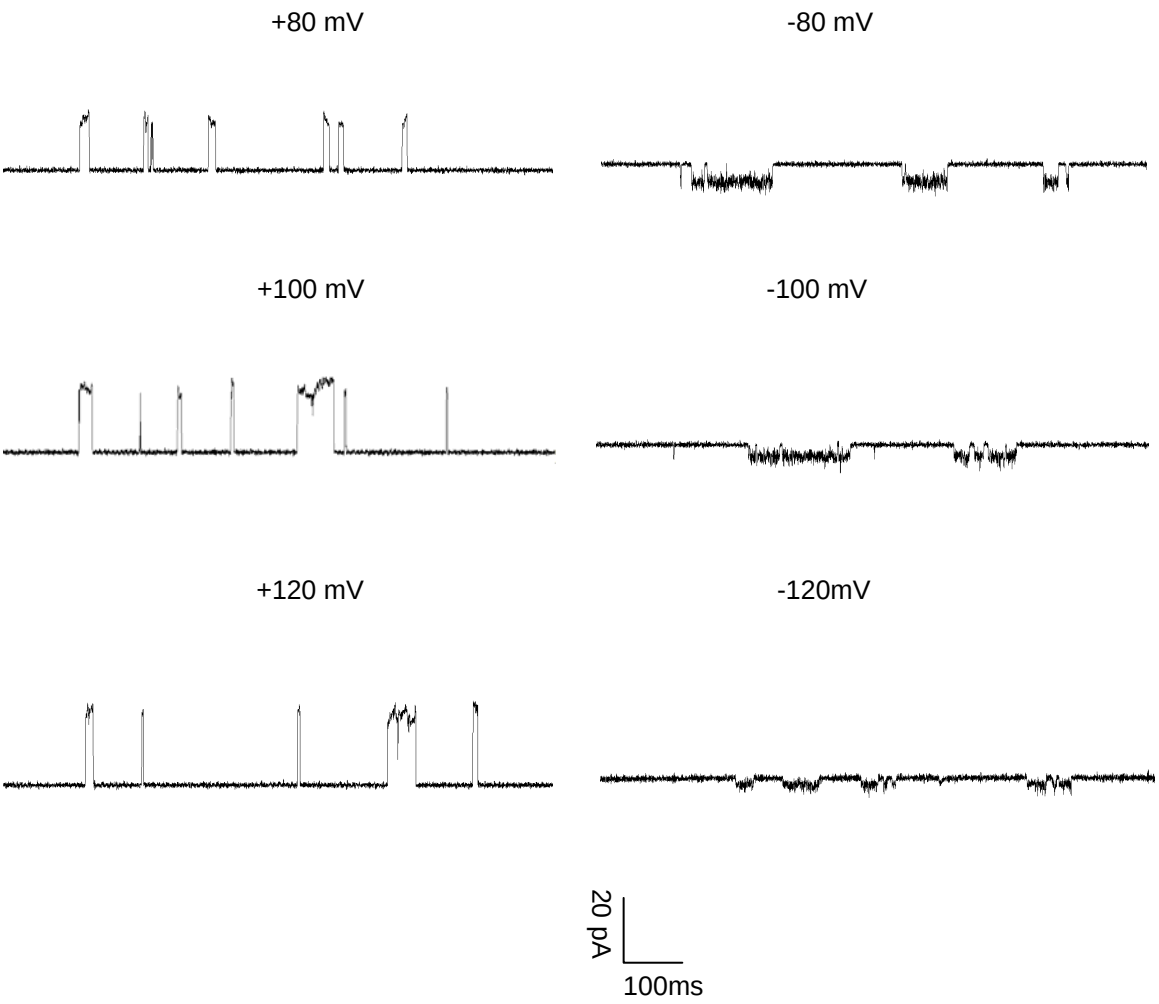

Figure 18. Single channel currents of the wild-type Kcv channel at high positive and negative voltages. The data was obtained from single channel currents recorded in symmetrical solutions containing 150 mM KCl in both *trans* and *cis* side. Compared with the currents at positive voltages, the currents at negative voltages show decayed amplitudes and higher level of noise.

2.4. Advantages of the hetero-channel method

The unique property of the miniature Kcv provides a straightforward strategy for detecting subunit roles in the channel functionality. First of all, the stability of the Kcv tetramer in SDS enables us to study the electrophysiology properties of individual types of hetero-Kcv tetramers that are directly purified from the electrophoresis gel. It has been known that many β-barrel protein pores, as exemplified by α-hemolysin, retain their oligomeric structure and pore-forming capabilities after being treated with SDS (Braha et al., 1997; Cheley et al., 1999; Miles et al., 2001). Therefore, the synthetic Kcv represents an alpha-helix channels that retain both structural and functional integrity under harsh biological conditions. Furthermore, the tagged-Kcv we identified (N8) allows for separation and purification of hetero-Kcv tetramers from the gel. This is similar to the traditional mass-tagging method for effectively inferring the subunit stoichiometry (the number of subunits) of ion channels (Gouaux et al., 1994; Miles et al., 2002). However, the role of the tagged-Kcv is more than that. The tagged-Kcv should function as a wild-type Kcv, therefore serving as the wild-type subunits in hetero-tetramers with the untagged mutant subunits. We have reported earlier that Kcv with a more complicated tag, N8H6 (eight asparagines followed by six histidines), can also form tetramers (Shim et al., 2007). However, this tagged-Kcv showed a low efficiency in channel formation. The advantage of this hetero-channel method is that the contributions of mutant subunits to the channel function can be independently revealed. This method does not require different subunits to be equally expressed and random associated in the membrane as in the co-expression method, and does not require tandem constructs as in the concatemer method**.**

2.5. Conclusion and perspectives

We established a simple, straightforward method of genetically manipulating individual subunits in the Kcv tetramer, thereby enabling the detection of the contribution from individual subunits to the channel functions. Using this approach, we are able to distinguish two mechanisms for regulation of ion permeation and gating by subunit composition, "all-or-none" channel inactivation by Gly65 in the selectivity filter, and "additive" regulation of ion permeation and fast gating by Leu70 near the extracellular entrance.

This approach could be useful in detecting a variety of subunit composition-determined molecular processes in channels. Kcv channel can be inhibited by a typical potassium channel blocker Ba^{2+} and the antiviral drug amantadine (Syeda et al., 2008). By using genetic selection methods, a mutant T63S, which exhibited both barium and amantadine-resistance, was identified. T63 is located in the innermost site of Kcv channel selectivity filter. A barium ion might be coordinated in this site, thereby block the K^+ flow (Chatelain et al., 2009). By investigating the blocker sensitivity of each type of hetero-channels with different number of T63S substitutions, it is possible to uncover the subunit contribution to the channel block. This study will make a better understanding the ion channel functions and be useful for development of channel-specific drugs.

This approach is applicable to the mechanistic study of other K^+ channels. Like Kcv, our preliminary data supports that the KcsA can tetramerize in the presence of SDS. The tetrameric KcsA retains the K+ channel functions when purified from the SDS gel (Fig. 19). The tagged KcsA (N8- or H6N8-) allows good separation of heteromers through SDS-polyarylamide electrophoresis (Fig. 20). These properties allow for detecting

hetero-KcsA channels, which is supposed to reveal the subunit contributions in channel functions. For example, the substitution of key proton binding residues near the bundle crossing region will disrupt inter- and intrasubunit interactions, thus favoring channel opening even in high intracellular pH 9.0. Detection of open probability of heteromeric KcsA channels with different number of mutated subunits will further clarify how these inter- and/or intrasubunit interactions modulate the gating behavior. Actually, during our detection with Kcv, the Bayley's group reported a similar hetero-channel approach that was successfully used to study the allosteric process in KcsA inactivation (Rotem et al., 2010).

Furthermore, by manipulating subunit composition, it is possible to construct protein channels with tunable functions for biosensing applications (Gu and Shim, 2010). As exemplified by the Leu70 mutants, we are able to stepwise regulate the conductance of the Kcv channel by using different mutants and adjusting the number of mutant subunits in the tetramer.

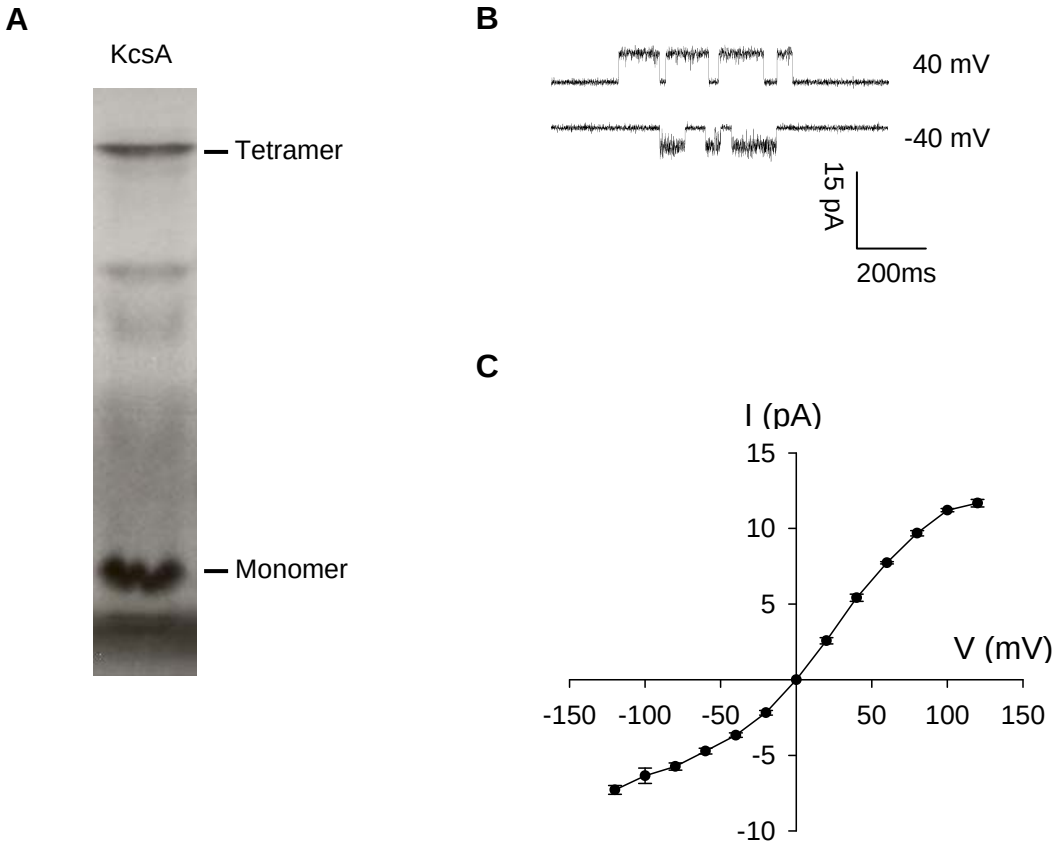

Figure 19. Single channel property of *in vitro* synthesized potassium channel KcsA. A. Electrophoretic separation of synthetized KcsA. The S^{35}-labeled protein KcsA was produced from coupled *in vitro*-transcription and translation (IVTT), run on a 12.5% SDS-polyacryamide gel for 8 hours, and visualized by autoradiograph. **B. Single channel currents of the KcsA tetramer purified from the SDS-PAGE gel.** All traces were recorded in symmetrical buffers containing 150 mM KCl and 10 mM Tris (pH 7.2). **C. I-V curve for the KcsA channel.**

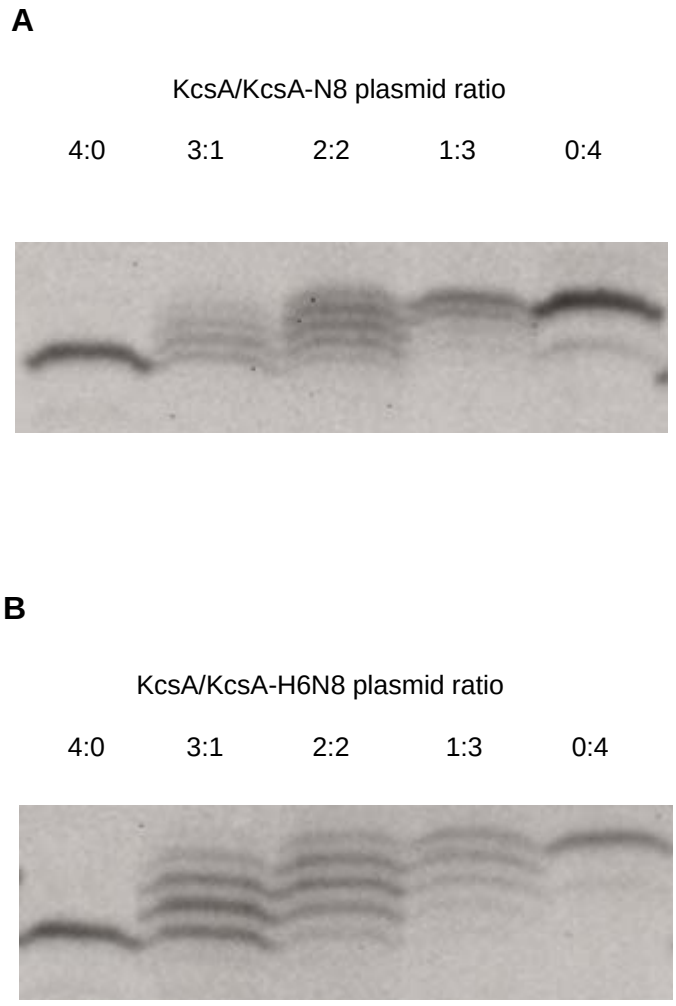

Figure 20. Electrophoretic separation of KcsA tetrameric channels. Tagged KcsA with N-terminus polypeptide extension containing NNNNNNNN (KcsA-N8) or HHHHHHNNNNNNNN (KcsA-H6N8) was co-assembled with untagged wild type KcsA at the indicated plasmid ratios. Homo- and heterotetrameic KcsA were run a 12.5% SDS-polyacrylamide gel for 8 hours. Longer extension in KcsA-H6N8 **(B)** leads to a better separation than shorter extension protein KcsA-N8 **(A)**.

CHAPTER 3

INHIBITION OF KCV CHANNEL BY TETRAETHYLAMONIUM (TEA)

3.1. Introduction

The quaternary ammonium ions (QAs) have been widely used for the study of the structure and function of potassium channels (French and Shoukimas, 1981; MacKinnon and Yellen, 1990; Choi et al., 1993). One of the most extensively used QAs is tetraethylamonium (TEA), a commonly used molecular probe in potassium channel blocking (Bretschneider et al., 1999; Andalib et al., 2004). It inhibits the potassium channel function by blocking the ion permeation pathway and occluding the potassium flow. The binding of TEA has been well studied through site-directed mutagenesis, X-ray crystallography and modeling studies. It can bind the potassium channel on the external or internal side of membrane with different properties. The external binding site is very selective to TEA, however, the internal binding site can bind many TEA derivates with even higher affinity than TEA (Meuser et al., 1999; Faraldo-Gómez et al., 2007). The external TEA binding exhibits much higher affinity than internal binding.

In this report, we examined the TEA block of Kcv, a virus potassium channel with high structural similarity to bacterium potassium channels. Sequence alignment of Kcv with KcsA indicates 42% aa similarity and 19% aa identity. The hypothetical model of Kcv shows high structural similarity with KcsA, especially in pore helix and selectivity

filter region (Gazzarrini et al., 2003). Here in vitro synthesized Kcv purified from SDS-PAGE gel was reconstituted into planar lipid bilayer and the TEA blockade at extracellular or intracellular side was investigated. Reduced apparent single channel amplitude upon addition of TEA from either side was observed in a voltage-dependent manor. Like KcsA, Kcv shows much higher TEA sensitivity when it is applied from extracellular side.

It has been well established the external blockade by TEA is strongly related to an aromatic residue Tyrosine near the extracellular entrance to the pore of the potassium channels (Y82 in KcsA and Y449 in Shaker), probably due to Π-cation interaction between TEA and aromatic side chain. For example, substitution of Tyr by Val, Ile, Ser and Thr at residue 449 in Shaker decresed the external TEA sensitivity significantly (Heginbotham and MacKinnon, 1992; Molina et al., 1997). Wild type KcsA is sensitive to external TEA blockade and the affinity of external TEA blockade is decreased in Y82T, Y82V and Y82C mutant channels (Meuser et al., 2001). In wild type Kcv, the residue at corresponding site 70 is Leucine. The substitution of Leucine at residue 70 by aromatic residue (Tyr, Phe), however, decreases the external TEA sensitivity. Higher sensitivity to external TEA block suggested a different mechanism other than Π-cation interaction in the presence of Leu. Consistent with previous studies, any other mutants at residue 70 decrease the external TEA sensitivity more significantly. Among these mutants, L70A exhibited more than 100 fold lower blocking efficiency of external TEA. In combination with the mass-tagging method, the hetero-tetrameric Kcv channels containing different number of L70A substitution were obtained and the contribution of each subunit to external TEA binding was investigated. The linear relationship between the free energy

of TEA binding and the number of the substitutions (zero, one, two, three and four) suggests that external TEA interacts simultaneously with the Leucine residue of the four subunits. Each subunit interacts with one ethyl group of TEA independently and contributes the binding free energy change equally.

3.2. Methods

3.2.1. Construction of the Kcv mutants

The Kcv mutants at residue L70 were constructed using QuikChange® Site-Directed Mutagenesis Kit (Stratagene 200519) as described earlier. Briefly, the PCR was performed as the following condition: 95^0C 30sec – (95^0C 30sec, 55^0C 1min, 68^0C 5min) x 16 cycles. 50 µl PCR product was digested with 1 µl DpnI (10 U/µL) at 37 $^{\circ}$C for 1 hour to digest the DNA template. The PCR product was then transformed into XL-1 blue supercompetent cells and the plasmids were extracted using QIAprep Spin Miniprep Kit (Qiagen 27104). Primers for gene construction of Kcv mutants were:

L70Y:

Forward: CCGTTGGTTTCGGTGATATC**TAT**CCAAAAACGACGGGC

Reverse: GCCCGTCGTTTTTGG**ATA**GATATCACCGAAACCAACGG

L70F:

Forward: CCGTTGGTTTCGGTGATATC**TTT**CCAAAAACGACG

Reverse: CGTCGTTTTTGG**AAA**GATATCACCGAAACCAACGG

L70W:

Forward: CCGTTGGTTTCGGTGATATC**TGG**CCAAAAACGACGGGC

Reverse: GCCCGTCGTTTTTGG**CCA**GATATCACCGAAACCAACGG

L70H:

Forward: CGTTGGTTTCGGTGATATC**CAT**CCAAAAACGACGGGCGCG

Reverse: CGCGCCCGTCGTTTTTGG**ATG**GATATCACCGAAACCAACG

L70A:

Forward: CGTTGGTTTCGGTGATATC**GCA**CCAAAAACGACGGGCG

Reverse: CGCCCGTCGTTTTTGG**TGC**GATATCACCGAAACCAACG

L70V:

Forward: TTGGTTTCGGTGATATC**GTA**CCAAAAACGACGGGC

Reverse: GCCCGTCGTTTTTGG**TAC**GATATCACCGAAACCAA

L70I:

Forward: TTGGTTTCGGTGATATC**ATA**CCAAAAACGACGGGC

Reverse: GCCCGTCGTTTTTGG**TAT**GATATCACCGAAACCAA

L70M:

Forward: GTTGGTTTCGGTGATATC**ATG**CCAAAAACGACGGGCGC

Reverse: GCGCCCGTCGTTTTTGG**CAT**GATATCACCGAAACCAAC

L70T:

Forward: CGTTGGTTTCGGTGATATC**ACA**CCAAAAACGACGGGCG

Reverse: CGCCCGTCGTTTTTGG**TGT**GATATCACCGAAACCAACG

L70S:

Forward: CCGTTGGTTTCGGTGATATC**TCA**CCAAAAACGACGG

Reverse: CCGTCGTTTTTGG**TGA**GATATCACCGAAACCAACGG

L70C:

Forward: CCGTTGGTTTCGGTGATATC**TGC**CCAAAAACGACGGGC

Reverse: GCCCGTCGTTTTTGG**GCA**GATATCACCGAAACCAACGG

L70K:

Forward: CGTTGGTTTCGGTGATATC**AAA**CCAAAAACGACGGGCG

Reverse: CGCCCGTCGTTTTTGG**TTT**GATATCACCGAAACCAACG

L70E:

Forward: CGTTGGTTTCGGTGATATC**GAA**CCAAAAACGACGGGCG

Reverse: CGCCCGTCGTTTTTGG**TTC**GATATCACCGAAACCAACG

3.2.2. Synthesis and purification of Kcv proteins

S^{35}-labeled Kcv proteins were synthesized from coupled *in vitro* transcription and translation (IVTT) in *E. coli* T7 S30 Extract System for circular DNA (L1130, Promega). To get the hetero-tetramer, the 4ul of template with various ration of tagged DNA to untagged DNA (4:0, 3:1, 2:2, 1:3, 0:4) was added. The IVTT mix was incubated at 37 C for 1 hour. The radio-labeled tetrameric Kcv proteins were resolved in 12.5% SDS polyacrylamide gel and purified from the dried gel. The purified Kcv channel proteins were aliquoted and stored at -20^0C.

3.2.3. Single channel recording on lipid bilayer

The apparatus and method for single channel recording has been described earlier. Briefly, the lipid bilayer was formed with 1,2-diphytanoylsn-glycerophosphatidylcholine

(Avanti Polar Lipids) by merging two lipid monolayers over a ~100 μm wide aperture in a 25 μm thick Teflon film that partitions the *cis* and *trans* chambers. The Kcv protein purified from the gel was added to the *cis* chamber. The voltage was applied from the *trans* chamber and the *cis* chamber was grounded. The recording solutions in both *trans* and *cis* side containing 150mM KCl, 10mM Tris.Cl, pH = 7.2. Electrophysiology data were collected with an Axopatch 200B patch clamp amplifier (Molecular Device Inc.). The current signal was filtered at 1 kHz with a low-pass Bessel filter, and acquired at a sampling rate of 20 kHz.

3.2.4. Data analysis

Kcv channel inhibition by TEA was measured at different concentration of TEA. The inhibition constant IC_{50} values were then calculated by fitting the dose-response data with single-component Langmuir equation:

$$\text{Fraction blocked} = 1 - I/I_0 = [TEA]/([TEA] + IC_{50}) \qquad (2)$$

In this equation, I_0 is the control current when TEA is not applied.

The voltage dependence of TEA block was assessed through the Woodhull equation:

$$IC_{50}(V) = IC_{50}(0) \exp(\delta VzF/RT) \qquad (3)$$

Where δ is the electrical distance and F, R and T are thermodynamic constant.

3.3. Results

3.3.1. Inhibition of Kcv channel by TEA

For structure-function study of ion channel, it is very important to know its orientation in the membrane under study. When studied in the cells, the transmembrane orientation of ion channels is apparent. However, transmembrane orientation of channel needs to be experimentally established when an ion channel is investigated as a purified protein reconstituted into an artificial planar lipid bilayer (Fig. 21). For example, by using the asymmetric channel blocker (i.e. Na+, TEA and charybdotoxin), extracellular side of KcsA was demonstrated to face the *cis* side when it is added to the *cis* chamber which is grounded in the planar lipid bilayer system (Heginbotham et al., 1999). Due to its high structural similarity with KcsA, Kcv may also adopt the same orientation in the similar planar lipid bilayer system.

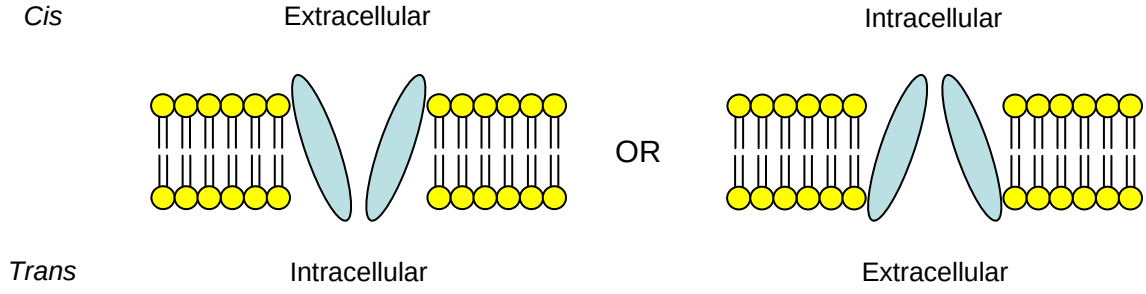

Figure 21. Orientations of a purified ion channel in artificial lipid bilayer.

3.3.1.1. Inhibition of Kcv channel by TEA from the *cis* or *trans* side

In this study, we first examined the block of Kcv by TEA at *trans* or *cis* side. *In vitro* synthesized tetrameric Kcv channel was resolved in SDS-polyacrylamide electrophoresis.

Purified Kcv channels from gel were reconstituted into planar lipid bilayer, both sides of which contain 150mM KCl, 10mM Tris.Cl pH 7.2. After channel formation, TEA was applied to *trans* or *cis* side and the ion current was monitored at different voltages (-100mV to 100mV). Decrease current amplitude was observed when TEA was applied from either side. Due to the rapid kinetics of TEA block, the fast current fluctuation can not be resolved by the recording electronics. Consequently, TEA reduces the Kcv apparent single channel current amplitude (Fig. 22). The current decreased in a TEA concentration dependent manner from either *cis* or *trans* side (Fig. 23, 24, 25). By using equation 2 (Methods), the inhibition curve was fitted to obtain the inhibition constant IC_{50}, which represents the inhibition potency. For *cis* TEA, the IC_{50} values were 0.41mM at +60mV and 0.10mM at -60mV. For *trans* TEA, the IC_{50} values were 12.71mM at +60mV and 47.32mM at -60mV (Fig. 26). The observed higher sensitivity of Kcv to *cis* side applied TEA (Fig. 27), a well known strong external potassium channel blocker, suggested that extracellular side of Kcv face the *cis* side and intracellular face *trans* side in planar lipid bilayer.

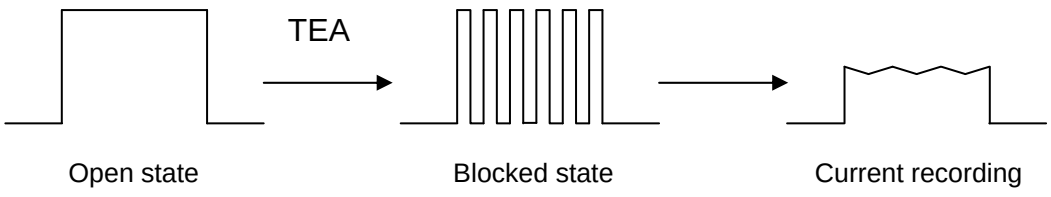

Figure 22. Reduced apparent current amplitude in the presence of TEA. Due to the rapid kinetics TEA block, the open-close flicking can not be fully resolved the electrophysiology instrument. Accordingly, average current amplitude is reduced in accompany with higher flicking-like current noise.

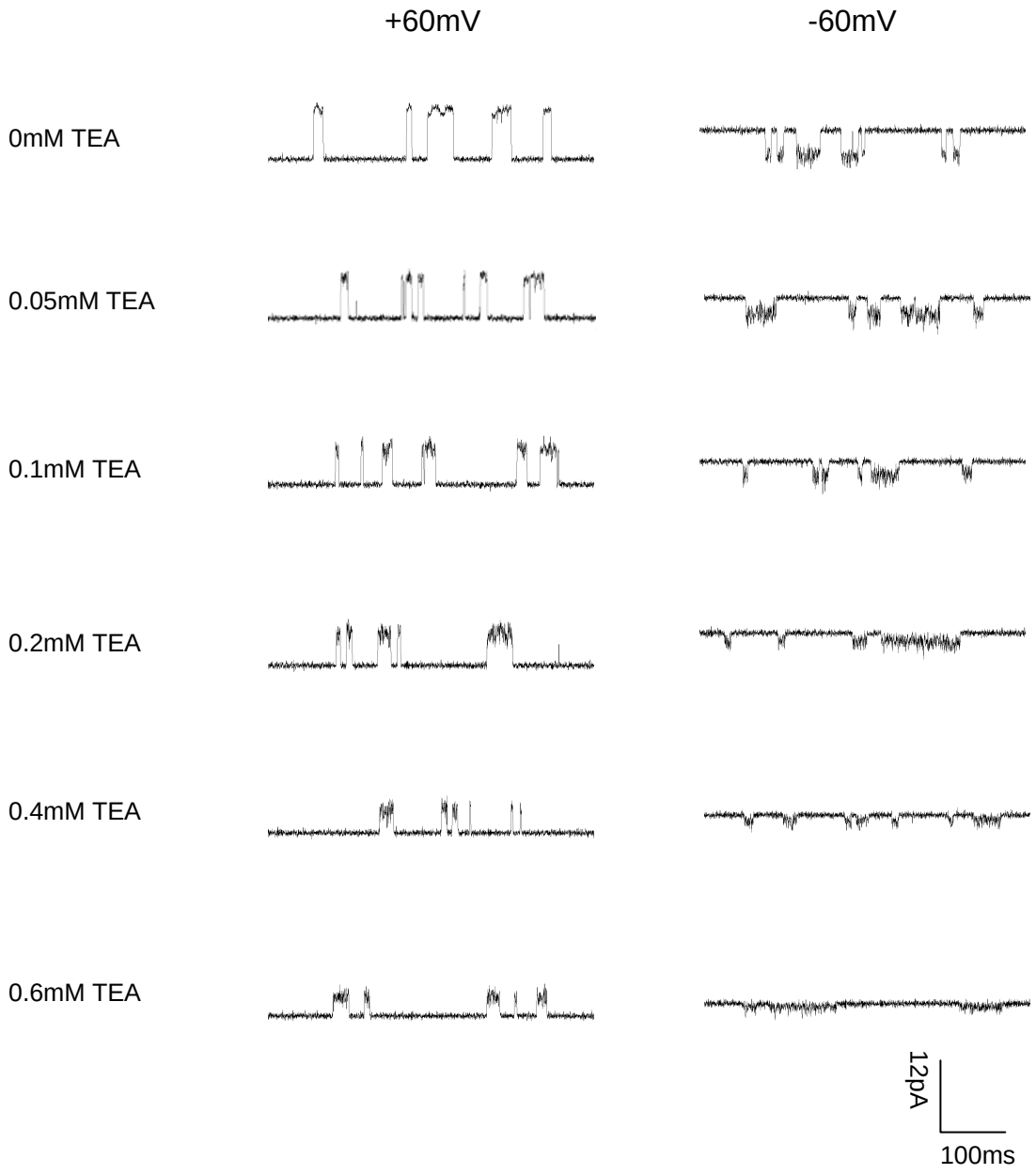

Figure 23. Inhibition of Kcv by *cis* TEA. Gel purified Kcv channel was reconstituted on a DPhPC lipid bilayer. Single channel currents were recorded at -100mV to 100mV in 150mM KCl symmetric solution with indicated TEA concentration added to the *cis* side of the channel. Representative currents recorded at +60mV and -60mV are shown.

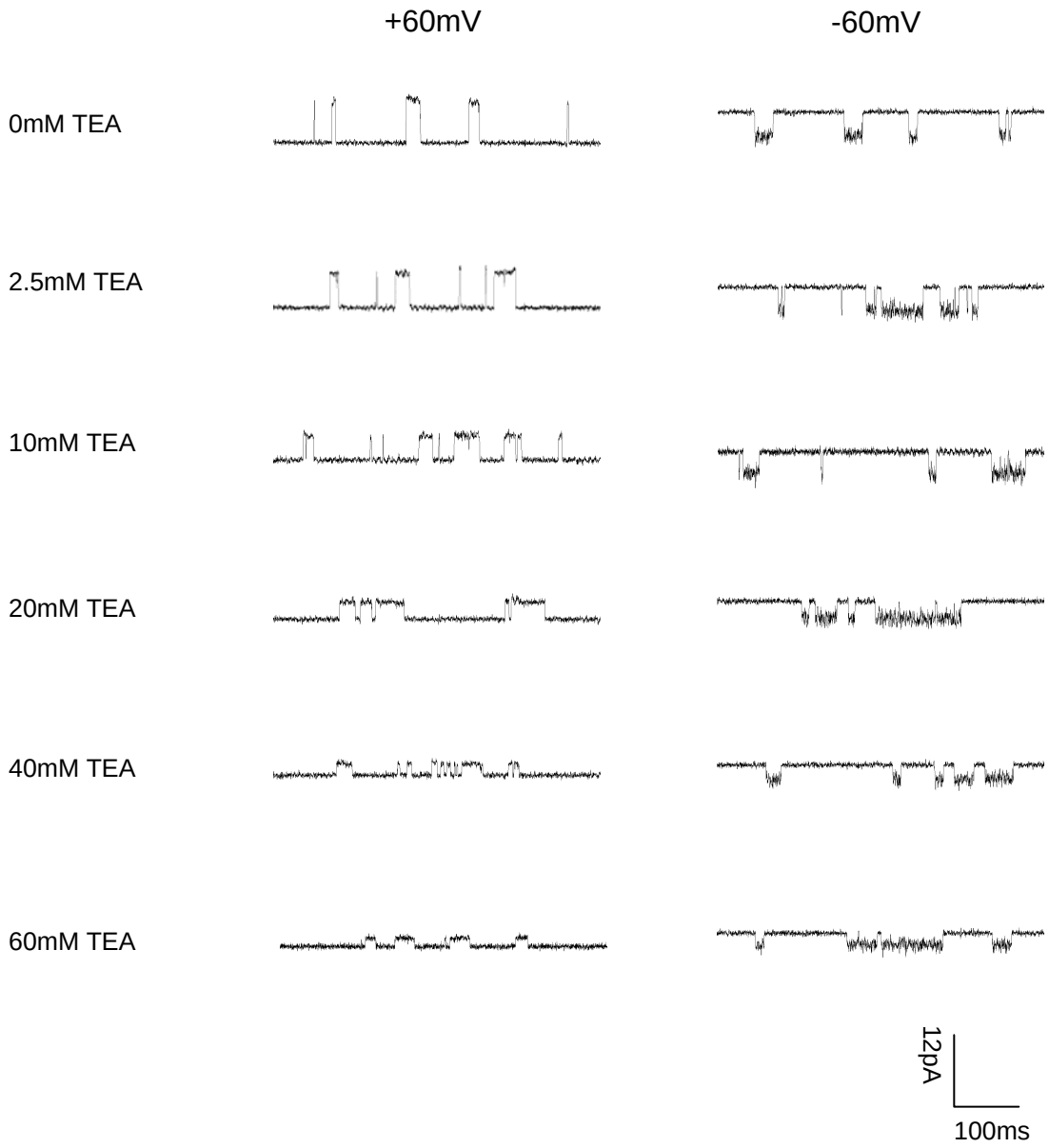

Figure 24. Inhibition of Kcv by *trans* TEA. Single channel currents of Kcv were recorded at -100mV to 100mV with indicated TEA concentration added to the *trans* side of the channel. All traces were recorded in 150mM KCl symmetric solution. Representative currents recorded at +60mV and -60mV are shown.

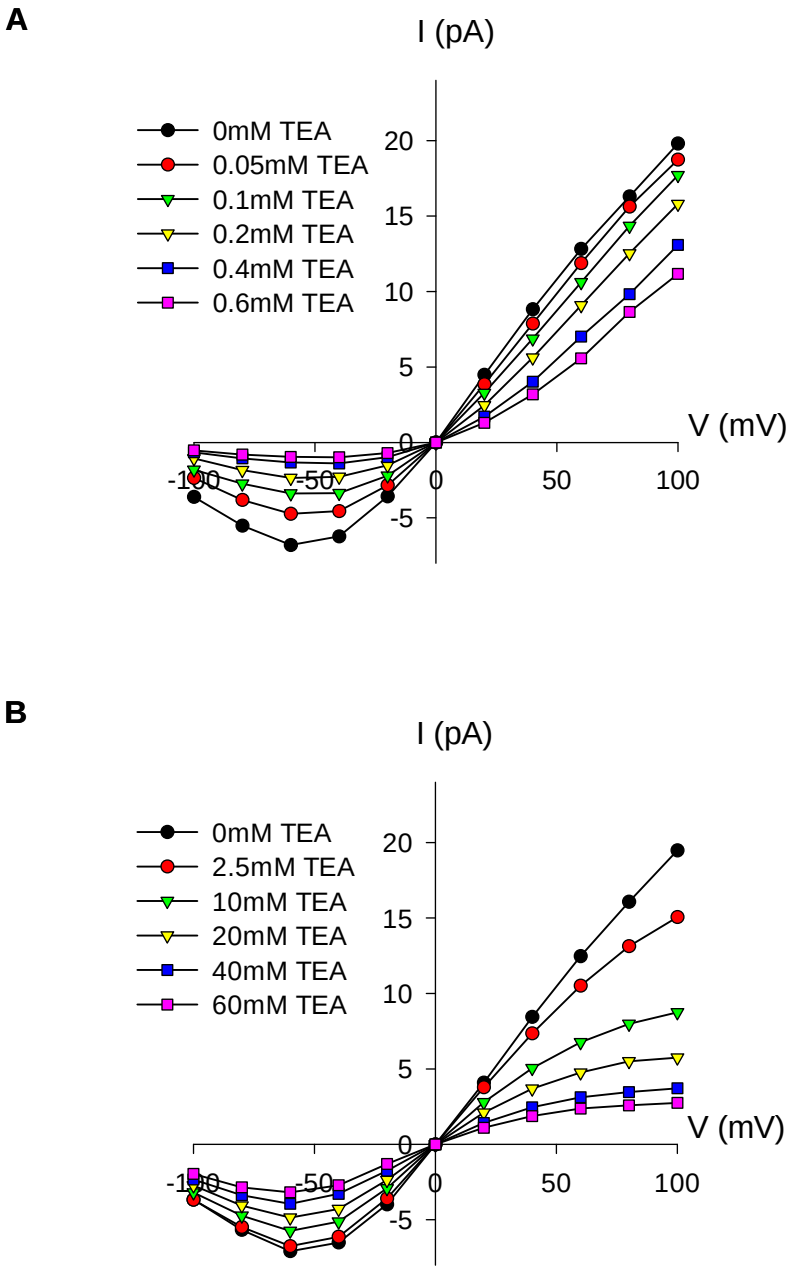

Figure 25. Kcv conductance inhibition by *cis* or *trans* applied TEA. The indicated amount of TEA was applied from *cis* **(A)** or *trans* side **(B)**. The Kcv channel inhibition by TEA from either side is dose-dependent from -100mV to 100mV.

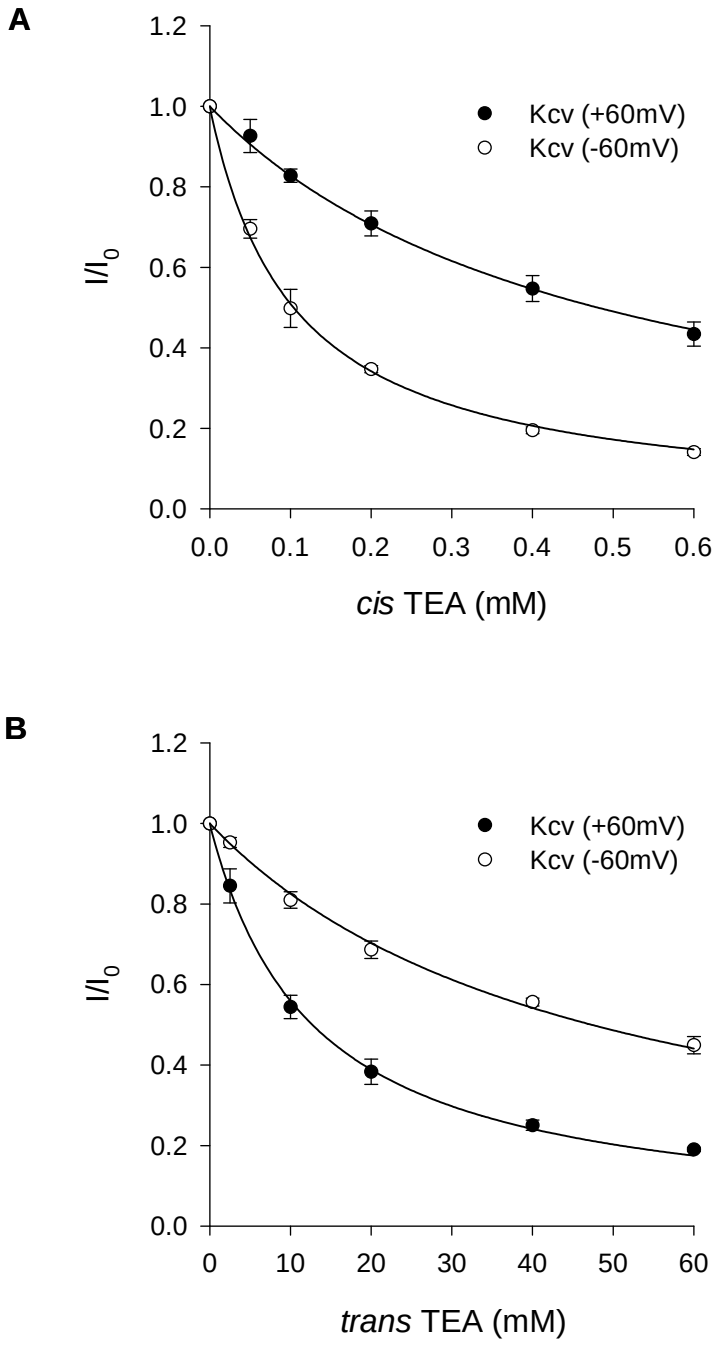

Figure 26. Dose response of Kcv inhibition by *cis* or *trans* TEA. The inhibition constants IC_{50} were calculated by fitting the inhibition curves with Langmuir equation. IC_{50} values are 0.41mM and 0.10mM for *cis* TEA inhibition at +60mV and -60mV, respectively **(A)**. For *trans* TEA inhibition, IC_{50} values are 12.71mM and 47.32mM at +60mV and -60mV, respectively **(B)**.

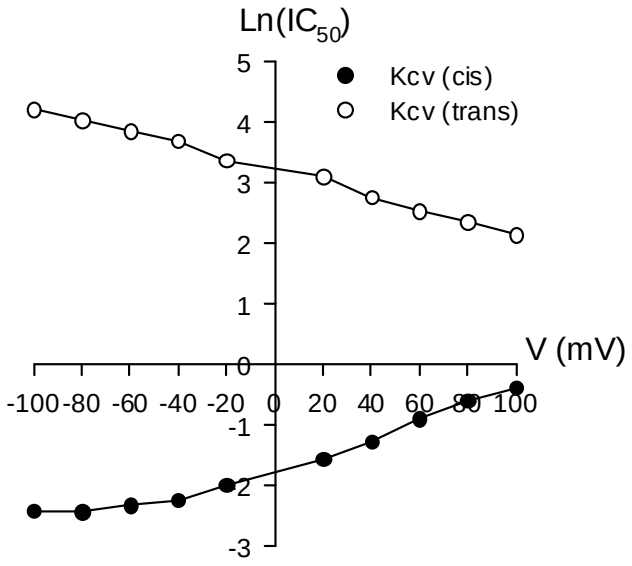

Figure 27. Inhibition of Kcv by *cis* or *trans* applied TEA. The IC50 values were obtained from dose-response data in Figure 25. Kcv shows much higher sensitivity to cis applied TEA at voltages from +100mV to -100 mV.

3.3.1.2. Inhibition of Kcv mutants (L70Y and L70A) by *cis*/*trans* TEA

To further verify the orientation of Kcv in lipid bilayer, the TEA block of Kcv from *cis* or *trans* side was tested upon substitution of Leu70 (corresponding site of Tyr82 in KcsA) by Tyr. Similarly, apparent current amplitude was decreased upon addition of TEA from either side. The IC_{50} values for *cis* TEA were 2.01mM at +60mV and 0.86mM at -60mV. In contrast, the IC_{50} values for *trans* TEA were 19.89mM at +60mV and 74.87mM at -60mV. Like Kcv, Kcv-L70Y also showed higher TEA block when TEA was applied from *cis* side (Fig. 28).

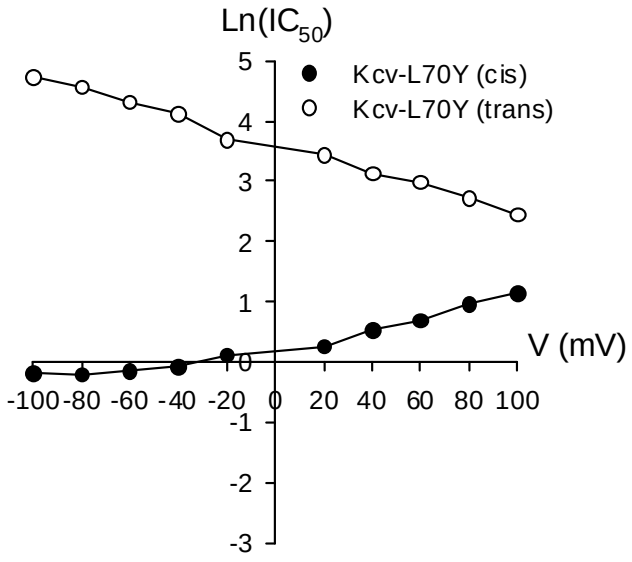

Figure 28. Inhibition of Kcv-L70Y by *cis* or *trans* applied TEA. Like wild type Kcv, substitution of Leu70 in Kcv (equivalent site of Tyr 82 in KcsA) by Tyr also shows much stronger inhibition by *cis* applied TEA at voltages from +100mV to -100 mV.

It has been well established that the key residue Tyr82 in KcsA contributes the high external TEA sensitivity and the substitutions at this site alter the external TEA block significantly. Here, we tested the effects of the substitution at equivalent site Leu70 in Kcv on TEA block. We found that the substitution (L70A) decreased the TEA block drastically from the cis side (IC_{50} = 71.81mM at 60mV, see described below). However, no significant difference for TEA block of Kcv from the *trans* side was observed (Wild type, IC_{50} = 12.71mM; L70Y, IC_{50} =19.89mM; L70A, IC_{50} = 15.08mM at 60mV) (Fig. 29). This result also argues that extracellular side of Kcv face the *cis* side when studied in our lipid bilayer system.

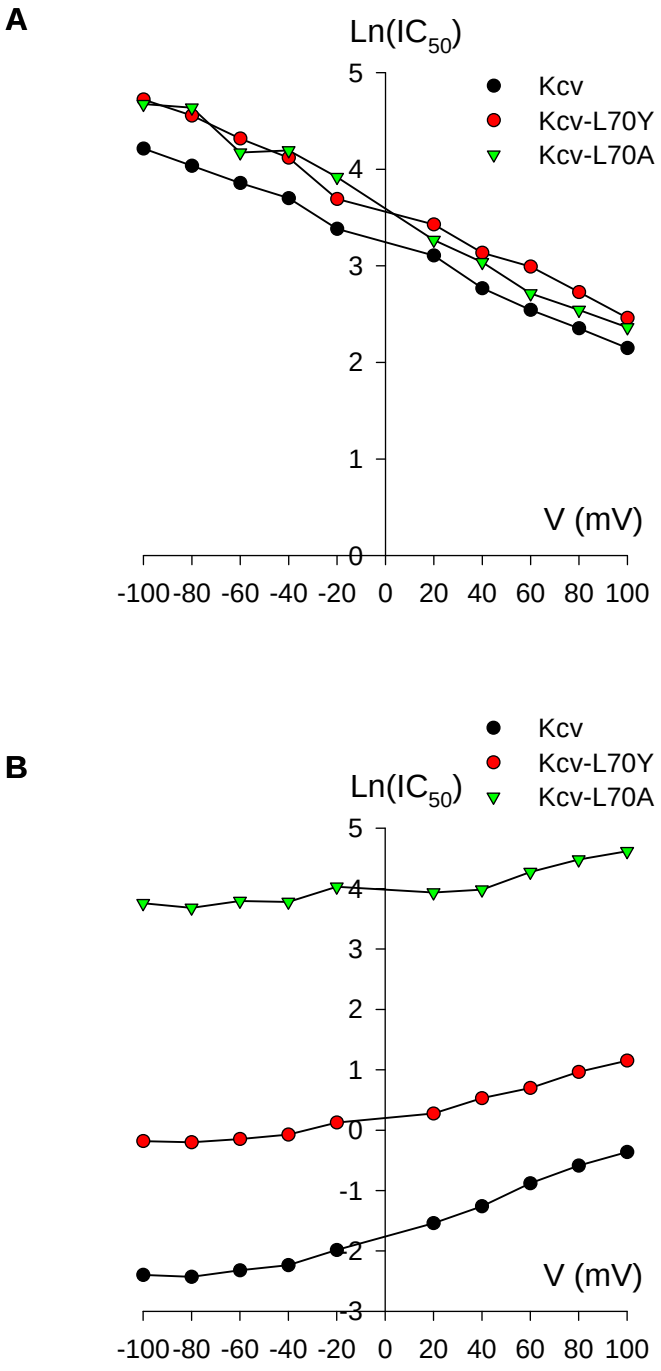

Figure 29. Effect of mutation at Leu70 on TEA inhibition from *cis* or *trans* side. Three types Kcv channel show similar sensitivity to *trans* applied TEA **(A)**. In contrast, significant TEA sensitivity difference among three types of Kcv channel is shown when TEA is applied from *cis* side **(B)**.

Our findings demonstrate that Kcv channel shows much higher sensitivity to TEA applied from external (*cis*) side. Several more mutants at Leu70 corresponding to external TEA binding site Tyr 82 in KcsA were further constructed to explore the effect of the substitutions of Leu70 by different type of amino acids on external TEA inhibition (Section 3.3.2). By using the hetero-channels, the contribution of each subunit in a tetrameric Kcv channel to external TEA binding was also investigated (Section 3.3.3).

3.3.2. Altered sensitivity of mutant channels to external TEA block

3.3.2.1. K^+ conductance of mutant channels

Previous studies suggest that a single aromatic residue Tyr/Phe (82 in KcsA or 449 in *Shaker)* confer high external TEA block. Here a series of mutants at residue Leu70 in Kcv, which corresponds to Tyr 82 in KcsA, were generated by site-directed mutagenesis for the study of external TEA block. All the mutants can form the SDS-stable tetrameric channels and show different ion conductance at negative voltage, thus affect the rectifying properties of Kcv channel (Fig. 30). Substitution by aromatic residues (Tyr, Phe, or Trp) and Cys increase the current amplitude dramatically at negative voltages. Notably, the positive charged lysine substitution shows no conductance at negative voltage and significant decrease of conductance at positive voltages. This is perhaps due to the reduction of net negative surface charge near the extracellular entryway. All other substitutions including negative charged Glu show a modest increase of current magnitude at negative voltages.

A

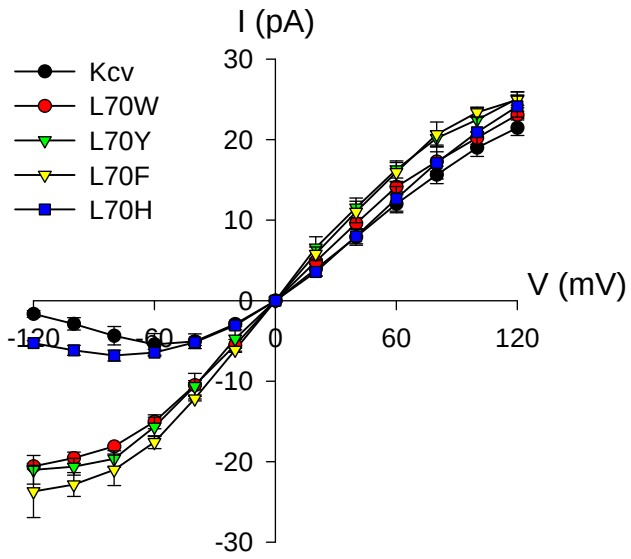
I (pA)
Kcv
L70W
L70Y
L70F
L70H
30
20
10
0
-10
-20
-30
V (mV)
-120
-60
0
60
120

B

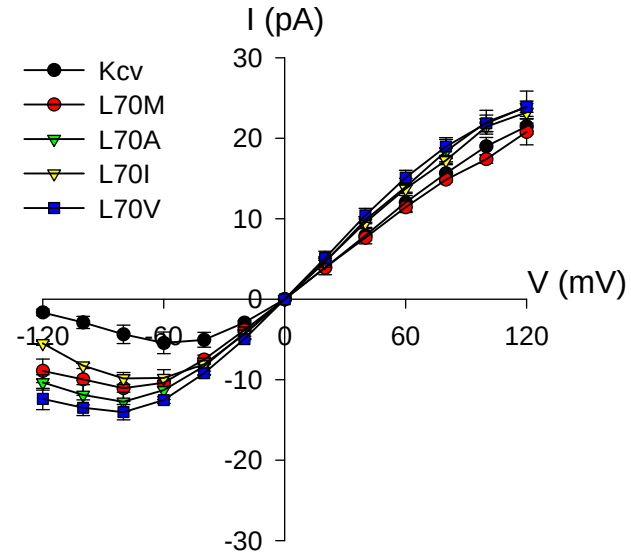
I (pA)
Kcv
L70M
L70A
L70I
L70V
30
20
10
0
-10
-20
-30
V (mV)
-120
-60
0
60
120

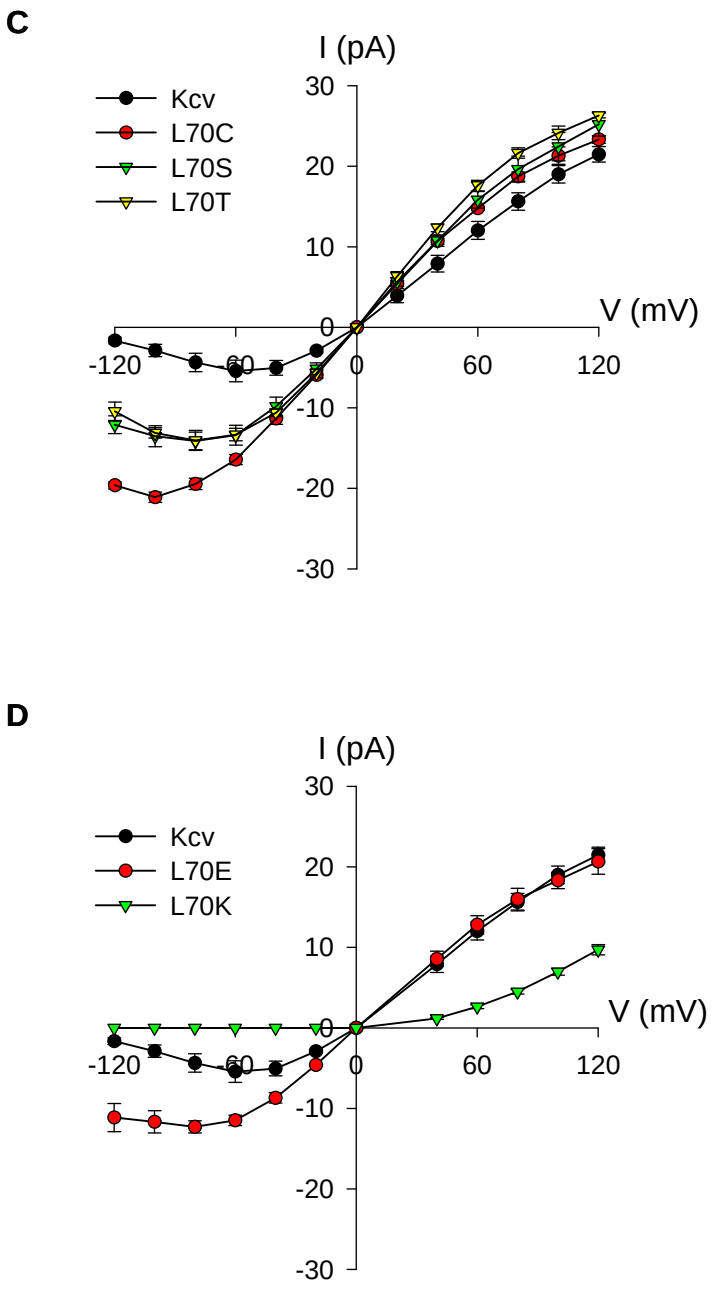

Figure 30. Current-voltage relations of Kcv and its mutants. The data was obtained from single channel currents recorded in symmetrical solutions containing 150 mM KCl. Mutants L70Y, L70F, L70W and L70C demonstrated a significant increase for negative current **(A** and **C)**. Notably, L70K shows no conductance at negative voltage and significant decrease of conductance at positive voltages **(D)**. All other mutants show moderate increase for negative current. **(B**,**C** and **D)**.

The varying conductance with different amino acid type at residue 70 may be due to a fast gating mechanism, which was proposed to interpret the decayed apparent current at negative voltages. It has been suggested that the voltage-dependent fast gating in MaxiK channel are modulated by ion occupying in selectivity filter (Schroeder and Hansen, 2007). At high voltage, K^+ ions are pulled out of the filter more rapidly than K^+ can be supplemented from solution. Since the selectivity filter has been shown to be involved in channel gating and this process is sensitive to the ion occupancy in filter (Bernèche and Roux, 2005), the K^+ depletion in selectivity filter can influence the fast gating pattern, consequently alter the apparent currents. In Kcv, the residue 70 near the outer vestibule of Kcv may regulate the K^+ entry from extracellular side, especially at high negative voltages, thereby modulate the fast gating in a same mechanism. Indeed, we found that high concentration of K^+ (1M KCl) in either extracellular or intracellular side increased the apparent conductance and decreased the flickering noise at the same driving forces. This observation confirms that the ion depletion mechanism which accounts for the fast gating behavior at high voltages in Kcv.

3.3.2.2. Inhibition of Kcv mutants by external TEA

Although wild type Kcv has high sensitivity to external block, we expect that the substitution of Leu 70, by aromatic residue (Tyr/Phe) will enhance the sensitivity. However, our data shows that these substitutions lead to a decrease of external TEA sensitivity. The IC_{50} values for L70Y and L70F are 1.87mM and 2.01mM at 60mV, respectively. Presence of His at residue 70 shows similar external TEA sensitivity (IC_{50}= 3.57mM at 60mV), probably due to its aromatic properties of side chain. Other Kcv mutants demonstrate more significant decrease of external TEA sensitivity. IC_{50} values(mM) at 60mV for Kcv and its mutants are increased in the following order： L70 (0.48)< L70C(11.65) <L70I(18.51) ≈L70M(19.58) ≈L70S(20.85) ≈L70W(22.36)< L70V(31.60)<L70T(41.11)<L70A(71.81) (Table 4). Substitution of Leu70 by charged amino acids (L70K and L70E) showed no external TEA sensitivity at all.

The block of Kcv channels by external TEA was measured at different voltages (-100mV to +100mV). According to Woodhull model, the relative electric distance (б) was calculated by fitting the curve with equation 3 (Methods) (Fig. 31). Kcv and its mutants showed varying degree of voltage dependence. For outward current at positive voltage, the apparent relative electric distances were distributed from 16% to 35%. WT-Kcv (L70) and L70W show highest б values (35% and 34%) and L70H, L70S, L70I, L70M, and L70A show lower б values (16%, 21%, 21%, 22% and 22% respectively). For the inward current at negative voltage, lower б values (from 15% to ~0%) were shown (Table 4). No correlation was observed between relative electric distance and external TEA sensitivity.

Table 4. Block of Kcv and its mutants by external TEA

	IC_{50} (mM) at +60mV	IC_{50} (mM) at -60mV	δ at positive voltage	δ at negative voltage
Kcv	0.41	0.10	36%	12%
Aromatic				
Kcv-L70Y	2.01	0.86	26%	9%
Kcv-L70F	1.87	0.74	29%	6%
Kcv-L70W	22.36	8.55	34%	9%
Kcv-L70H	3.57	3.30	16%	0%
Nonpolar				
Kcv-L70A	71.81	44.50	22%	8%
Kcv-L70V	31.60	17.07	25%	9%
Kcv-L70M	19.68	6.80	22%	15%
Kcv-L70I	18.51	9.76	21%	6%
Polar				
Kcv-L70T	41.11	22.83	29%	12%
Kcv-L70S	20.85	14.48	21%	0%
Kcv-L70C	11.65	4.88	25%	6%
Charged				
Kcv-L70K	ns	nd	nd	nd
Kcv-L70E	ns	79.28	nd	nd

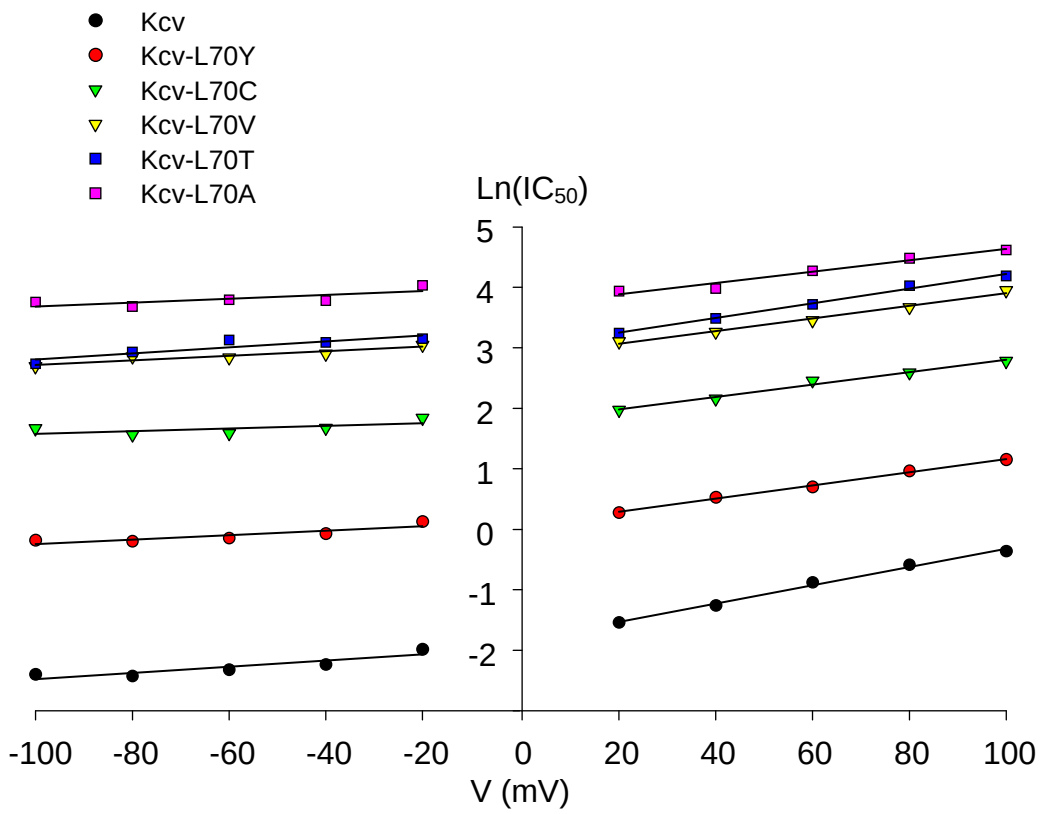

Figure 31. Voltage dependence of the external TEA block. The $Ln(IC_{50})$ of external TEA block is shown as a function of applied voltage. The relative electrical distances (δ) were calculated by fitting the curve with Woodhull equation.

3.3.3. External TEA binding energy additivity

3.3.3.1. Affinities of external TEA binding to Kcv/Kcv-L70A tetramers

The observation that substitution of residue 70 in Kcv leads to significant decrease of external TEA block raises the following question. How is the TEA affinity affected by different number of substitutions in a tetrameric Kcv channel? To address this question, hetero-tetrameric Kcv with one, two or three substitutions was obtained by mass-tagging

method. As described before, the tagged Kcv (N8-Kcv) can not only allow for separation and purification of heteromeric Kcv channels, but also retain the same channel functions such as ion conductance and selectivity. More importantly, attachment of eight neutral amino acids to N-terminus doesn't change the external TEA sensitivity of N8-Kcv channel (IC_{50}=0.38mM at 60mV and 0.11mM at -60mV). So we use N8-Kcv as a "wild-type background" protein to produce the hetero-tetrameric Kcv channels containing different number of mutated subunits. By co-expression of N8-Kcv and Kcv-L70A, which most affect the external TEA block, the hetero-tetrameric Kcvs with different number of Leu and Ala at position 70 (A_1L_3, A_2L_2 and A_3L_1) were synthesized and resolved by SDS-polyacrylamide gel electrophoresis (Fig. 32).

External TEA block of each category of gel purified N8/L70A Kcv tetramer was tested in 150mM KCl symmetric solution at +60mV and -60mV. And the inhibition constant IC_{50} was calculated by fitting the dose-response data with equation 2 (Fig. 33). The N8-Kcv(L4) and Kcv-L70A(A_4) reveals significant difference in external TEA sensitivity (IC_{50}= 0.38mM and 72mM at 60mV for N8-Kcv(L4), 0.11mM and 45mM at -60mV for L70A(A_4)). The hetero-tetrameric Kcv channels L_3A_1, L_2A_2 and L_1A_3 shows IC_{50} (mM) of 1.16, 3.99, and 13.92 at +60mV, 0.33, 1.32, 8.47 at -60mV (Table 5). Here we use IC_{50} as the apparent disassociation constant K*d*. By using the following equation, free energy of TEA binding to each type of tetrameric Kcv channel was calculated.

$$\Delta G_i^o = RT\ (\ln Kd_i) \qquad (4)$$

In this expression, i is the number of Ala at position 70 (i=0, 1, 2, 3, 4) and R, T is the thermal constant. Fig. 34 demonstrates a linear relationship between the TEA binding

energy and the number of Ala at residue 70. Fig. 35 shows the single channel currents recorded at the TEA concentration close to IC_{50} of each N8/L70A tetramer.

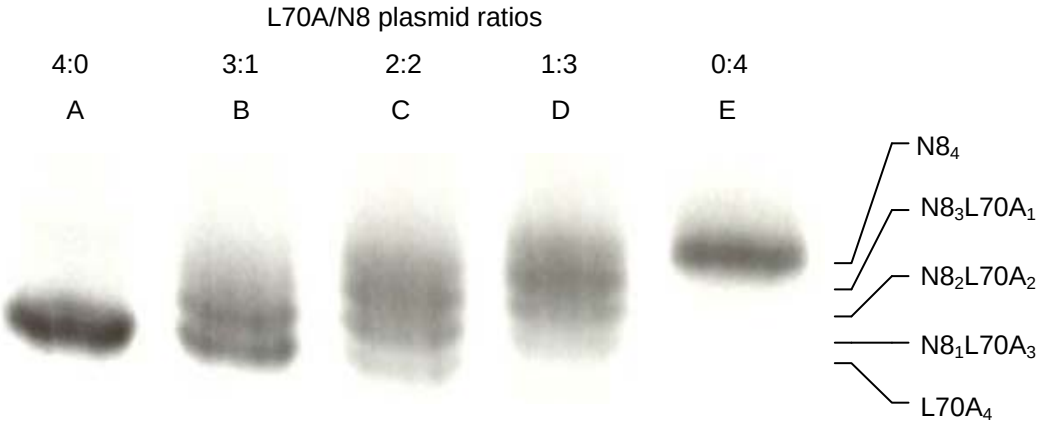

Figure 32. Electrophoretic separation of N8/L70A tetramers. The synthesized S^{35}-labeled proteins were run on a 12.5% SDS-polyacryamide gel for 16 hours. Lane A through E were tetramers formed at L70A/N8 plasmid ratios of 4:0, 3:1, 2:2, 1:3 and 0:4. The five bands identified represent all possible subunit combinations, $L70A_{4-n}N8_n$ (n = 0, 1, 2, 3 and 4 is the number N8 in the tetramer).

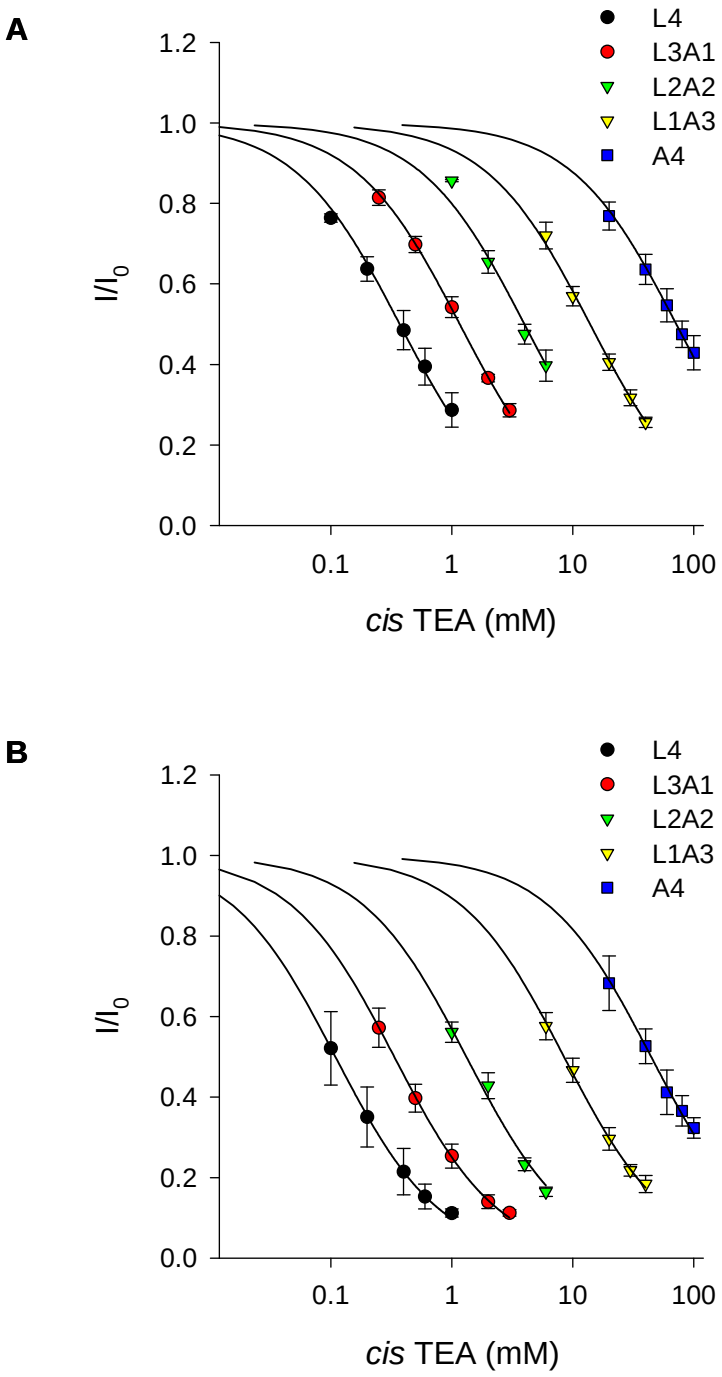

Figure 33. External TEA inhibition of N8/L70A tetramers. Normalized current (I/I_0) is plotted as a function of semi-logarithmic TEA concentration. IC_{50} of each type of Kcv tetramer (L4, L3A1, L2A2, L1A3 and A4) at +60mV (**A**) or -60mV (**B**) was obtained from the inhibition curve.

Table 5. External TEA sensitivities of N8/L70A tetramers

	IC_{50} (mM) at +60mV	IC_{50} (mM) at -60mV
WT_4 (L_4)	0.38	0.11
WT_3L70A_1 (L_3A_1)	1.16	0.34
WT_2L70A_2 (L_2A_2)	3.99	1.32
WT_1L70A_3 (L_1A_3)	13.92	8.48
$L70A_4$ (A_4)	71.81	44.51

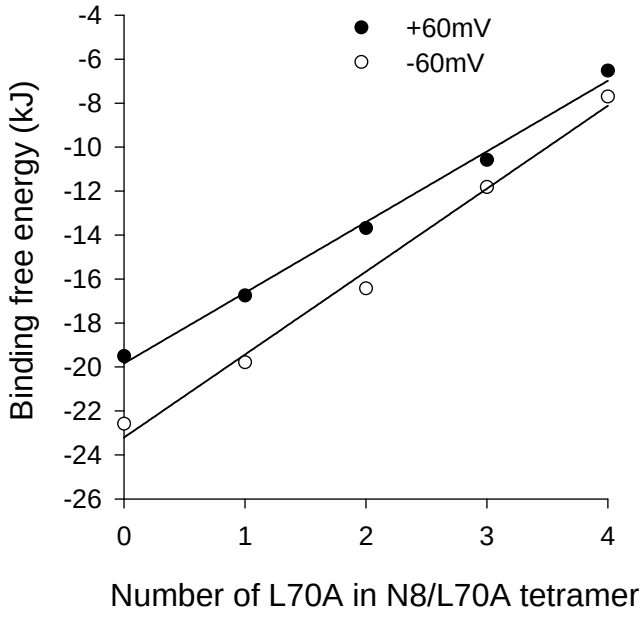

Figure 34. Dependence of external TEA binding on the number of L70A in N8/L70A tetramer. The TEA binding free energy for each N8/L70A tetramer was deduced from IC_{50} (Table 5) by using equation 4. The linear relationship between binding energy and number of mutated subunit L70A suggests that four subunits in a tetrameric Kcv channel interact simultaneously with a TEA molecule.

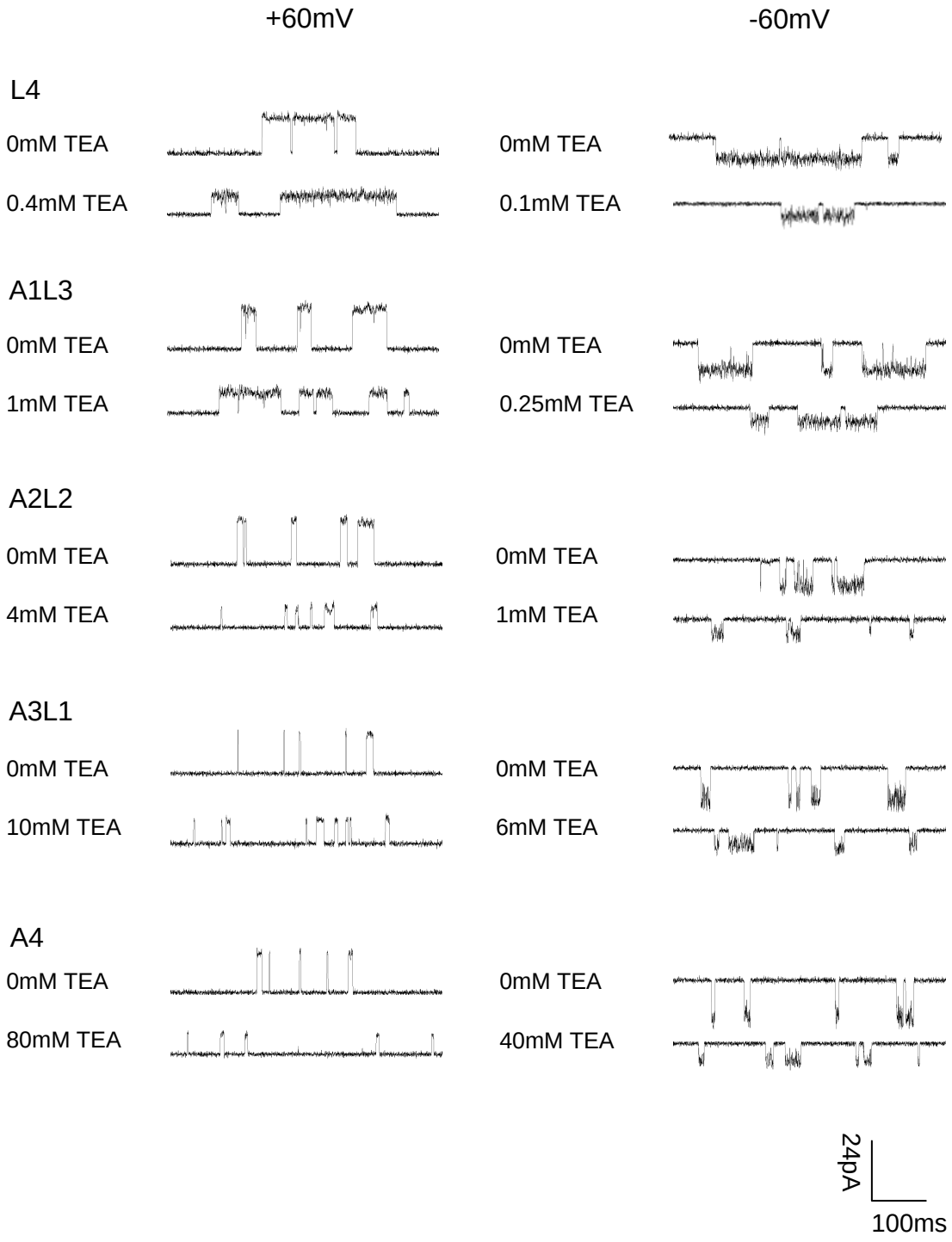

Figure 35. Current recording of external TEA block for N8/L70A tetramers. The indicated TEA concentration is close to IC50 value (Table 5).

3.3.3.2. Affinities of external TEA binding to Kcv-L70Y/Kcv-L70A tetramers

In KcsA, the residue 82 is Tyrosine. After introducing a Tyrosine at corresponding site 70 in Kcv, IC_{50} for external TEA block is 2.01mM at +60mV and 0.86mM at -60mV in 150mM KCl solution. Single channel study of KcsA reveal similar external TEA block (IC_{50}=2.2mM at +60mV and 1.56mM at -60mV) in 100mM KCl buffer. Due to the similarity in structure and external TEA sensitivity, Kcv-L70Y may be used as a relevant ion channels to provide more insights on TEA interaction with KcsA. This tagged Kcv (N8-L70Y) showed the same external TEA sensitivity (IC_{50}=2.06mM at 60mV and 0.83mM at -60mV) as untagged Kcv-L70Y. Co-assembly of N8-L70Y and L70A produced hetero-channels revealed by SDS-PAGE (Fig. 36). The heteromeric Kcv Y_3A_1, Y_2A_2 and Y_1A_3 shows IC_{50} (mM) of 3.44, 9.07, and 21.87 at +60mV, 1.78, 5.87, 15.8 at -60mV (Table 6, Fig. 37). Again, the linear relationship between the TEA binding energy and the number of L70A substitution was observed (Fig. 38). Fig. 39 shows the currents recorded at the TEA concentration close to IC_{50} of each N8/L70A tetramer.

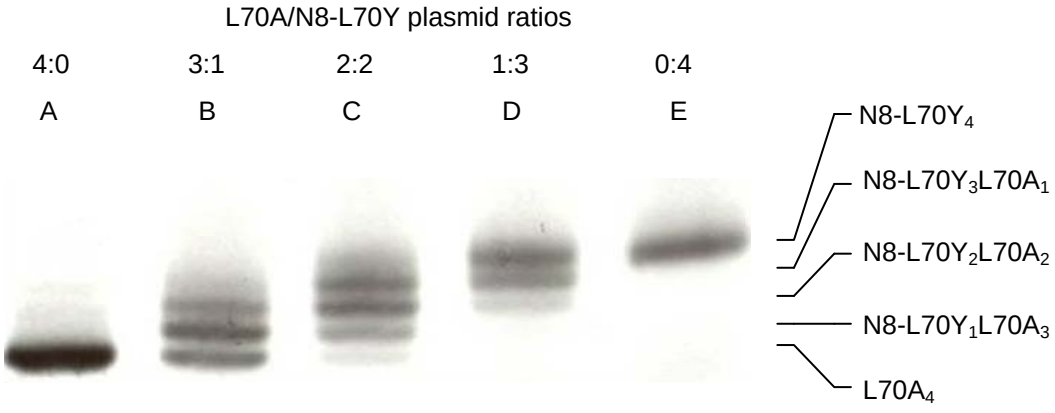

Figure 36. Electrophoretic separation of N8-L70Y/L70A tetramers. The synthesized S^{35}-labeled proteins were run on a 12.5% SDS-polyacrylamide gel for 16 hours. The five bands represent all possible subunit combinations, $L70A_{4-n}N8\text{-}L70Y_n$ (n = 0, 1, 2, 3 and 4 is the number N8-L70Y in the tetramer).

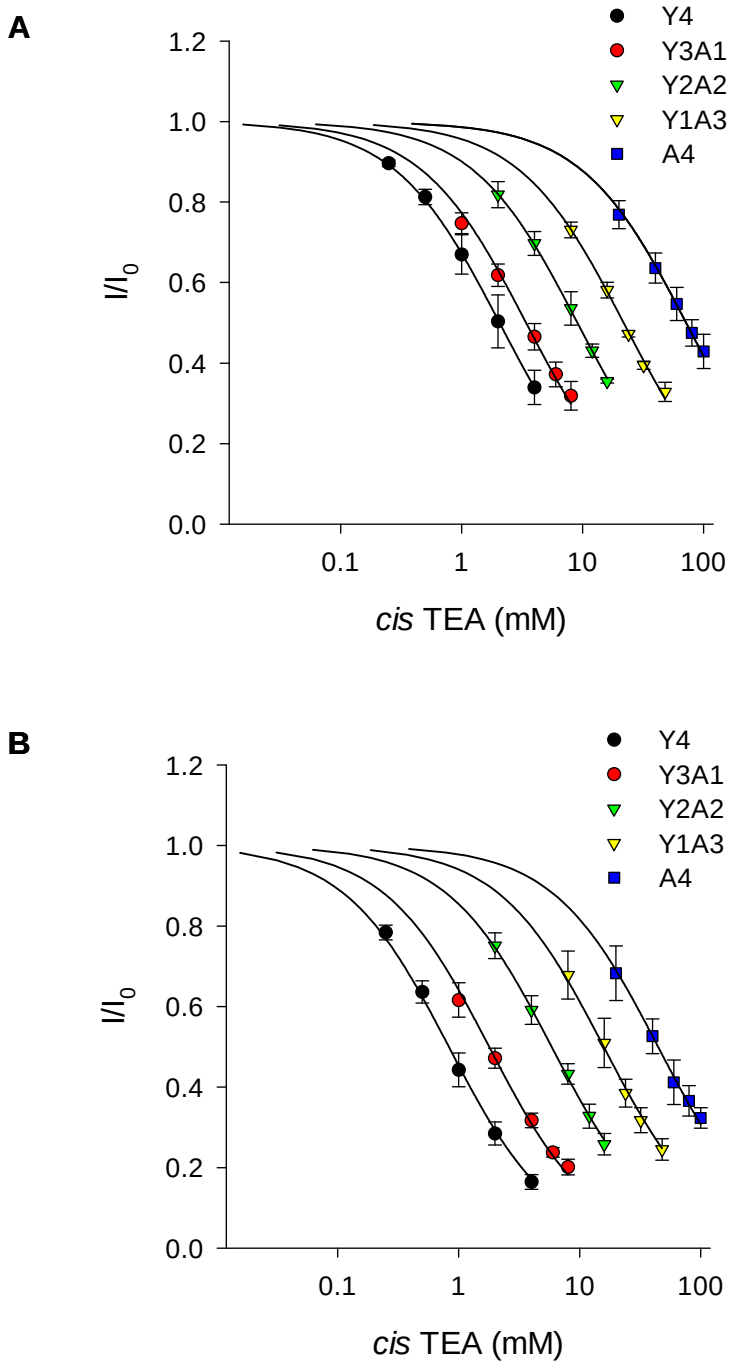

Figure 37. External TEA inhibition of N8-L70Y/L70A tetramers. External TEA inhibition of Kcv tetramers with different number of Tyr and Ala at position 70 was tested at +60mV (**A**) or -60mV (**B**). IC_{50} of each type of Kcv tetramer (Y4, Y3A1, Y2A2, Y1A3 and A4) was calculated from the inhibition curve.

Table 6. External TEA sensitivities of N8-L70Y/L70A tetramers

	IC_{50} (mM) at +60mV	IC_{50} (mM) at -60mV
$L70Y_4$ (Y_4)	2.06	0.83
$L70Y_3L70A_1$ (Y_3A_1)	3.42	1.79
$L70Y_2L70A_2$ (Y_2A_2)	9.08	5.87
$L70Y_1L70A_3$ (Y_1A_3)	21.87	15.80
$L70A_4$ (A_4)	71.81	44.51

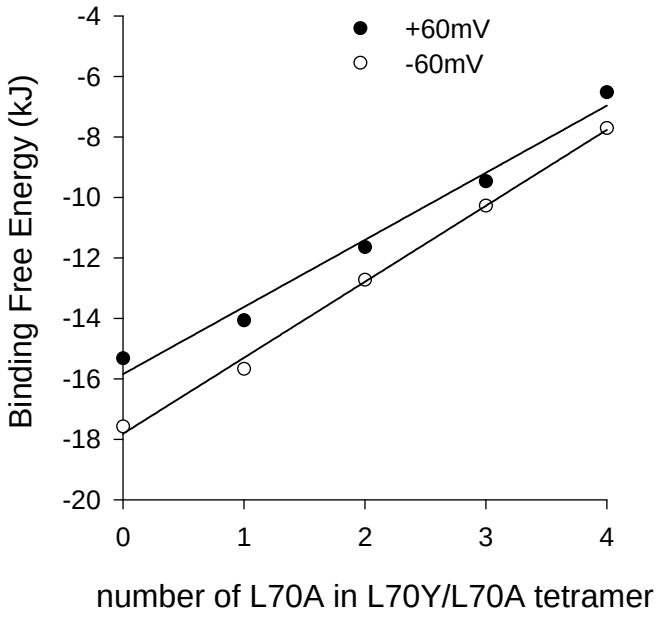

Figure 38. Dependence of external TEA binding on the number of L70A in N8-L70Y/L70A tetramer. The TEA binding free energy for each tetramer was calculated from IC_{50} (Table 6). The similar binding energy additivity is revealed by the linear relationship between binding energy and number of L70A substitution.

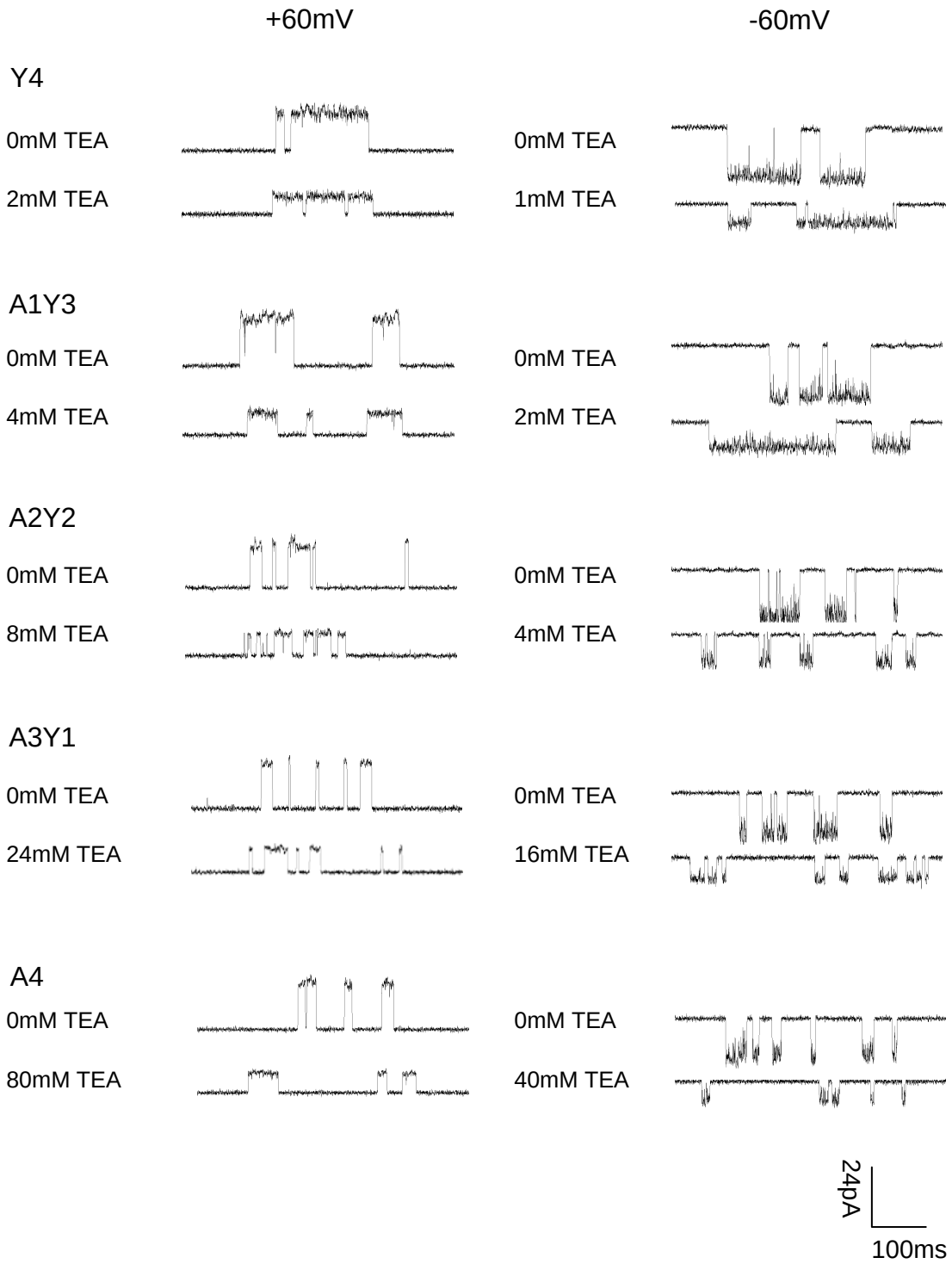

Figure 39. Current recording of external TEA block for N8-L70Y/L70A tetramers. The indicated TEA concentration is close to IC50 value (Table 6).

3.4. Conclusion and Discussion

3.4.1. Mechanism of TEA binding to potassium channels

A single aromatic residue (Tyr82 in KcsA and Tyr449 in Shaker) in potassium channels was shown to be required for high sensitivity to external TEA block. The substitution of Tyr by Trp, Thr, Ser, Cys, Ile and Val reduce the external TEA block in Shaker or KcsA (Heginbotham and MacKinnon, 1992; Meuser et al., 2001). Π-cation interaction between the positive charged TEA and quadrupole aromatic ring was implicated in the binding of external TEA. Consistently, the substitutions by these residues at the corresponding site Leu70 in Kcv decrease the external TEA block significantly. The substitution of Leu by Tyr/Phe in Kcv leads to similar external TEA sensitivity with WT KcsA, which suggests a structural similarity upon the substitution of Leu70 by Trosine in Kcv. However, higher sensitivity to external TEA block in WT Kcv suggests that the external TEA binding to Kcv channel may not arise from Π-cation interaction in the presence of Leu. Even in KcsA where the Try82 is present, the position and orientation of the aromatic ring of Tyrosine are not really favorable for the Π-cation interaction. To form favorable Π-cation interaction, an “en face” orientation is required, in which center of aromatic ring directly face the TEA molecule. By using nonsense suppression method, an “en face” orientation of Tyr449 was suggested in *Shaker* to support the Π-cation interaction (Ahern et al., 2006). However, crystallography studies showed an “edge-on” configuration in KcsA, where aromatic rings of Tyrosine are tilted relative to the pore central axis (Lenaeus et al., 2005). Simulation analysis in KcsA also demonstrated that, rather than Π-cation interaction, the high binding affinity was attributed to stabilizing hydrophobic interaction between TEA and potassium channels

(Crouzy et al., 2001; Luzhkov and Åqvist, 2001; Guidoni and Carloni, 2002). Indeed, shorter hydrophobic side chains (Val, Ala) lead to significant decrease of TEA affinity to Kcv. Substitution by charged residues (Glu/Lys) showed no sensitivity of external TEA block at all. Furthermore, the stabilization of external TEA may be influenced by subtle conformational difference of the side chain. For example, substitution of Leu by Ile which has similar structure and hydrophobicity, showed significant decrease of external TEA block. In WT Kcv, the presence of Leu may help the extracellular entrance of channel adopt an optimal conformation which makes these interactions energetically favorable, thus confer high TEA affinity. Alternatively, the varying TEA sensitivity in different Kcv mutants at residue 70 may be attributed to a combination effect from multiple sites. It has been suggested that external TEA block is modulated by multiple sites. For example, although the corresponding site Y380 in Kv 2.1 channel is important for the external TEA affinity, other residues in selectivity filter (T373, Y376) and outer vestibule (D378, K382) were also found to influence the TEA block, likely via direct or indirect interactions (Pascual et al., 1995). In rat RBK1, V381T didn't change the TEA sensitivity at all. The TEA sensitivity was decreased 27-fold upon substitution of Tyr by Val at equivalent site 379. However, double mutant Y379V/V381T decreased TEA sensitivity by 225-fold (Kavanaugh et al., 1991).

Our comprehensive mutagenesis study has provided some consistent results with other reports about TEA sensitivity of mutated or naturally occurring potassium channels which have different residue types at the equivalent site. However, some different data were obtained in our study. Compared with aromatic residue (Phe/Tyr), presence of Leu70 in Kcv shows higher TEA sensitivity. Presence of His showed similarly high

sensitivity to external TEA block (IC_{50} (mM) = 1.87, 2.01and 3.57 for L70Y, L70F and L70H at 60mV, respectively). Surprisingly, substitution of corresponding site His401 in rat RGK5 by Tyr (H401Y) decreased IC_{50} from 11mM to 0.55mM. The discrepancy about the TEA sensitivity difference between Tyr and His may be due to the varying degree of ionization of His in different potassium channels. Wild type RGK5 (H401) showed less TEA sensitivity at lower pH, while mutant RGK5 (H401Y) channel showed no difference in TEA sensitivity at varying pH. This implied that TEA binding can be affected by ionization of the imidazole ring of Histidine (Kavanaugh et al., 1991). Since KcsA and Shaker has been widely used for the mechanistic study for TEA binding, effect of substitution by Leu or His in KcsA and Shaker on external TEA affinity need to be further investigated.

3.4.2. Voltage dependence of TEA block

Voltage dependence of external TEA block is a well-known phenomenon. In KcsA, voltage sensitivity has been measured in several channel types. The relative electric distances (б) for WT (Y82), Y82T, Y82V and Y82C are 20%, 17%, 18% and 16%, respectively (Meuser et al., 2001). According to Woodhull model, it was argued that TEA has about the same position in the pore of each channel type. Consistent with the KcsA study, no significant difference in voltage dependence among four Kcv channel types was observed. The relative electric distance at positive voltages for each channel type is 26% (L70Y), 29% (L70T), 25% (L70V) and 24% (L70C). These results seem to contradict with the study of external TEA block in Shaker channel. When the Tyr is substituted by Thr at position 449, the voltage dependence increased from 4% to 19%.

This observation argued that replacing Tyr with Thr make TEA enters much more deeply into the Shaker pore (Heginbotham and MacKinnon, 1992). To reconcile this contradiction, more consideration should be taken in term of the physical position of TEA deduced from the experimentally observed voltage dependence. The classic explanation of voltage-dependence is that the charged TEA enters deeply into the pore within the electric field. However, this explanation has been called in some questions. The diameter of TEA molecule is about 6-8 angstroms. It is difficult for the TEA to get deeply into the narrow pore. Simulation studies also demonstrated that external TEA binding site was outside the selectivity filter (Crouzy et al., 2001; Guidoni and Carloni, 2002). Because transmembrane potential is mainly across the selectivity filter (Roux et al., 2000), the TEA binding site can not be within the membrane electric field. Therefore, external TEA block should be independent of voltage for both the high and low affinity channel types. However, instead of direct interaction between the voltage and the charged TEA, the observed voltage dependence may be related to many other processes such as voltage-gated channel opening and K^+ occupancy in the pore (Ikeda and Korn, 1995). It has been suggested that the apparent voltage dependence of external TEA block in Shaker channel arises from the net effect of two oppositely directed voltage-dependent processes, the K^+ distribution in selectivity filter and K^+ occupancy near the inner end of the pore (Thompson and Begenisich, 2003). More investigations about the complex interplay among potassium channel, permeant ions and channel blocker TEA are needed to further clarify the origin of the observed voltage-dependence and make a better understanding of the relationship between TEA sensitivity and voltage dependence.

3.4.3. Additivity of TEA binding energy

To study the contribution of each subunit of a tetrameric K^+ channel to external TEA binding, the affinity of each type of heteromeric channel with different number of low affinity subunit was determined. For example, coexpression of wild-type rabbit RBK1 and its low affinity mutant (Y379V) RNAs in *Xenopus* oocytes yields a mixture of all five channel types which contains zero, one, two, three or four substituted subunits. The relative proportion of each type is governed by the relative proportion of RNA injected. The TEA sensitivity of each channel type was deduced by statistic analysis of overall dose-dependence data. The energy additivity for external TEA binding was observed. This additivity effect was further confirmed by using tandem constructs of RBK1. The tandem RBK1 dimers were constructed by linking two subunits (wild type-wild type, wild type-mutant and mutant-mutant) with an amino acid linker. When a tandem dimer cDNA or RNA was injected into Xenopus oocytes, two expressed tandem dimer formed a tetrameric channel. A uniform population of concatenated channels with zero, two or four mutated subunits was generated in cells and the TEA sensitivity of each channel type was determined (Kavanaugh et al., 1992). By using this tandem method, the additivity effect of TEA binding was also observed in Shaker (Heginbotham and MacKinnon, 1992) and Kv2.1 (Pascual et al., 1995) channels. In this report, a whole set of gel-purified terameric channels which contain zero, one, two, three or four mutated subunits were generated for individual analysis of external TEA sensitivity. We have found that the substitution of residue (Leu70 or Tyr70) by Ala decrease the external TEA sensitivity significantly. Consistent with the observations from co-injection or tandem dimer studies, the linear relationship between TEA binding free energy and the number of mutated subunits

(L70A) was observed. Therefore, our study provides direct evidence that external TEA interacts simultaneously with the four Kcv subunits. Each subunit interacts with one ethyl group of TEA independently and contributes the binding free energy change equally. The simulation and crystallgraphy data also suggest that ethyl group of TEA closely approach the side chain Tyr82 from all four subunits in KcsA and make a simultaneous contact with the edge of each aromatic ring (Lenaeus et al., 2005). The similar binding energy additivity observed in several K+ channels suggests a shared mechanism of external TEA block. As a symmetric molecule, TEA can simultaneously bind to each subunit of a potassium channel with four fold symmetry (Fig. 40). It is reasonable to speculate that other TEA analogues, for example, tetrabutylamoinium (TBA), may bind to potassium channel in the same way due to their symmetric molecular structure. In contrast, single wild-type subunit grants the Shaker channel's high sensitivity to Charybdotoxin (CTX), indicating that this asymmetric molecule interact strongly with only one subunit of Shaker channel (MacKinnon, 1991).

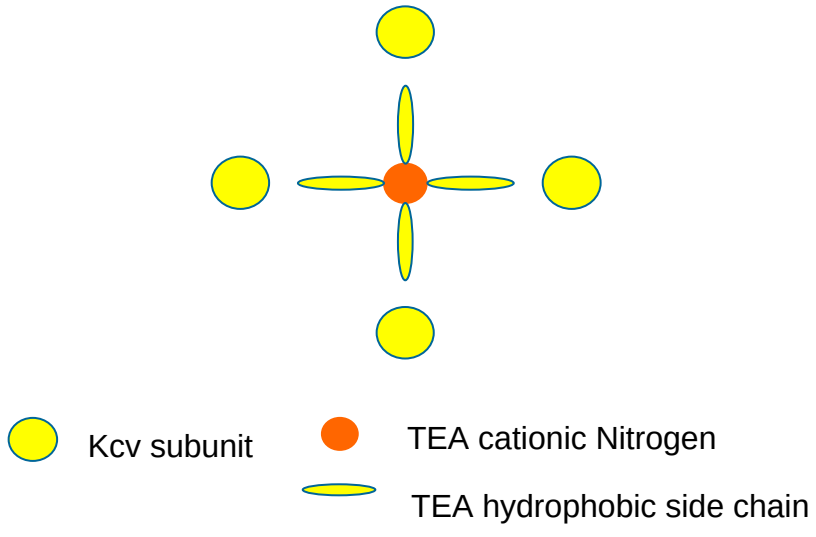

Figure 40. Simultaneous interaction of TEA with each subunit of potassium channel.

CHAPTER 4

CONCLUSION AND DISCUSSION

By using a SDS-stable tetrameric Kcv channel as a model, we propose a simple, straightforward approach that can genetically manipulate individual subunits in the tetramer, thereby enabling the detection of contribution from individual subunits to the channel functions. We designed a tagged Kcv that possesses a polypeptide tag at the N-terminal and retains the same function including ion conductance and K^+ selectivity as the wild-type protein. The tagged-Kcv (N8-Kcv) can hybridize with a mutant Kcv to form hetero-tetramers that can be separated using electrophoresis. Due to the stability in SDS, each hetero-tetramer directly purified from the gel can be examined for its electrophysiology properties. Using this method, we can detect how the channel function is altered by genetically manipulating individual subunits.

4.1. Two different mechanisms for ion permeation by subunit composition in Kcv channel

In the report, we uncovered that the mutation in the selectivity filter of Kcv (G65C) alters the permeability in an "all-or-none" manner. Substitution in one subunit in the tetramer is sufficient to permanently abolish the channel permeability. This "all-or-none" functional stoichiometry could be correlated with the selectivity filter's function in gating regulation. The substitution of Gly^{65} by Cys may give rise to a "reorientation" of the selectivity filter that "locks" the Kcv channel in the non-conducting state. In contrast, the

mutation near the extracellular entrance of the channel (L70Y) regulates the ion permeation governed by an "additive" mechanism. The channel's rectifying current can be additively modified with increasing number of mutant subunits in the tetramer. The "additive" regulation of ion permeation could originate from the "fast" gating, a mechanism proposed to interpret the Kcv's decayed conductance at the high voltages. Based on the this fast gating model, we infer that that Leu^{70} is a key position to modulate the fast gating activity, and each subunit independently contributes a fast gating pattern to the overall conductance. Therefore, the observed apparent conductance is an accumulation of four fast gating patterns, rather than a simple open-close two-state flicking. A sophistical mathematical analysis will be applied to clarify this process.

4.2. Regulation of external TEA block by subunit composition of Kcv

The TEA blockade of Kcv channel was further explored through mutagenesis and stoichiometric studies. Kcv shows high sensitivity to external TEA blockade in a voltage–dependent manor. Higher sensitivity to external TEA block in the presence of Leu at corresponding site 70 in WT Kcv than aromatic residues (Tyr/Phe) suggests different mechanisms other than Π-cation interaction. Any other residues (Thr, Cys, Val, Ala, etc.) lead to significant decreases of external TEA binding affinity. Among them, mutant L70A exhibited more than 100 fold lower blocking efficiency of external TEA. By investigating the TEA sensitivity of each heteromeric Kcv channel with different number of L70A substitution, a linear relationship between the free energy of TEA binding and the number of the substitution (zero, one, two, three and four) was observed. The linear relationship suggests that external TEA interacts simultaneously with four

subunits. Each subunit interacts with one ethyl group of TEA independently and contributes the binding free energy change equally. The binding energy additivity suggests a shared mechanism of external TEA block. As a symmetric molecule, TEA can simultaneously bind to each subunit of a potassium channel with four fold symmetry.

4.3. Producing native heteromeric channels by mass-tagging method

Compared to previous functional stoichiometric studies, our hetero-channel method exhibits several advantages. The contributions of mutant subunits to the channel function can be independently revealed. This method does not require different subunits to be equally expressed and random associated in the membrane as in the co-expression method, and does not require tandem constructs as in the concatemer method**.** This approach could be useful in detecting a variety of subunit composition-determined molecular processes in potassium channels. And this technique may also be beneficial for construction of engineering channels with tunable functions for biosensing by manipulating subunit composition.

The mass-tagging method proves a useful tool for study of subunit contribution to the overall function of homotetrameric potassium channels. It might also be used to in vitro produce naturally occurring heteromeric channel subtypes composed of different type of subunits. For example, Shaker-related voltage-gated potassium channel (Kv1) consists of four transmembrane pore-forming α (Kv1.1-Kv1.8) subunits and four cytoplasmic β subunits (Rhodes et al., 1997). Combination of different type of Kv1α could generate a variety of tissue-specific heterotetrameric channels with distinct biophysical and pharmacological properties. These Kv1 heteromers serve numerous functions including

maintenance of resting membrane potential, control of action potential duration and frequency and neurotransmitter release (Scott et al., 1994; Shamotienko et al., 1997; Shamotienko et al., 1999). Due to their physiological and pharmacological importance, to create these tissue-specific heteromeric receptors is necessary not only for the analysis of the properties of the channels themselves but also for development of novel experimental probes and subtype-specific therapeutics. Because of the different size, each subunit may have different electrophoretic mobility. The heteromeric channels, for example, Kv 1.2-1.6 will be gel-purified by using SDS-PAGE. The preliminary study need to be performed to determine whether Kv protein can multimerize in the presence of SDS and the function of gel purified heterotetramer with defined subunit composition need to be verified in an appropriate lipid bilayer.

Another important tetrameric K+ channel is G protein–activated inward rectifying potassium channel (GIRK) (Wickman and Clapham, 1995a; Wickman and Clapham, 1995b). For example, heteromeric channel (GIRK1/4) can be activated by acetylcholine through G protein-coupled receptors (GPCRs) such as M2 muscarinic receptors. Binding of receptors by ligands leads to release of G-protein βγ subunits (Gβγ), which interact with GIRK channels, thereby causes an inward current of potassium (Krapivinsky et al., 1995a; Krapivinsky et al., 1995b; Krapivinsky et al., 1995c). GIRK channels can be also activated by phosphatidylinositol 4,5-bisphosphate (PIP2) generated by ATP-dependent lipid kinases (Huang et al., 1998). It is important to produce these heteromeric GIRK channels for examining how the activation mechanisms of PIP2 and Gβγ are related.

Rather than tetrameric potassium channels, the heteromeric receptors containing more subunits may also be produced by using this method. For example, pentameric nicotinic

acetylcholine receptors (nAChR) can contain as many as four different types of subunits (Conroy and Berg, 1995; Corriveau et al., 1995; Forsayeth and Kobrin, 1997; Moretti et al., 2004). Assembly of combinations of subunits results in a large variety of heteromeric receptors such as (α1)2β1δε (muscle type), (α3)2(β4)3 (ganglion type) and (α4)2(β2)3 (CNS type), etc. For those nAChRs with two types of subunits, the heteromeric channel (α3)2(β4)3 or (α4)2(β2)3 may be synthesized in vitro and gel-purified in a similar way. However, the exact subunit arrangement in this hetero-pentameric channel needs to be determined.

4.4. Further improvements of current method

In this study, we utilize a mass-tagging strategy to produce heteromeric channels which are purified from SDS-PAGE gel. To carry out this study, there are two prerequisites. First, the multimeric channel should be SDS-stable. The second, the tagged channel should retain the same function as the untagged wild type channel. However, not every channel can meet these two requirements. To solve this problem, several modified methods will be proposed.

4.4.1. Purification of SDS-sensitive oligomeric channels

As a strong detergent, SDS may denature the protein, thus leading to nonfunctional channels. Native gel electrophoresis might be used for the separation and purification of oligomeric proteins that are not resistant to SDS. Alternatively, the hetero-channel proteins can be separated and purified by HPLC method. The tagged and untagged

proteins are co-assembled into homo- and heteromeric channels in *Escherichia coli* or eukaryotic expression system. The cells are collected after centrifugation and suspended in homogenization buffer. The cell membrane containing a mixture of multimeric channel proteins are then detergent-solubilized for further purification. Since the attachment a tag will change the physical or biochemical properties such as molecular size, net charge and hydrophobicity, the multimeric channels with different number of tagged subunits will be purified by various HPLC **(**High performance liquid chromatography**)** methods, for example, ion exchange chromatography (IC) and size exclusion chromatography (SEC).

4.4.2. Construction of tagged protein with cleavable tags

As mentioned earlier, the composition and size of the tag may influence significantly the channel functions including multimerization efficiency and channel activity. Alternatively, a cleavable tag can be introduced. In a similar study, Bayley's group introduced a polypeptide extension containing a tobacco etch virus (TEV) protease recognition site (ENLYFQG) (Rotem et al., 2010). After purification from SDS-PAGE gel, the polypeptide tags of tetrameric channels were removed by proteolysis with TEV protease (Fig. 41A). Many proteases has been widely used for cleavage of tags (His6 and glutathione *S*-transferase GST) linked with proteins by a specific protease recognition sequence. Several protease and their recognition sites are shown in Table 7.

Table 7. Specific protease and their recognition sequence

Protease	Recognition sequence
TEV protease	Glu-Asn-Leu-Tyr-Phe-Gln-Gly
Enterokinase	Asp-Asp-Asp-Asp-Lys
Thrombin	Leu-Val-Pro-Arg-Gly-Ser
Factor Xa	Ile-Glu/Asp-Gly-Arg
Signal peptidase	Signal sequence

The cleavage of tags can also be achieved by a chemical modification method. For example, modification of a single cysteine residue with thiol-reactive agent 4-acetamido-4'-[(iodoacetyl)amino]stilbene-2-2'-disulfonate (IASD) has been used to alter the electrophoretic mobility of subunit, thus permit separation of heteromeric pores with different subunit combinations (Gouaux et al., 1994). And this tag can be further removed by reducing agent dithiothreitol (DTT) (Fig. 41B).

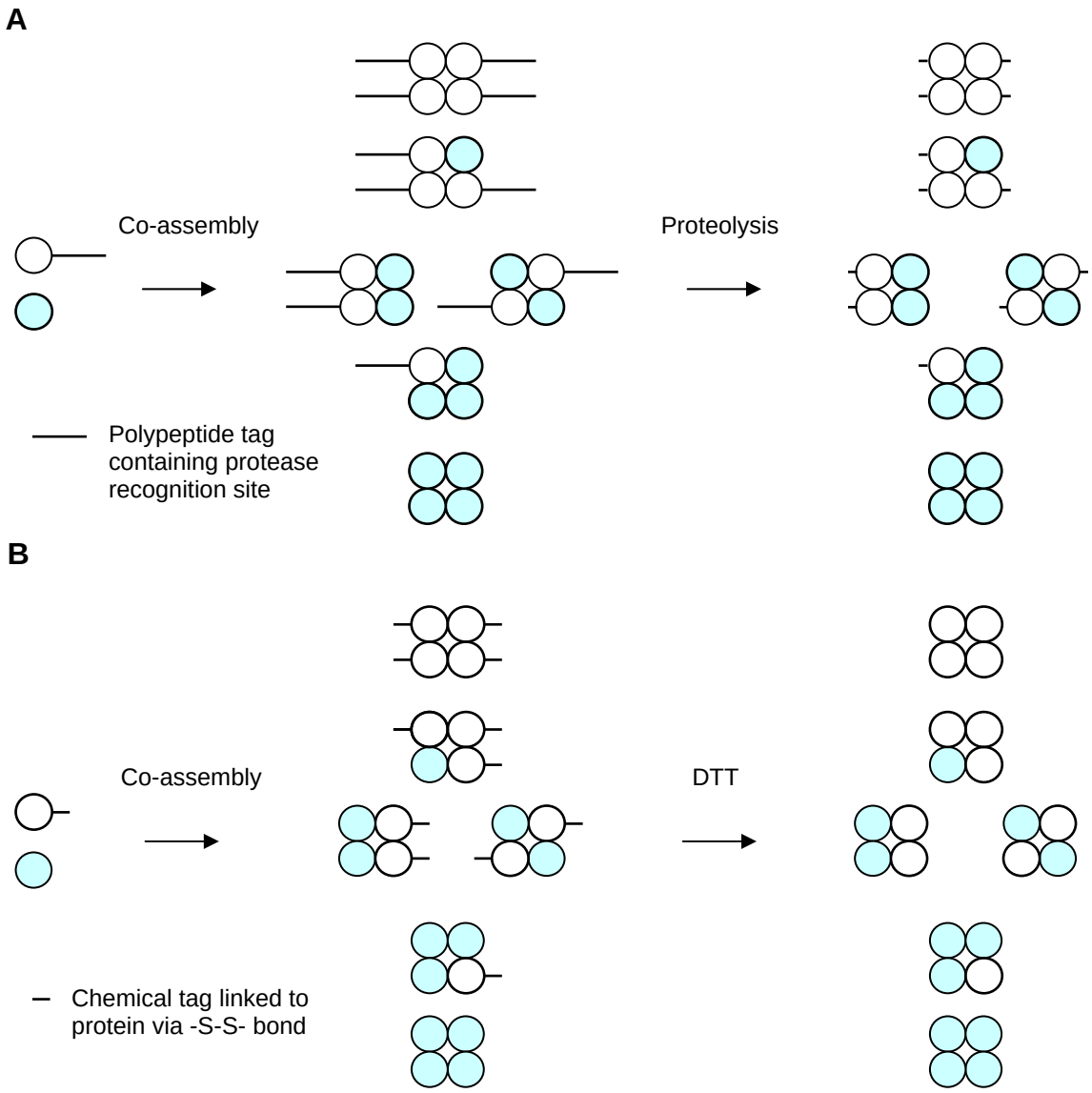

Figure 41. Cleavage of tagged protein. A. The polypeptide tag containing protease recognition site can be cleaved from the protein by specific protease. **B.** The chemical tag covalently linked to protein via disulfide bond can be removed by reducing agent DTT.

REFERENCES

Abenavoli, A., M.L. DiFrancesco, I. Schroeder, S. Epimashko, S. Gazzarrini, U.P. Hansen, G. Thiel, and A. Moroni. 2009. Fast and slow gating are inherent properties of the pore module of the K+ channel Kcv. *Journal of General Physiology*. 134:219-229.

Ahern, C.A., A.L. Eastwood, H.A. Lester, D.A. Dougherty, and R. Horn. 2006. A cation-π interaction between extracellular TEA and an aromatic residue in potassium channels. *Journal of General Physiology*. 128:649-657.

Akhtar, S., O. Shamotienko, M. Papakosta, F. Ali, and J. Oliver Dolly. 2002. Characteristics of brain Kv1 channels tailored to mimic native counterparts by tandem linkage of α subunits. Implications for K+ channelopathies. *Journal of Biological Chemistry*. 277:16376-16382.

Alvis, S.J., I.M. Williamson, J.M. East, and A.G. Lee. 2003. Interactions of Anionic Phospholipids and Phosphatidylethanolamine with the Potassium Channel KcsA. *Biophysical Journal*. 85:3828-3838.

Andalib, P., J.F. Consiglio, J.G. Trapani, and S.J. Korn. 2004. The external TEA binding site and C-type inactivation in voltage-gated potassium channels. *Biophysical Journal*. 87:3148-3161.

Baker, O.S., H.P. Larsson, L.M. Mannuzzu, and E.Y. Isacoff. 1998. Three transmembrane conformations and sequence-dependent displacement of the S4 domain in Shaker K+ channel gating. *Neuron*. 20:1283-1294.

Bernèche, S., and B. Roux. 2005. A gate in the selectivity filter of potassium channels. *Structure*. 13:591-600.

Blunck, R., J.F. Cordero-Morales, L.G. Cuello, E. Perozo, and F. Bezanilla. 2006. Detection of the opening of the bundle crossing in KcsA with fluorescence lifetime spectroscopy reveals the existence of two gates for ion conduction. *Journal of General Physiology*. 128:569-581.

Braha, O., B. Walker, S. Cheley, J.J. Kasianowicz, L. Song, J.E. Gouaux, and H. Bayley. 1997. Designed protein pores as components for biosensors. *Chemistry and Biology*. 4:497-505.

Bretschneider, F., A. Wrisch, F. Lehmann-Horn, and S. Grissmer. 1999. External tetraethylammonium as a molecular caliper for sensing the shape of the outer vestibule of potassium channels. *Biophysical Journal*. 76:2351-2360.

Chanda, B., O.K. Asamoah, R. Blunck, B. Roux, and F. Bezanilla. 2005. Gating charge displacement in voltage-gated ion channels involves limited transmembrane movement. *Nature*. 436:852-856.

Chatelain, F.C., S. Gazzarrini, Y. Fujiwara, C. Arrigoni, C. Domigan, G. Ferrara, C. Pantoja, G. Thiel, A. Moroni, and D.L. Minor Jr. 2009. Selection of inhibitor-resistant viral potassium channels identifies a selectivity filter site that affects barium and amantadine block. *PLoS ONE*. 4.

Cheley, S., O. Braha, X. Lu, S. Conlan, and H. Bayley. 1999. A functional protein pore with a 'retro' transmembrane domain. *Protein Science*. 8:1257-1267.

Choi, K.L., C. Mossman, J. Aube, and G. Yellen. 1993. The internal quaternary ammonium receptor site of Shaker potassium channels. *Neuron*. 10:533-541.

Conroy, W.G., and D.K. Berg. 1995. Neurons can maintain multiple classes of nicotinic acetylcholine receptors distinguished by different subunit compositions. *Journal of Biological Chemistry*. 270:4424-4431.

Cordero-Morales, J.F., L.G. Cuello, and E. Perozo. 2006a. Voltage-dependent gating at the KcsA selectivity filter. *Nature Structural and Molecular Biology*. 13:319-322.

Cordero-Morales, J.F., L.G. Cuello, Y. Zhao, V. Jogini, D.M. Cortes, B. Roux, and E. Perozo. 2006b. Molecular determinants of gating at the potassium-channel selectivity filter. *Nature Structural and Molecular Biology*. 13:311-318.

Corriveau, R.A., S.J. Romano, W.G. Conroy, L. Oliva, and D.K. Berg. 1995. Expression of neuronal acetylcholine receptor genes in vertebrate skeletal muscle during development. *Journal of Neuroscience*. 15:1372-1383.

Cortes, D.M., L.G. Cuello, and E. Perozo. 2001. Molecular architecture of full-length KcsA role of cytoplasmic domains in ion permeation and activation gating. *Journal of General Physiology*. 117:165-180.

Crouzy, S., S. Bernèche, and B. Roux. 2001. Extracellular blockade of K+ channels by TEA: Results from molecular dynamics simulations of the KcsA channel. *Journal of General Physiology*. 118:207-217.

Cuello, L.G., J.G. Romero, D. Marien Cortes, and E. Perozo. 1998. pH-dependent gating in the Streptomyces lividans K+ channel. *Biochemistry*. 37:3229-3236.

Del Camino, D., and G. Yellen. 2001. Tight steric closure at the intracellular activation gate of a voltage-gated K+ channel. *Neuron*. 32:649-656.

Doyle, D.A., J.M. Cabral, R.A. Pfuetzner, A. Kuo, J.M. Gulbis, S.L. Cohen, B.T. Chait, and R. MacKinnon. 1998. The structure of the potassium channel: Molecular basis of K+ conduction and selectivity. *Science*. 280:69-77.

Faraldo-Gómez, J.D., E. Kutluay, V. Jogini, Y. Zhao, L. Heginbotham, and B. Roux. 2007. Mechanism of Intracellular Block of the KcsA K+ Channel by Tetrabutylammonium: Insights from X-ray Crystallography, Electrophysiology and Replica-exchange Molecular Dynamics Simulations. *Journal of Molecular Biology*. 365:649-662.

Forsayeth, J.R., and E. Kobrin. 1997. Formation of oligomers containing the β3 and β4 subunits of the rat nicotinic receptor. *Journal of Neuroscience*. 17:1531-1538.

French, R.J., and J.J. Shoukimas. 1981. Blockage of squid axon potassium conductance by internal tetra-n-alkylammonium ions of various sizes. *Biophysical Journal*. 34:271-291.

Frohns, F., A. Käsmann, D. Kramer, B. Schäfer, M. Mehmel, M. Kang, J.L. Van Etten, S. Gazzarrini, A. Moroni, and G. Thiel. 2006. Potassium ion channels of chlorella viruses cause rapid depolarization of host cells during infection. *Journal of Virology*. 80:2437-2444.

Gazzarrini, S., J.L. Etten, D. DiFrancesco, G. Thiel, and A. Moroni. 2002. Voltage-dependence of virus-encoded miniature K+ channel Kcv. *Journal of Membrane Biology*. 187:15-25.

Gazzarrini, S., M. Kang, A. Abenavoli, G. Romani, C. Olivari, D. Gaslini, G. Ferrara, J.L. Van Etten, M. Kreim, S.M. Kast, G. Thiel, and A. Moroni. 2009. Chlorella virus ATCV-1 encodes a functional potassium channel of 82 amino acids. *Biochemical Journal*. 420:295-303.

Gazzarrini, S., M. Severino, M. Lombardi, M. Morandi, D. DiFrancesco, J.L. Van Etten, G. Thiel, and A. Moroni. 2003. The viral potassium channel Kcv: Structural and functional features. *FEBS Letters*. 552:12-16.

Gouaux, J.E., O. Braha, M.R. Hobaugh, L. Song, S. Cheley, C. Shustak, and H. Bayley. 1994. Subunit stoichiometry of staphylococcal α-hemolysin in crystals and on membranes: A heptameric transmembrane pore. *Proceedings of the National Academy of Sciences of the United States of America*. 91:12828-12831.

Groot-Kormelink, P.J., S.D. Broadbent, J.P. Boorman, and L.G. Sivilotti. 2004. Incomplete incorporation of tandem subunits in recombinant neuronal nicotinic receptors. *Journal of General Physiology*. 123:697-708.

Gu, L.Q., and J.W. Shim. 2010. Single molecule sensing by nanopores and nanopore devices. *Analyst*. 135:441-451.

Guidoni, L., and P. Carloni. 2002. Tetraethylammonium binding to the outer mouth of the KcsA potassium channel: Implications for ion permeation. *Journal of Receptors and Signal Transduction*. 22:315-331.

Heginbotham, L., M. LeMasurier, L. Kolmakova-Partensky, and C. Miller. 1999. Single Streptomyces lividans K+ channels. Functional asymmetries and sidedness of proton activation. *Journal of General Physiology*. 114:551-559.

Heginbotham, L., Z. Lu, T. Abramson, and R. MacKinnon. 1994. Mutations in the K+ channel signature sequence. *Biophysical Journal*. 66:1061-1067.

Heginbotham, L., and R. MacKinnon. 1992. The aromatic binding site for tetraethylammonium ion on potassium channels. *Neuron*. 8:483-491.

Heginbotham, L., E. Odessey, and C. Miller. 1997. Tetrameric stoichiometry of a prokaryotic K+ channel. *Biochemistry*. 36:10335-10342.

Ho, K., C.G. Nichols, W.J. Lederer, J. Lytton, P.M. Vassilev, M.V. Kanazirska, and S.C. Hebert. 1993. Cloning and expression of an inwardly rectifying ATP-regulated potassium channel. *Nature*. 362:31-38.

Huang, C.L., S. Feng, and D.W. Hilgemann. 1998. Direct activation of inward rectifier potassium channels by PIP2 and its stabilization by Gβγ. *Nature*. 391:803-806.

Hurst, R.S., M.P. Kavanaugh, J. Yakel, J.P. Adelman, and R.A. North. 1992. Cooperative interactions among subunits of a voltage-dependent potassium channel. Evidence from expression of concatenated cDNAs. *Journal of Biological Chemistry*. 267:23742-23745.

Ikeda, S.R., and S.J. Korn. 1995. Influence of permeating ions on potassium channel block by external tetraethylammonium. *Journal of Physiology*. 486:267-272.

Isacoff, E.Y., Y.N. Jan, and L.Y. Jan. 1990. Evidence for the formation of heteromultimeric potassium channels in Xenopus oocytes. *Nature*. 345:530-534.

Jan, L.Y., and Y.N. Jan. 1994. Potassium channels and their evolving gates. *Nature*. 371:119-122.

Jongsma, H.J., and R. Wilders. 2001. Channelopathies: Kir2.1 mutations jeopardize many cell functions. *Current Biology*. 11:R747-R750.

Kang, M., A. Moroni, S. Gazzarrini, D. DiFrancesco, G. Thiel, M. Severino, and J.L. Van Etten. 2004. Small potassium ion channel proteins encoded by chlorella viruses. *Proceedings of the National Academy of Sciences of the United States of America*. 101:5318-5324.

Kavanaugh, M.P., R.S. Hurst, J. Yakel, M.D. Varnum, J.P. Adelman, and R.A. North. 1992. Multiple subunits of a voltage-dependent potassium channel contribute to the binding site for tetraethylammonium. *Neuron*. 8:493-497.

Kavanaugh, M.P., M.D. Varnum, P.B. Osborne, M.J. Christie, A.E. Busch, J.P. Adelman, and R.A. North. 1991. Interaction between tetraethylammonium and amino acid residues in the pore of cloned voltage-dependent potassium channels. *Journal of Biological Chemistry*. 266:7583-7587.

Kirsch, G.E., J.M. Pascual, and C.C. Shieh. 1995. Functional role of a conserved aspartate in the external mouth of voltage- gated potassium channels. *Biophysical Journal*. 68:1804-1813.

Krapivinsky, G., E.A. Gordon, K. Wickman, B. Velimirovic, L. Krapivinsky, and D.E. Clapham. 1995a. The G-protein-gated atrial K+ channel I(KACh) is a heteromultimer of two inwardly rectifying K+-channel proteins. *Nature*. 374:135-141.

Krapivinsky, G., L. Krapivinsky, B. Velimirovic, K. Wickman, B. Navarro, and D.E. Clapham. 1995b. The cardiac inward rectifier K+ channel subunit, CIR, does not comprise the ATP-sensitive K+ channel, I(KATP). *Journal of Biological Chemistry*. 270:28777-28779.

Krapivinsky, G., L. Krapivinsky, K. Wickman, and D.E. Clapham. 1995c. Gβγ binds directly to the G protein-gated K+ channel, I(KACh). *Journal of Biological Chemistry*. 270:29059-29062.

Lenaeus, M.J., M. Vamvouka, P.J. Focia, and A. Gross. 2005. Structural basis of TEA blockade in a model potassium channel. *Nature Structural and Molecular Biology*. 12:454-459.

Liman, E.R., J. Tytgat, and P. Hess. 1992. Subunit stoichiometry of a mammalian K+ channel determined by construction of multimeric cDNAs. *Neuron*. 9:861-871.

Liu, Y.S., P. Sompornpisut, and E. Perozo. 2001. Structure of the KcsA channel intracellular gate in the open state. *Nature Structural Biology*. 8:883-887.

Long, S.B., E.B. Campbell, and R. MacKinnon. 2005a. Crystal structure of a mammalian voltage-dependent Shaker family K + channel. *Science*. 309:897-903.

Long, S.B., E.B. Campbell, and R. MacKinnon. 2005b. Voltage sensor of Kv1.2: Structural basis of electromechanical coupling. *Science*. 309:903-908.

Lopatin, A.N., E.N. Makhina, and C.G. Nichols. 1994. Potassium channel block by cytoplasmic polyamines as the mechanism of intrinsic rectification. *Nature*. 372:366-369.

Lu, T., A.Y. Ting, J. Mainland, L.Y. Jan, P.G. Schultz, and J. Yang. 2001. Probing ion permeation and gating in a K+ channel with backbone mutations in the selectivity filter. *Nature Neuroscience*. 4:239-246.

Luzhkov, V.B., and J. Åqvist. 2001. Mechanisms of tetraethylammonium ion block in the KcsA potassium channel. *FEBS Letters*. 495:191-196.

Ma, L., M. Melegari, M. Colombini, and J.T. Davis. 2008. Large and stable transmembrane pores from guanosine-bile acid conjugates. *Journal of the American Chemical Society*. 130:2938-2939.

MacKinnon, R. 1991. Determination of the subunit stoichiometry of a voltage-activated potassium channel. *Nature*. 350:232-235.

MacKinnon, R., R.W. Aldrich, and A.W. Lee. 1993. Functional stoichiometry of Shaker potassium channel inactivation. *Science*. 262:757-759.

MacKinnon, R., S.L. Cohen, A. Kuo, A. Lee, and B.T. Chait. 1998. Structural conservation in prokaryotic and eukaryotic potassium channels. *Science*. 280:106-109.

MacKinnon, R., and G. Yellen. 1990. Mutations affecting TEA blockade and ion permeation in voltage-activated K+ channels. *Science*. 250:276-279.

Manganas, L.N., and J.S. Trimmer. 2000. Subunit composition determines Kv1 potassium channel surface expression. *Journal of Biological Chemistry*. 275:29685-29693.

Mannuzzu, L.M., and E.Y. Isacoff. 2000. Independence and cooperativity in rearrangements of a potassium channel voltage sensor revealed by single subunit fluorescence. *Journal of General Physiology*. 115:257-268.

Meuser, D., H. Splitt, R. Wagner, and H. Schrempf. 1999. Exploring the open pore of the potassium channel from Streptomyces lividans. *FEBS Letters*. 462:447-452.

Meuser, D., H. Splitt, R. Wagner, and H. Schrempf. 2001. Mutations stabilizing an open conformation within the external region of the permeation pathway of the potassium channel KcsA. *European Biophysics Journal*. 30:385-391.

Miles, G., S. Cheley, O. Braha, and H. Bayley. 2001. The staphylococcal leukocidin bicomponent toxin forms large ionic channels. *Biochemistry*. 40:8514-8522.

Miles, G., L. Movileanu, and H. Bayley. 2002. Subunit composition of a bicomponent toxin: Staphylococcal leukocidin forms an octameric transmembrane pore. *Protein Science*. 11:894-902.

Minier, F., and E. Sigel. 2004. Techniques: Use of concatenated subunits for the study of ligand-gated ion channels. *Trends in Pharmacological Sciences*. 25:499-503.

Molina, A., A.G. Castellano, and J. López-Barneo. 1997. Pore mutations in Shaker K+ channels distinguish between the sites of tetraethylammonium blockade and C-type inactivation. *Journal of Physiology*. 499:361-367.

Moretti, M., S. Vailati, M. Zoli, G. Lippi, L. Riganti, R. Longhi, A. Viegi, F. Clementi, and C. Gotti. 2004. Nicotinic acetylcholine receptor subtypes expression during rat retina development and their regulation by visual experience. *Molecular Pharmacology*. 66:85-96.

Moroni, A., C. Viscomi, V. Sangiorgio, C. Pagliuca, T. Meckel, F. Horvath, S. Gazzarrini, P. Valbuzzi, J.L. Van Etten, D. DiFrancesco, and G. Thiel. 2002. The short N-terminus is required for functional expression of the virus-encoded miniature K+ channel Kcv. *FEBS Letters*. 530:65-69.

Nichols, C.G., K. Ho, and S. Hebert. 1993. ROMK1 expressed in Xenoyus oocytes encodes a Mg2+-dependent inwardly rectifying potassium channel. *Journal of Physiology*. 473.

Nishida, M., M. Cadene, B.T. Chait, and R. MacKinnon. 2007. Crystal structure of a Kir3.1-prokaryotic Kir channel chimera. *EMBO Journal*. 26:4005-4015.

Noskov, S.Y., S. Bernéche, and B. Roux. 2004. Control of ion selectivity in potassium channels by electrostatic and dynamic properties of carbonyl ligands. *Nature*. 431:830-834.

Ogielska, E.M., W.N. Zagotta, T. Hoshi, S.H. Heinemann, J. Haab, and R.W. Aldrich. 1995. Cooperative subunit interactions in C-type inactivation of K channels. *Biophysical Journal*. 69:2449-2457.

Pagliuca, C., T.A. Goetze, R. Wagner, G. Thiel, A. Moroni, and D. Parcej. 2007. Molecular properties of Kcv, a virus encoded K+ channel. *Biochemistry*. 46:1079-1090.

Pascual, J.M., C.C. Shieh, G.E. Kirsch, and A.M. Brown. 1995. Multiple residues specify external tetraethylammonium blockade in voltage- gated potassium channels. *Biophysical Journal*. 69:428-434.

Pathak, M., L. Kurtz, F. Tombola, and E. Isacoff. 2005. The cooperative voltage sensor motion that gates a potassium channel. *Journal of General Physiology*. 125:57-69.

Perozo, E., D.M. Cortes, and L.G. Cuello. 1999. Structural rearrangements underlying K+-channel activation gating. *Science*. 285:73-78.

Plaster, N.M., R. Tawil, M. Tristani-Firouzi, S. Canún, S. Bendahhou, A. Tsunoda, M.R. Donaldson, S.T. Iannaccone, E. Brunt, R. Barohn, J. Clark, F. Deymeer, A.L. George Jr, F.A. Fish, A. Hahn, A. Nitu, C. Ozdemir, P. Serdaroglu, S.H. Subramony, G. Wolfe, Y.H. Fu, and L.J. Ptáček. 2001. Mutations in Kir2.1 cause the developmental and episodic electrical phenotypes of Andersen's syndrome. *Cell*. 105:511-519.

Plugge, B., S. Gazzarrini, M. Nelson, R. Cerana, J.L. Van Etten, C. Derst, D. DiFrancesco, A. Moroni, and G. Thiel. 2000. A potassium channel protein encoded by chlorella virus PBCV-1. *Science*. 287:1641-1644.

Preisig-Müller, R., G. Schlichthörl, T. Goerge, S. Heinen, A. Brüggemann, S. Rajan, C. Derst, R.W. Veh, and J. Daut. 2002. Heteromerization of Kir2.x potassium channels contributes to the phenotype of Andersen's syndrome. *Proceedings of the National Academy of Sciences of the United States of America*. 99:7774-7779.

Rhodes, K.J., B.W. Strassle, M.M. Monaghan, Z. Bekele-Arcuri, M.F. Matos, and J.S. Trimmer. 1997. Association and colocalization of the Kvβ1 and Kvβ2 β-subunits with Kv1 α-subunits in mammalian brain K+ channel complexes. *Journal of Neuroscience*. 17:8246-8258.

Rotem, D., A. Mason, and H. Bayley. 2010. Inactivation of the KcsA potassium channel explored with heterotetramers. *Journal of General Physiology*. 135:29-42.

Roux, B., S. Berneche, and W. Im. 2000. Ion channels, permeation, and electrostatics: Insight into the function of KcsA. *Biochemistry*. 39:13295-13306.

Ruta, V., J. Chen, and R. MacKinnon. 2005. Calibrated measurement of gating-charge arginine displacement in the KvAP voltage-dependent K+ channel. *Cell*. 123:463-475.

Schachtman, D.P., J.I. Schroeder, W.J. Lucas, J.A. Anderson, and R.F. Gaber. 1992. Expression of an inward-rectifying potassium channel by the Arabidopsis KAT1 cDNA. *Science*. 258:1654-1658.

Schrempf, H., O. Schmidt, R. Kümmerlen, S. Hinnah, D. Müller, M. Betzler, T. Steinkamp, and R. Wagner. 1995. A prokaryotic potassium ion channel with two predicted transmembrane segments from Streptomyces lividans. *EMBO Journal*. 14:5170-5178.

Schroeder, I., and U.P. Hansen. 2007. Saturation and microsecond gating of current indicate depletion-induced instability of the MaxiK selectivity filter. *Journal of General Physiology*. 130:83-97.

Scott, V.E.S., Z.M. Muniz, S. Sewing, R. Lichtinghagen, D.N. Parcej, O. Pongs, and J.O. Dolly. 1994. Antibodies specific for distinct Kv subunits unveil a heterooligomeric basis for subtypes of α-dendrotoxin-sensitive K+ channels in bovine brain. *Biochemistry*. 33:1617-1623.

Shamotienko, O., S. Akhtar, C. Sidera, F.A. Meunier, B. Ink, M. Weir, and J.O. Dolly. 1999. Recreation of neuronal Kv1 channel oligomers by expression in mammalian cells using semliki forest virus. *Biochemistry*. 38:16766-16776.

Shamotienko, O.G., D.N. Parcej, and J.O. Dolly. 1997. Subunit combinations defined for K+ channel Kv1 subtypes in synaptic membranes from bovine brain. *Biochemistry*. 36:8195-8201.

Shealy, R.T., A.D. Murphy, R. Ramarathnam, E. Jakobsson, and S. Subramaniam. 2003. Sequence-function analysis of the K+-selective family of ion channels using a comprehensive alignment and the KcsA channel structure. *Biophysical Journal*. 84:2929-2942.

Shim, J.W., M. Yang, and L.Q. Gu. 2007. In vitro synthesis, tetramerization and single channel characterization of virus-encoded potassium channel Kcv. *FEBS Letters*. 581:1027-1034.

Sokolov, M.V., O. Shamotienko, S.N. Dhochartaigh, J.T. Sack, and J.O. Dolly. 2007. Concatemers of brain Kv1 channel α subunits that give similar K+ currents yield pharmacologically distinguishable heteromers. *Neuropharmacology*. 53:272-282.

Splitt, H., D. Meuser, I. Borovok, M. Betzler, and H. Schrempf. 2000. Pore mutations affecting tetrameric assembly and functioning of the potassium channel KcsA from Streptomyces lividans. *FEBS Letters*. 472:83-87.

Syeda, R., M.A. Holden, W.L. Hwang, and H. Bayley. 2008. Screening blockers against a potassium channel with a droplet interface bilayer array. *Journal of the American Chemical Society*. 130:15543-15548.

Takeuchi, K., H. Takahashi, S. Kawano, and I. Shimada. 2007. Identification and characterization of the slowly exchanging pH-dependent conformational rearrangement in KcsA. *Journal of Biological Chemistry*. 282:15179-15186.

Thompson, A.N., D.J. Posson, P.V. Parsa, and C.M. Nimigean. 2008. Molecular mechanism of pH sensing in KcsA potassium channels. *Proceedings of the National Academy of Sciences of the United States of America*. 105:6900-6905.

Thompson, J., and T. Begenisich. 2003. External TEA block of Shaker K+ channels is coupled to the movement of K+ ions within the selectivity filter. *Journal of General Physiology*. 122:239-246.

Tombola, F., M.M. Pathak, and E.Y. Isacoff. 2006. How does voltage open an ion channel? *In*. Annu. Rev. Cell Dev. Biol. 23-52.

Tytgat, J., and P. Hess. 1992. Evidence for cooperative interactions in potassium channel gating. *Nature*. 359:420-423.

VanDongen, A.M.J. 2004. K channel gating by an affinity-switching selectivity filter. *Proceedings of the National Academy of Sciences of the United States of America*. 101:3248-3252.

Vergara, C., R. Latorre, N.V. Marrion, and J.P. Adelman. 1998. Calcium-activated potassium channels. *Current Opinion in Neurobiology*. 8:321-329.

White, M.M. 2006. Pretty subunits all in a row: Using concatenated subunit constructs to force the expression of receptors with defined subunit stoichiometry and spatial arrangement. *Molecular Pharmacology*. 69:407-410.

Wickman, K., and D.E. Clapham. 1995a. Ion channel regulation by G proteins. *Physiological Reviews*. 75:865-885.

Wickman, K.D., and D.E. Clapham. 1995b. G-protein regulation of ion channels. *Current Opinion in Neurobiology*. 5:278-285.

Williamson, I.M., S.J. Alvis, J.M. East, and A.G. Lee. 2003. The potassium channel KcsA and its interaction with the lipid bilayer. *Cellular and Molecular Life Sciences*. 60:1581-1590.

Williamson, I.M., S.J. Alvis, J. Malcolm East, and A.G. Lee. 2002. Interactions of phospholipids with the potassium channel KcsA. *Biophysical Journal*. 83:2026-2038.

Wong, A., and G. Wu. 2003. Selective Binding of Monovalent Cations to the Stacking G-Quartet Structure Formed by Guanosine 5´-Monophosphate: A Solid-State NMR Study. *Journal of the American Chemical Society*. 125:13895-13905.

Yuan, C., R.J. O'Connell, P.L. Feinberg-Zadek, L.J. Johnston, and S.N. Treistman. 2004. Bilayer thickness modulates the conductance of the BK channel in model membranes. *Biophysical Journal*. 86:3620-3633.

Zhou, M., and R. MacKinnon. 2004. A mutant KcsA K+ channel with altered conduction properties and selectivity filter ion distribution. *Journal of Molecular Biology*. 338:839-846.

VITA

Qiulin Tan was born in Chongqing, People's Republic of China in August, 1972. He obtained his bachelor degree in laboratory medicine from West China Medical University in 1995. He achieved Master of Science degree in Toxicology in 2005 at Texas AM University and Doctor of Philosophy degree in Biological engineering in 2010 from University of Missouri-Columbia.